



US Army Corps
of Engineers

MISCELLANEOUS PAPER CERC-88-3

AN ANALYTICAL MODEL OF WAVE-INDUCED LONGSHORE CURRENT BASED ON POWER LAW WAVE HEIGHT DECAY

by

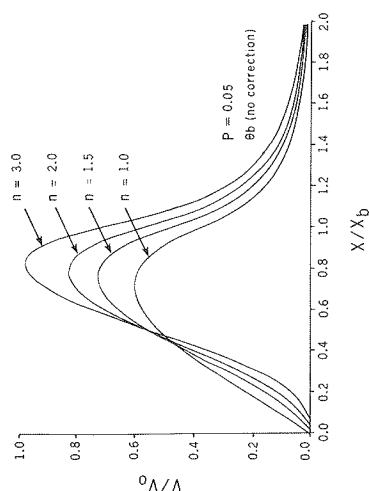
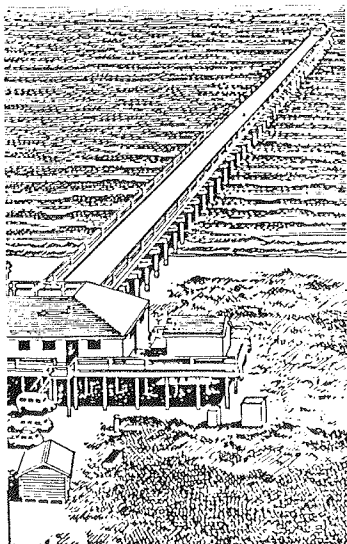
Jane McKee Smith, Nicholas C. Kraus

Coastal Engineering Research Center

DEPARTMENT OF THE ARMY

Waterways Experiment Station, Corps of Engineers

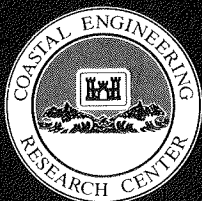
PO Box 631, Vicksburg, Mississippi 39180-0631



January 1988

Final Report

Approved For Public Release; Distribution Unlimited



Prepared for DEPARTMENT OF THE ARMY
US Army Corps of Engineers
Washington, DC 20314-1000

Destroy this report when no longer needed. Do not return
it to the originator.

The findings in this report are not to be construed as an official
Department of the Army position unless so designated
by other authorized documents.

The contents of this report are not to be used for
advertising, publication, or promotional purposes.
Citation of trade names does not constitute an
official endorsement or approval of the use of
such commercial products.

Unclassified

SECURITY CLASSIFICATION OF THIS PAGE

REPORT DOCUMENTATION PAGE				Form Approved OMB No. 0704-0188	
1a. REPORT SECURITY CLASSIFICATION Unclassified			1b. RESTRICTIVE MARKINGS		
2a. SECURITY CLASSIFICATION AUTHORITY			3. DISTRIBUTION/AVAILABILITY OF REPORT Approved for public release; distribution unlimited.		
2b. DECLASSIFICATION/DOWNGRADING SCHEDULE					
4. PERFORMING ORGANIZATION REPORT NUMBER(S) Miscellaneous Paper CERC-88-3			5. MONITORING ORGANIZATION REPORT NUMBER(S)		
6a. NAME OF PERFORMING ORGANIZATION USAEWES, Coastal Engineering Research Center		6b. OFFICE SYMBOL (If applicable) CEWES-CR-0	7a. NAME OF MONITORING ORGANIZATION		
6c. ADDRESS (City, State, and ZIP Code) PO Box 631 Vicksburg, MS 39180-0631			7b. ADDRESS (City, State, and ZIP Code)		
8a. NAME OF FUNDING/SPONSORING ORGANIZATION US Army Corps of Engineers		8b. OFFICE SYMBOL (If applicable) DAEN CWH-D	9. PROCUREMENT INSTRUMENT IDENTIFICATION NUMBER		
8c. ADDRESS (City, State, and ZIP Code) Washington, DC 20314-1000			10. SOURCE OF FUNDING NUMBERS		
			PROGRAM ELEMENT NO.	PROJECT NO.	TASK NO.
					WORK UNIT ACCESSION NO. 31592
11. TITLE (Include Security Classification) An Analytical Model of Wave-Induced Longshore Current Based on Power Law Wave Height Decay					
12. PERSONAL AUTHOR(S) Smith, Jane M., and Kraus, Nicholas C.					
13a. TYPE OF REPORT Final		13b. TIME COVERED FROM Jul 85 TO Oct 86		14. DATE OF REPORT (Year, Month, Day) January 1988	
15. PAGE COUNT 134					
16. SUPPLEMENTARY NOTATION Available from National Technical Information Service, 5285 Port Royal Road, Springfield, VA 22161.					
17. COSATI CODES			18. SUBJECT TERMS (Continue on reverse if necessary and identify by block number)		
FIELD	GROUP	SUB-GROUP	Longshore Current Current Distribution		
			Wave Breaking Power Law		
			Wave Decay Surf Zone		
19. ABSTRACT (Continue on reverse if necessary and identify by block number)					
<p>An analytical model of the wave-induced longshore current is derived. A unique feature of the model is an empirical power law expression, developed in this study, employed to describe the broken wave height in the surf zone. The model also includes the effect of wave setup, finite incident wave angle, and lateral mixing. The power law expression represents the surf zone wave height decay significantly better than the linear decay profile assumed in previous longshore current models. The exponent in the power law expression is determined to be a function of the beach slope and the wave height to water depth ratio at wave breaking. The longshore current model is derived by balancing the longshore stresses: local wave stress, lateral mixing stress, and bottom friction stress. The solution for the longshore current distribution is an infinite power series which is truncated to second order. The model gives the longshore current as a function of distance offshore, breaking wave conditions (height, depth, and angle), beach slope,</p>					
20. DISTRIBUTION/AVAILABILITY OF ABSTRACT <input checked="" type="checkbox"/> UNCLASSIFIED/UNLIMITED <input type="checkbox"/> SAME AS RPT. <input type="checkbox"/> DTIC USERS			21. ABSTRACT SECURITY CLASSIFICATION Unclassified		
22a. NAME OF RESPONSIBLE INDIVIDUAL			22b. TELEPHONE (Include Area Code)		22c. OFFICE SYMBOL

DD Form 1473, JUN 86

Previous editions are obsolete.

SECURITY CLASSIFICATION OF THIS PAGE
Unclassified

Unclassified

SECURITY CLASSIFICATION OF THIS PAGE

19. ABSTRACT (Continued).

friction coefficient, and a parameter, P , that expresses the relative importance of lateral mixing and bottom friction. Estimates of the longshore current distribution using this model agree with previous results in the appropriate limits, but the estimated current varies significantly under certain breaking wave conditions and beach slopes. Wave setup is also derived using the power law expression of the broken wave height. For the limited amount of setup data examined, the setup based on the power law wave height decay represents the data better than the calculated setup based on linear wave height decay.

Unclassified

SECURITY CLASSIFICATION OF THIS PAGE

PREFACE

The investigation described in this report was authorized as a part of the Civil Works Research and Development Program by the Office, Chief of Engineers (OCE), US Army Corps of Engineers. Work was performed under Wave Estimation for Design Work Unit 31592, Coastal Flooding Program, at the Coastal Engineering Research Center (CERC) of the US Army Engineer Waterways Experiment Station (CEWES). Messrs. John H. Lockhart, Jr., and John G. Housley were OCE Technical Monitors. Dr. C. Linwood Vincent is CERC Program Manager.

The study was conducted from July 1985 through October 1986 by Ms. Jane McKee Smith, Hydraulic Engineer, and Dr. Nicholas C. Kraus, Research Physical Scientist, CERC. This report is substantially the same as the thesis submitted to Mississippi State University by Ms. Smith in partial fulfillment of the requirements for an M.S. degree in civil engineering. Dr. Kraus was the thesis advisor.

This study was done under general supervision of Dr. James R. Houston and Mr. Charles C. Calhoun, Jr., Chief and Assistant Chief, CERC, respectively; and under direct supervision of Mr. H. Lee Butler, Chief, Research Division; Dr. Edward F. Thompson, Chief, Coastal Oceanography Branch (CR-O); and Dr. Robert E. Jensen, Principal Investigator, Wave Estimation for Design Work Unit, CR-O, CERC.

The author gratefully acknowledges Dr. Kiyoshi Horikawa, Department of Civil Engineering, University of Tokyo, who provided his extensive data on breaking waves, and Dr. Tsuguo Sunamura, Institute of Geosciences, University of Tsukuba, who assisted in obtaining other wave data reported in the Japanese literature.

COL Dwayne G. Lee, CE, was Commander and Director of CEWES during report publication. Dr. Robert W. Whalin was Technical Director.

CONTENTS

	Page
PREFACE	1
LIST OF TABLES	3
LIST OF FIGURES	3
CHAPTER I: INTRODUCTION	7
CHAPTER II: WAVE HEIGHT DECAY	17
CHAPTER III: DERIVATION OF THE LONGSHORE CURRENT DISTRIBUTION MODEL	44
CHAPTER IV: WAVE SETUP	75
CHAPTER V: CONCLUSIONS	80
REFERENCES	83
APPENDIX A: WAVE HEIGHT DECAY DATA	88
APPENDIX B: COMPUTER PROGRAM	123
APPENDIX C: NOTATION	129

LIST OF TABLES

No.		Page
1-1	Comparison of Longshore Current Models	11
1-2	Longshore Current Model Assumptions	12
2-1	Data Summary for Wave Height Decay	21
2-2	Regression Results for $n = f(\text{slope})$	35
3-1	Mizuguchi et al. (1978) Longshore Current Data	71

LIST OF FIGURES

No.		Page
2-1	Idealized profiles of experimentally determined wave height decay after initial breaking on plane beaches of different slope	18
2-2	Comparison of gamma calculated by the expression of McCowan (1891) and experimental results	24
2-3	Comparison of gamma calculated by the expression of Galvin (1969) and experimental results	25
2-4	Comparison of gamma calculated by the expression of Collins and Weir (1969) and experimental results	25
2-5	Gamma as a function of the water depth at breaking to deepwater wave length ratio (after Goda 1970)	26
2-6	Comparison of gamma calculated by the expression of Weggel (1972) and experimental results	26
2-7	Comparison of gamma calculated by the expression of Singamsetti and Wind (1980) and experimental results	27

2-8	Comparison of γ calculated by the expression of Sunamura (1981) and experimental results	27
2-9	γ versus wave steepness for experimental results	29
2-10	γ versus beach slope for experimental results	29
2-11	γ versus surf similarity parameter for experimental results	30
2-12	Power law exponent versus beach slope for experimental results (exponent determined from each experimental run)	32
2-13	Power law exponent versus wave steepness for experimental results (exponent determined from each experimental run)	32
2-14	Power law exponent versus deepwater surf similarity parameter for experimental results (exponent determined from each experimental run)	33
2-15	Power law exponent versus surf similarity parameter at wave breaking for experimental results (exponent determined from each experimental run)	33
2-16	Power law exponent versus $1/\text{slope}$ for experimental results and regression equations (exponent determined from combined data for each slope)	36
2-17	Power law exponent versus wave steepness for experimental results (exponent determined from combined data for each slope)	36
2-18	Power law exponent versus wave steepness for experimental results with slope = $1/20$ (exponent determined from each experimental run)	37
2-19	Power law exponent versus γ for experimental results with slope = $1/20$ (exponent determined from each experimental run)	37

2-20	Power law exponent versus gamma from Equation 2-8 and experimental results from Horikawa and Kuo (1967) (exponent determined from combined data with similar gamma and slope)	39
2-21	Power law exponent versus gamma from Equation 2-8 and experimental results (exponent determined from combined data with similar gamma and slope)	39
2-22	Comparison of wave height decay from experimental results, power law model ($n=1.10$, $\gamma=0.84$, and slope= $1/20$), and Dally et al. (1985a, 1985b) model	40
2-23	Comparison of wave height decay from experimental results, power law model ($n=1.61$, $\gamma=1.18$, and slope= $1/20$), and Dally et al. (1985a, 1985b) model	40
2-24	Comparison of wave height decay from experimental results, power law model ($n=1.40$, $\gamma=0.86$, and slope= $1/30$), and Dally et al. (1985a, 1985b) model	41
2-25	Comparison of wave height decay from experimental results, power law model ($n=2.09$, $\gamma=0.78$, and slope= $1/65$), and Dally et al. (1985a, 1985b) model	41
2-26	Comparison of wave height decay from experimental results, power law model ($n=2.39$, $\gamma=0.87$, and slope= $1/65$), and Dally et al. (1985a, 1985b) model	42
2-27	Comparison of wave height decay from experimental results, power law model ($n=1.75$, $\gamma=0.61$, and slope= $1/80$), and Dally et al. (1985a, 1985b) model	42
3-1	Definition sketch for momentum balance	46
3-2	Longshore current distribution showing the dependence on the power law exponent ($n=1.0$, 1.5 , 2.0 , 3.0 ; $P=0.05$; $\theta_b=0.0^\circ$).	66
3-3	Longshore current distribution showing the dependence on the parameter P ($P=0.00$, 0.01 , 0.05 , 0.10 , 0.50 ; $n=1.0$; $\theta_b=0.0^\circ$).	67
3-4	Longshore current distribution showing the dependence on the parameter P ($P=0.00$, 0.01 , 0.05 , 0.10 , 0.50 ; $n=1.5$; $\theta_b=0.0^\circ$).	67

3-5	Longshore current distribution showing the dependence on the breaking wave angle ($\theta_b = 0.0^\circ, 10.0^\circ, 20.0^\circ, 30.0^\circ$; $n=1.00$; $P=0.05$)	68
3-6	Comparison of the longshore current distribution from Case 1 experimental results of Mizuguchi et al. (1978), the present model, and the model of Longuet-Higgins (1970b).	69
3-7	Comparison of the longshore current distribution from Case 2 experimental results of Mizuguchi et al. (1978), the present model, and the model of Longuet-Higgins (1970b).	69
3-8	Comparison of the longshore current distribution from Case 3 experimental results of Mizuguchi et al. (1978), the present model, and the model of Longuet-Higgins (1970b).	70
3-9	Comparison of the longshore current distribution from Case 4 experimental results of Mizuguchi et al. (1978), the present model, and the model of Longuet-Higgins (1970b).	70
3-10	Infinite series solution for the longshore current distribution showing the dependence on the breaking wave angle ($\theta_b = 0.0^\circ, 10.0^\circ, 20.0^\circ, 30.0^\circ$; $n=1.00$; $P=0.05$)	73
3-11	Longshore current distribution showing the dependence on the breaking wave angle ($\theta_b = 0.0^\circ, 10.0^\circ, 20.0^\circ, 30.0^\circ$; $n=2.00$; $P=0.05$)	74
3-12	Infinite series solution for the longshore current distribution showing the dependence on the breaking wave angle ($\theta_b = 0.0^\circ, 10.0^\circ, 20.0^\circ, 30.0^\circ$; $n=2.00$; $P=0.05$)	74
4-1	Comparison of the wave setup from the small-scale experimental results of Stive (1985), setup based on the power law wave height decay ($n=1.79$), and setup based on linear wave height decay	79
4-2	Comparison of the wave setup from the large-scale experimental results of Stive (1985), setup based on the power law wave height decay ($n=1.52$), and setup based on linear wave height decay	79

CHAPTER I: INTRODUCTION

Wind generated or short period waves continually arrive at the coast. The approaching waves become unstable at a certain depth and the tops of their crests spill down or plunge over their forward faces. The wave height decreases as the wave energy is converted into turbulent eddies in the surf zone. If waves break at an angle to the shore, they induce a longshore current in the surf zone. The current acts somewhat analogous to a river, transporting sediment mobilized by the breaking waves. Coastal engineers have long worked to correlate sediment movement and current velocities to predict sediment transport, shoreline evolution, and pollutant transport. This requires accurate estimation procedures, or models, of the longshore current. This report presents an analytical longshore current model for engineering use. The model employs an expression developed in this report to describe the nonlinearity of the wave height decay, and it also includes the effect of wave setup, finite incident wave angles, and lateral mixing. The advantages of an analytical model over a numerical model are the ease of discerning the functional dependencies of the physical parameters and the ease of applying the model.

Waves transfer momentum from offshore to the nearshore. In the nearshore, the waves break when they reach a depth comparable to their height, and the wave energy is dissipated in the surf zone. Waves breaking at an angle to the shoreline induce a current parallel to the shoreline due to changes in the longshore component of momentum. The balance of momentum is conserved in the surf zone by the external forces of bottom and surface shear stresses. The change in the onshore component of momentum also causes a change in the mean water level in the surf zone, known as wave setup. Momentum is also diffused or transported by turbulent eddies.

Water motion in the surf zone is extremely complex. The flow is unsteady and three-dimensional, with dynamic upper and lower boundaries. No adequate theoretical description of water motion in the surf zone presently exists. Therefore, to predict longshore currents it is necessary to simplify

the problem by considering an idealized environment and to include a certain amount of empiricism. Applying various degrees of simplification, many investigators have calculated longshore currents analytically and numerically using empirical correlations, continuity of water mass, energy flux, and momentum flux.

In 1967 Galvin reviewed the state of the art of longshore current prediction. He concluded that the best approach at the time was the prediction of longshore current velocity through empirical correlation of data, but he cautioned that the available data were not reliable. Much progress has been made in the prediction of longshore currents since the review by Galvin. The progress mainly is due to the introduction of the concept of radiation stress by Longuet-Higgins and Stewart (1962, 1963, 1964). Radiation stress is used to calculate the flux of momentum parallel to the shoreline due to incident waves. Bowen (1969), Longuet-Higgins (1970a, 1970b), and Thornton (1971) were the first to apply radiation stress concepts in the equations of motion to predict longshore currents.

In the radiation stress approach it is necessary to specify the wave height through the surf zone a priori, but the mechanisms that determine the wave height in the surf zone (wave breaking, wave deformation, and energy dissipation) are not well understood. No quantitative, first-principle theoretical model of wave height decay exists; therefore an empirical approach is taken in longshore current modeling. The standard assumption is made that, in the surf zone (after initial wave breaking), the wave height, H , is described as a linear function of water depth, h , in the form

$$H = \gamma h \quad (1-1)$$

where γ is a constant of proportionality. This is known as the spilling breaker assumption because it holds fairly well for waves classified as spilling breakers. However, several investigators show that this is not valid in general (Horikawa and Kuo 1967; Nakamura, Shirashi, and Sasaki 1967; Street and Camfield 1967; Divoky, Le Mehaute, and Lin 1970; Dally, Dean, and Dalrymple, 1985a, 1985b), and it is especially inappropriate for mild bottom slopes, on which waves tend to break by plunging.

Investigators following Bowen, Longuet-Higgins, and Thornton built on the radiation stress approach by eliminating some of the simplifying assumptions and making more general models. But, all have retained the spilling breaker assumption despite its proven invalidity.

This investigation examines the effects of using nonlinear wave height decay, namely a power law decay, on the prediction of the longshore currents distribution. The power law wave height decay is of the form

$$H = H_b (h/h_b)^n \quad (1-2)$$

where the subscript b indicates breaking conditions, and the exponent n , to be determined empirically, is assumed to be dependent on the beach slope and the breaking wave conditions. It will be shown in this report that a closed-form solution for the longshore current distribution can still be derived if Equation 1-2 is employed instead of Equation 1-1.

The main body of this report begins with a review of previous longshore current models. Special attention is paid to the Longuet-Higgins model because it has served as the basis for most models that followed. Next, the wave height decay portion of this study is presented. Seven independent data sets are empirically fit to the wave height decay power law, and the exponent of the power law is parameterized. Then, an analytical longshore current model is derived from the equations of motion based on the radiation stress approach. The effects of large angles of wave incidence and of lateral mixing are included in the model. The current model gives the longshore current as a function of distance offshore, incident wave conditions, beach slope, friction coefficient, and a parameter, P , expressing the relative importance of lateral mixing and bottom friction as introduced by Longuet-Higgins (1970b).

Review of Previous Models

The radiation stress approach to modeling longshore currents was developed independently by Bowen (1969), Longuet-Higgins (1970a, 1970b), and Thornton (1971). Although the three models are similar, there are differences in the assumptions made in the bottom shear stress and lateral mixing terms.

The former two authors developed analytical solutions for a plane beach; the latter developed a numerical solution for arbitrary profiles of straight, parallel contours, using a more realistic bottom friction stress. The Longuet-Higgins model is the easiest and most straightforward to use (the solution of Bowen is in terms of Bessel functions and the model of Thornton requires a numerical solution), and appears to give very acceptable results for a plane beach. The Longuet-Higgins model, therefore, has been used as the basis for more recent longshore current models. A review of the Longuet-Higgins model is given, followed by overviews of other momentum-based models. Basco (1982) presents a thorough review of surf zone current literature with an annotated bibliography (Basco and Coleman 1982). Table 1-1 gives an intercomparison of selected models of the longshore current distribution across the surf zone.

Longuet-Higgins. Longuet-Higgins (1970a, 1970b) derives an analytical model for the steady longshore current from the governing equations of water motion. He makes the assumptions given in Table 1-2; in addition he assumes linear wave height decay given by Equation 1-1. The equation of motion for the longshore direction for this idealized case reduces to a balance between the local wave stress, the stress due to horizontal turbulent eddies, and the time-averaged bottom friction stress. The local wave stress is the driving force of the currents, and it is the net stress in the longshore direction exerted by the waves on the water in the surf zone. This stress is calculated from the radiation stress. The bottom shear stress is linearized by assuming the incident wave angle is small and the steady current is weak compared with the wave orbital velocities. These assumptions reduce the bottom shear stress to the product of the orbital velocity and the longshore current speed. The lateral mixing stress is a function of the horizontal eddy coefficient. Longuet-Higgins assumes the horizontal eddy coefficient is proportional to the offshore distance multiplied by a typical velocity, the shallow-water wave celerity. The distances (measured from the mean shoreline) are nondimensionalized by the distance from the mean shoreline to the breaker line. The longshore current velocity is nondimensionalized by the velocity

TABLE 1-1

Comparison of Longshore Current Models

	Plane Beach	Parallel Contours	Numerical	Analytical	Linear Theory	Nonlinear Theory	Lateral Mixing	2-D	Non-Linear Bottom Stress	Finite Angle	Strong Current	$H = h$	$H = h_b(b/h_b)^n$
Bowen (1969)	X		X	X		X					X		
Longuet-Higgins (1970a)	X		X	X							X		
Longuet-Higgins (1970b)	X		X	X		X					X		
Thornton (1971)		X	X		X*	X					X		
James (1974)	X	X		X	X	X		X	X	X	X		
Jonsson et al. (1975)		X	X	X							X		
Keely and Bowen (1977)	X	X	X			X					X		
Liu and Dalrymple (1978)		X	X	X					X	X	X	X	
Kraus and Sasaki (1979a, 1979b)	X		X	X	X			X	X	X	X		
present study (1986)	X		X	X	X			X			X		

* solitary wave theory

o hyperbolic wave theory

Table 1-2

Longshore Current Model Assumptions

WAVE FIELD

Monochromatic waves
Linear, shallow-water wave theory
Steady state wave field

BEACH

Plane, sloping beach
Impermeable beach
Hydrostatic pressure distribution

FLUID

Incompressible, homogeneous fluid

CURRENT

Current constant through depth and time
Current homogeneous in the longshore direction
Current weak relative to the wave orbital velocity

NEGLECTED STRESSES

No wind stress
No atmospheric pressure gradient
No wave-current interaction
No Coriolis force
No tide

at the breaker line when the effect of lateral mixing is omitted. The stress balance is described by a second-order differential equation with a closed-form solution. The solution is a function of the relative effects of lateral mixing and bottom friction. Longuet-Higgins does not include wave setup explicitly, but he suggests modifying the beach slope to include the change in water depth due to wave setup. He also does not include refraction because the angle of wave incidence is assumed small.

The strong points of the Longuet-Higgins model are: (a) the model solution is simple and easy to apply and, (b) the model results compare well to available data. The weak points of the model are: (a) the numerous simplifying assumptions, and (b) the spilling breaker assumption in the lateral mixing and bottom stress terms was applied seaward of the breaker line where it is no longer valid.

Bowen. The Bowen (1969) model differs from the Longuet-Higgins model in several ways. Bowen assumes the bottom shear stress is proportional to the longshore current speed, neglecting the contribution of the wave orbital velocity. He also does not account for the effect of variation in depth in the lateral mixing stress. Although Bowen simplifies the stress terms considerably more than Longuet-Higgins, his solution is more complicated. The solution is in terms of Bessel functions and is, therefore, more difficult to use. On the positive side, Bowen explicitly includes wave setup in the surf zone, and he neglects it outside the surf zone where it is negligible compared to the depth.

Thornton. Thornton (1971) uses solitary wave theory in the surf zone to specify wave celerity and linear wave theory outside the surf zone. Thornton relaxes the plane beach assumption, but still assumes a beach of straight and parallel contours. He also includes setup and refraction inside and outside the surf zone. Thornton uses Prandtl's mixing length hypothesis to calculate the horizontal eddy coefficient in the lateral mixing stress. He assumes the horizontal eddy coefficient is equal to the amplitude of wave particle motion multiplied by water particle velocity fluctuations due to waves in the shore normal direction. The Jonsson (1967) friction factor for turbulent flow was used in the bottom stress term. Thornton also does not account for the

variation in depth in the lateral mixing stress. Thornton's model requires a numerical solution.

James. James (1974) uses hyperbolic wave theory in the surf zone and linear wave theory far outside the surf zone with a transition region in between to calculate the wave stress. Hyperbolic wave theory is an approximation of cnoidal wave theory which is believed to describe the wave form in the surf zone better than linear theory. James includes refraction, setup, and return flows (to insure the mean shoreward mass flux is zero). He also eliminates the weak current assumption. Outside the surf zone, he uses experimental results to define the eddy coefficient to be proportional to the inverse of the depth. James relaxes the plane beach assumption, but requires the beach slope to be mild. The mild slope assumption may invalidate the linear wave height decay assumption (as stated earlier). Also, the model is formulated as a set of differential equations that must be solved numerically. This model is much too complicated for practical engineering use.

Jonsson, Skovgaard, and Jacobsen. Jonsson, Skovgaard, and Jacobsen (1975) return to using linear wave theory throughout the nearshore region. They use a nonlinear bottom shear stress and introduce a friction factor that is an interpolation between the friction factor for waves only and the friction factor for currents only. Jonsson, Skovgaard, and Jacobsen adopt Thornton's (1971) formulation for the lateral mixing stress, but they do account for the variation in depth. The model is a differential equation which is solved numerically.

Keeley and Bowen. Keeley and Bowen (1977) take into account longshore variations in longshore currents, removing the assumption of the current being homogeneous in the longshore direction. Spatial variations in the longshore current, typical in the field, are caused by irregular bathymetry and spatial variations in the wave field. Keeley and Bowen follow the Longuet-Higgins derivation of the longshore current due to obliquely incident waves, but omit the lateral mixing stress. They linearly add the currents due to obliquely incident waves, variations in the wave height in the longshore direction, variations in the wave angle in the longshore direction, and nonlinear effects

(due to the advection term in the longshore momentum balance). They also include wave setup. The Keeley and Bowen model must be driven by a refraction model which provides the variation of wave heights and angles in the longshore direction. The contributions of the longshore variation in wave height and the nonlinear effects to the longshore current are small. The model requires a numerical solution.

Liu and Dalrymple. Liu and Dalrymple (1978) present a weak current model and a strong current model. Both models include the effects of large incident wave angle and wave setup, but exclude the lateral mixing stress. In the weak current model, the longshore current velocity is assumed small compared to the wave orbital velocity. In the strong current model, the longshore current is assumed to be of the same order of magnitude or larger than the wave orbital velocity. The absolute value of the total velocity (longshore current plus wave orbital motion) is approximated with a truncated binomial series. For the weak current model, the bottom stress term is simplified to a linear function of the current velocity using the weak current assumption. The solution of the weak current model is in closed form. The strong current model results in a nonlinear ordinary differential equation solved numerically. The solution of the strong current model is found iteratively because the setup is not known a priori. The neglect of lateral mixing limits the use of this model.

Kraus and Sasaki. Kraus and Sasaki (1979a, 1979b) add still another improvement to the lineage of momentum-based longshore current models. Their model includes the effects of large incident wave angles and the lateral mixing stress (omitted by Liu and Dalrymple). They assume that the magnitude of the longshore current is small compared to the wave orbital velocity. Setup is approximated by modifying the beach slope as suggested by Longuet-Higgins. Similar to the Liu and Dalrymple strong current model, Kraus and Sasaki approximate the absolute value of the total velocity (wave orbital plus longshore current) with a truncated binomial expansion. Inside the surf zone, they also apply the approximation

$$\cos\theta = (1 - h/h_b \sin^2\theta_b)^{1/2}$$

derived from a trigonometric identity, shallow-water approximations for the wave celerity, and Snell's law, where θ is the angle of wave incidence. The model has an analytic solution in the form of an infinite series of successively smaller terms. Kraus and Sasaki verified the model with laboratory data (Mizuguchi et al. 1978) and their own field data.

CHAPTER II: WAVE HEIGHT DECAY

The derivation of the wave-induced longshore current requires knowledge of the wave height and the gradient of the wave height in the surf zone. Historically, the wave height in the surf zone has been estimated as a linear function of the water depth,

$$H = Yh \quad (2-1)$$

Longuet-Higgins and Stewart (1964) and Bowen et al. (1968) suggest the similarity between the decrease in wave height and the decrease in water depth shoreward of breaking as the motivation for Equation 2-1. Bowen et al. support the assumption with laboratory data on a slope of 1/12. The Y-values ranged from 0.9 to 1.3. This empirical expression is attractive because of its simplicity, but the surf zone wave height decay is not linear in general as has been noted, for example, by Horikawa and Kuo (1967), Street and Camfield (1967), and Van Dorn (1977) on the basis of their carefully performed laboratory experiments. Figure 2-1 shows idealized curves fit to laboratory wave height decay data. The curves are increasingly concave upward with decreasing beach slope. The purpose of this chapter is to develop an empirical power law decay model to describe the wave height decay more accurately than the linear model, but still retain the useful simple form of the linear model. The simple form will allow the longshore current model to be solved analytically.

The dissipation of wave energy in the surf zone is due primarily to turbulence (Horikawa and Kuo 1967; Sawaragi and Iwata 1975; Mizuguchi 1981; Dally, Dean, and Dalrymple 1985a, 1985b; and others). The power law decay model is entirely empirical. The model is not meant to replace more sophisticated models based on the physics of the turbulent energy dissipation. These more sophisticated models solve the energy flux equation in the surf zone,

$$\partial(EC_g)/\partial x = \epsilon \quad (2-2)$$

where EC_g is the energy flux and ϵ is the energy dissipation rate.

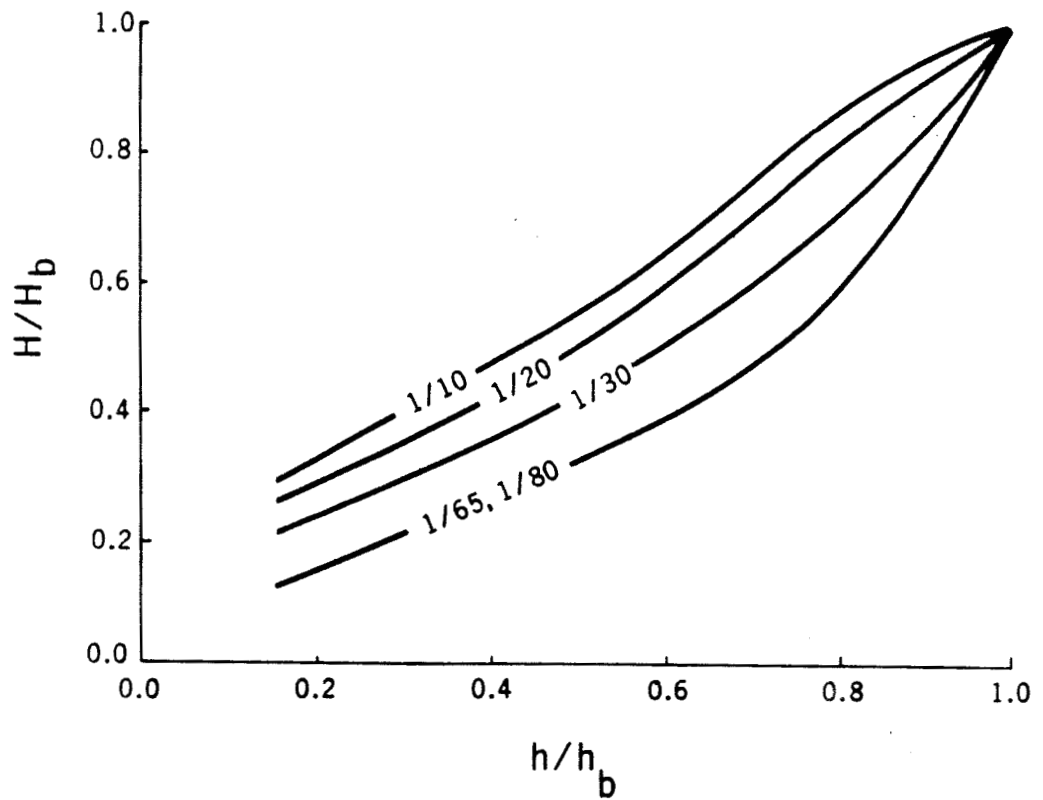


Figure 2-1. Idealized profiles of experimentally determined wave height decay after initial breaking on plane beaches of different slope

For completeness, some of these models are briefly described. Le Mehaute (1963) approximates a breaking wave as a hydraulic jump, substituting the energy dissipation of a hydraulic jump for ϵ in Equation 2-2. The same approach with some variations is applied to periodic laboratory waves by Divoky et al. (1970), Hwang and Divoky (1971), and Svendsen (1984, 1985). Battjes and Janssen (1979) also use the hydraulic jump model, but apply it to random laboratory waves. Thornton and Guza (1983) refine the approach of Battjes and Janssen and apply it to both laboratory and field data.

Although the hydraulic jump model appears to give the best explanation of the physics of wave breaking, three other approaches are mentioned because of their uniqueness and insight. Horikawa and Kuo (1967) model surf zone energy dissipation due to bottom friction and turbulence using solitary wave theory. The turbulence is assumed to decay exponentially with distance from the break point. The results are good for a horizontal bed, but poor for a plane sloping bed. Mizuguchi (1981) models the surf zone energy dissipation by replacing the molecular viscosity with the turbulent eddy viscosity in the solution for internal energy dissipation due to viscosity. Mizuguchi's model allows more complex beach profiles (step-type beaches) and reformation and second breaking of waves. The model gives good results when tested with laboratory data for wave breaking on a horizontal beach, a 1/10 slope plane beach, and a step-type beach. But, Mizuguchi admits that the eddy viscosity assumption is "obscure." The model requires a numerical solution. Dally et al. (1985a, 1985b) propose what they call an intuitive approach. The dissipation, ϵ , in Equation 2-2 is assumed to be proportional to the difference between the local energy flux, EC_g , and the "stable" energy flux, EC_{gs} , or

$$\epsilon = -(k/h) (EC_g - EC_{gs}) \quad (2-3)$$

where k is a dimensionless decay coefficient and h is the local still-water depth. The stable energy flux is found to be associated with a wave height equal to approximately 0.35 to 0.40 times the local depth. This approach allows a breaking wave to stabilize or reform and break again. The

formulation also allows for an arbitrary beach profile and the inclusion of wave setup, but this requires a numerical solution. Analytical solutions are derived for simple profiles (horizontal bottom, sloping bottom, and Dean's (1977) equilibrium profile). Results are good in comparison to laboratory data. Since this approach is so successful, the power law decay model will be compared to it.

Power Law Model of Wave Height Decay

In this study, the wave height decay is expressed as the power law

$$H = \gamma h_b (h/h_b)^n \quad (2-4)$$

This form was chosen because it is similar to the linear wave height decay model, and it reduces to the linear decay model (Equation 2-1) for an exponent, n , equal to 1.0. Equation 2-4 is applicable from the breaker line to the mean shoreline. Two constants, γ and n , must be specified in Equation 2-4. It is noted that the formulation of Dally et al. (1985a, 1985b) also requires specification of two parameters through empirical considerations. The importance of beach slope in the decay profile is clearly shown in Figure 2-1. Horikawa and Kuo also suggest the importance of the wave steepness, H_0/L_0 , where H_0 is the deepwater wave height and L_0 is the deepwater wavelength, and the breaking wave conditions (H_b/h_b) on the decay profile. Following a description of the wave height decay data, the procedures used to analyze the data and quantify γ and n are explained.

Seven independent sets of laboratory and prototype scale data comprising 135 experimental runs on slopes of 1/90 to 1/10 are used to quantify the wave height decay. These data sets were obtained through a comprehensive search of the literature in English and Japanese. Table 2-1 summarizes the data. The breaking wave heights (of monochromatic waves) range from 4.67 cm to 1.37 m, and the wave periods range from 1.2 s to 9.0 s. The wave steepnesses (H_0/L_0) are between 0.0031 and 0.091. The data are listed in Appendix A.

Table 2-1
Data Summary for Wave Height Decay

<u>Source</u>	<u>Slope</u>	<u>Number of Runs</u>
Horikawa and Kuo (1967) and Kuo (1965)	1/80	57
	1/65	16
	1/30	19
	1/20	21
Maruyama et al. (1983)	1/62.5	1
	1/45.5	1
	1/29.4	1
	1/22.2	1
Mizuguchi (1981)	1/10	1
Saeki and Sasaki (1973)	1/50	2
Sasaki and Saeki (1974)	1/90	1
Stive (1985)	1/40	2
Van Dorn (1977)	1/12	4
	1/25	4
	1/45	4

Horikawa and Kuo performed their experiment in two parts. The 1/20 and 1/30-slope data were collected in a flume 17 m long, 0.7 m wide, and 0.6 m deep. The slope was covered with a smooth rubber mat. The 1/65 and 1/80-slope data were collected in a flume 75 m long, 1.0 m wide, and 1.2 m deep. The slope was concrete. The Maruyama et al. data were collected in a prototype-scale flume 250 m long, 3.4 m wide, and 1.2 m deep. The initial slopes (1/22.2, 1/29.4, 1/45.5, and 1/62.5) were formed of sand and were, therefore, not constant throughout each run. The Mizuguchi data were collected in a wave basin 15 m long and 15 m wide, but the width was truncated to 9 m. The 1/50-slope Saeki and Sasaki data were collected in a flume 24 m long, 0.8 m wide, and 0.8 m deep. The 1/90-slope Sasaki and Saeki data were collected in a flume 24 m long, 0.6 m wide, and 1 m deep. The slope in both cases was formed of smooth plastic. The Stive data were collected at two scales to compare scale effects. The large flume was 233 m long, 5 m wide, and 7 m deep. The slope was sand with an initial slope of 1/40. The small flume was 55 m long, 1 m wide, and 1 m deep, with a concrete slope of 1/40. The Van Dorn data were collected in a flume 24 m long, 0.5 m wide, and at a still-water depth of 36 cm. The slopes were formed of plate glass.

The parameter γ is defined as the ratio of the wave height to the local water depth at breaking,

$$\gamma = H_b/h_b \quad (2-5)$$

by solving Equation 2-4 for γ with $H=H_b$ and $h=h_b$. This ratio is very significant because it specifies where a wave will break. This is important in the design of coastal structures, so the specification of γ has stimulated much interest.

McCowan (1891) calculates the critical H/h ratio for wave breaking from solitary wave theory. His value,

$$H_b/h_b = 0.78$$

gives a reasonable average of the measured γ -values from the data summarized

in Table 2-1, but it does not explain the measured variation in γ . Figure 2-2 shows McCowan's expression versus measured values of γ available from the data set (Appendix A). Galvin (1969) includes the effect of beach slope, m , in his empirical relationship

$$H_b/h_b = 1/\beta_b$$

where $\beta_b = 0.92$ for $m > 0.07$ and $\beta_b = 1.40 - 6.85 m$ for $m < 0.07$. Collins and Wier (1969) also include beach slope in their empirical expression

$$H_b/h_b = 0.72 + 5.6 m$$

Galvin, and Collins and Wier predict increasing γ with increasing slope. The data indicate that this trend is correct (Figures 2-3 and 2-4), but the large variations in γ for a given slope are not accounted for by these two equations. Goda (1970) gives H_b/h_b in terms of h_b/L_o and slope in graphical form (Figure 2-5) obtained by fitting field and laboratory data. Weggel (1972) gives a similar expression in terms of H_b/T^2 (where T is the wave period) and beach slope

$$H_b/h_b = b(m) - a(m) H_b/T^2$$

where $a(m) = 1.36 (1 - e^{-19m})$ and $1/b(m) = 0.64 (1 + e^{-19.5m})$. The units of $a(m)$ are sec^2/ft . Figure 2-6 shows Weggel's expression versus the measured values of γ . Singamsetti and Wind (1980) and Sunamura (1981) include the effects of beach slope and wave steepness (H_o/L_o) in expressions for H_b/h_b . Singamsetti and Wind's equation,

$$H_b/h_b = 1.16 (m/(H_o/L_o))^{1/2} 0.22 \quad (2-6)$$

is plotted in Figure 2-7 against the data summarized in Table 2-1. Sunamura's equation,

$$H_b/h_b = 1.1 (m)^{1/6} (H_o/L_o)^{-1/12} \quad (2-7)$$

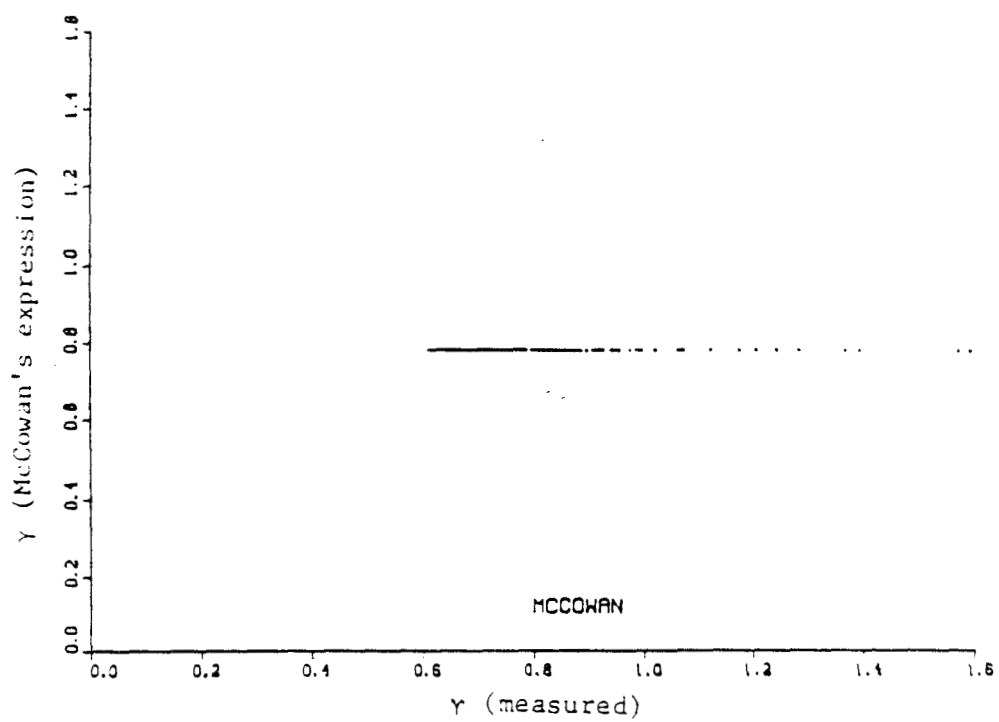


Figure 2-2. Comparison of γ calculated by the expression of McCowan (1891) and experimental results

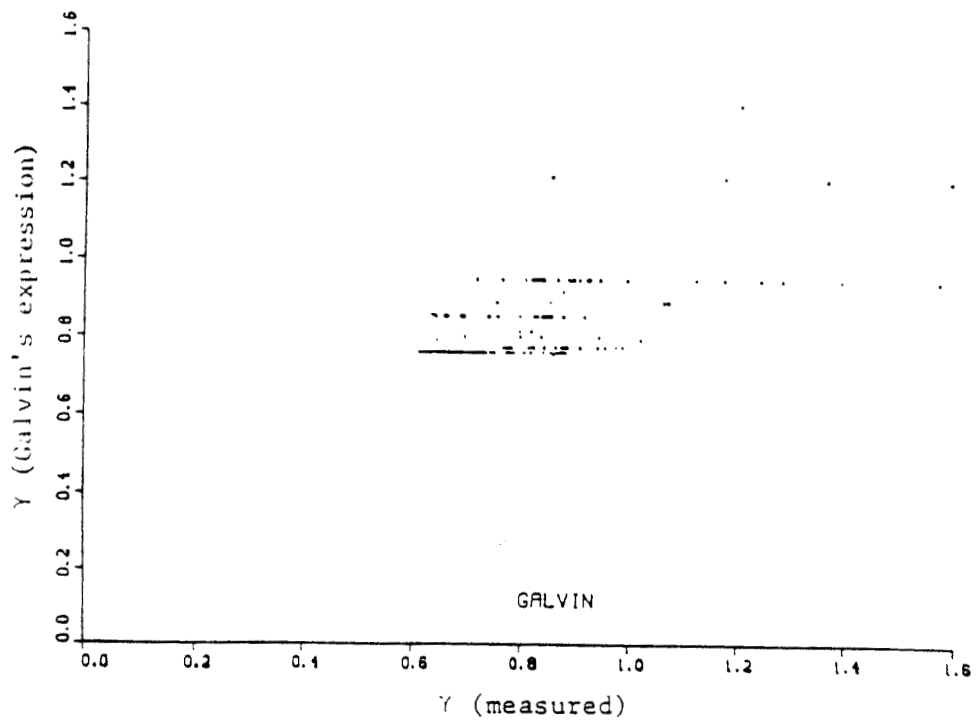


Figure 2-3. Comparison of Y calculated by the expression of Galvin (1969) and experimental results

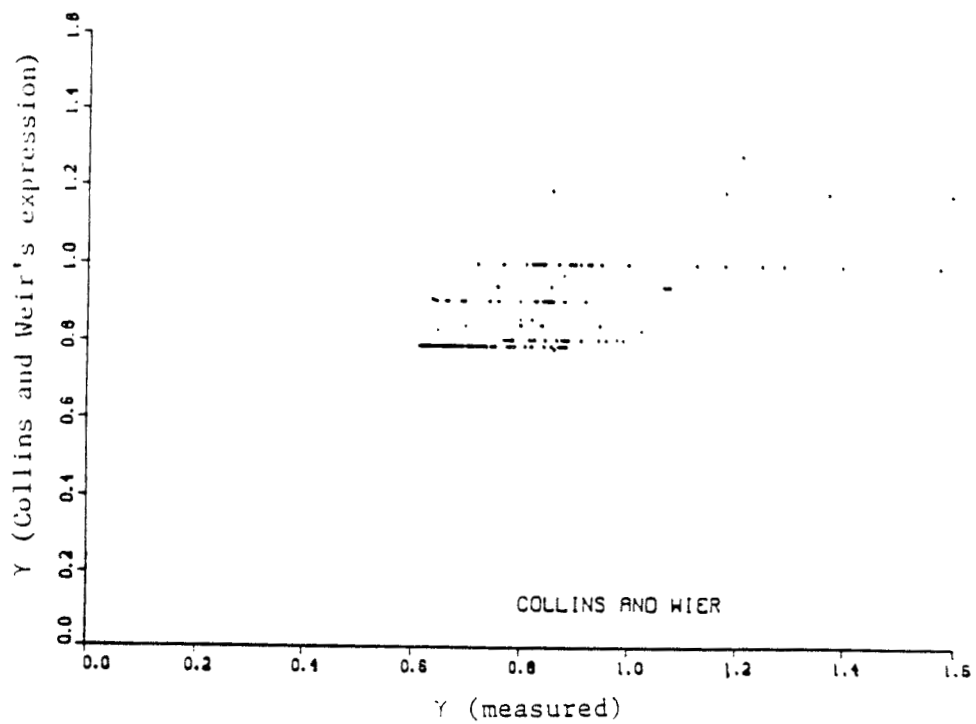


Figure 2-4. Comparison of Y calculated by the expression of Collins (1969) and experimental results

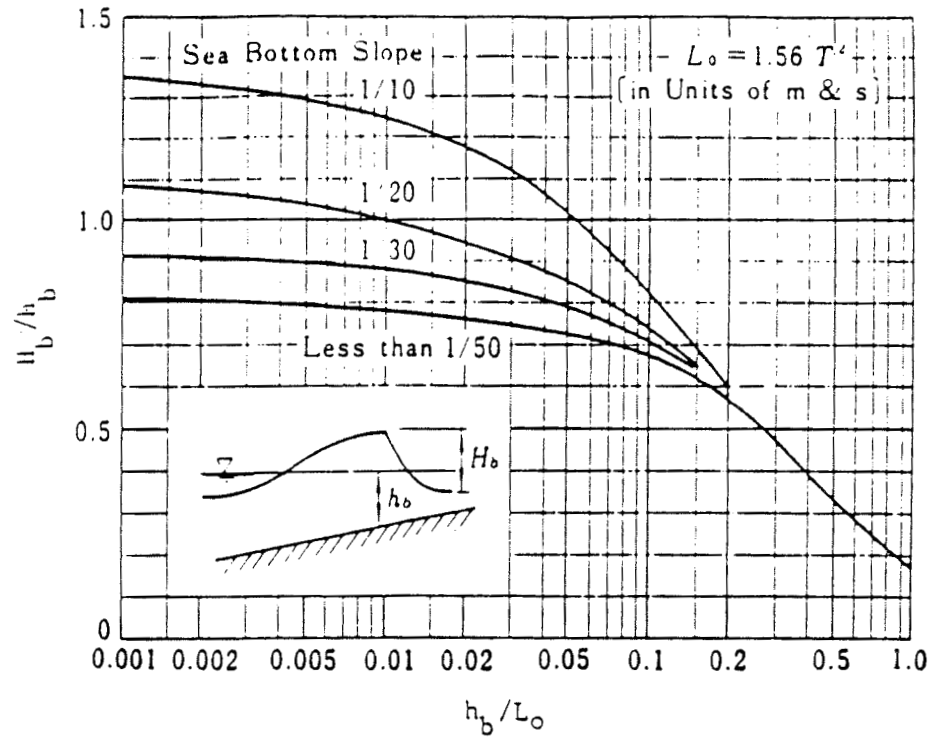


Figure 2-5. Gamma as a function of the water depth at breaking to deepwater wavelength ratio (after Goda 1970)

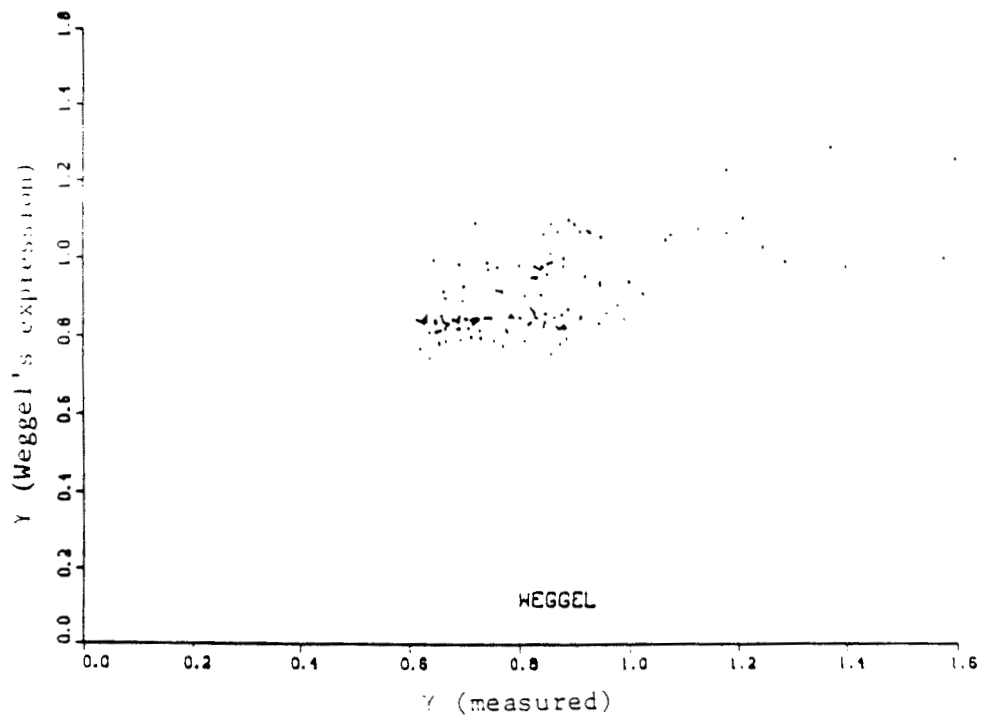


Figure 2-6. Comparison of γ calculated by the expression of Weggel (1972) and experimental results

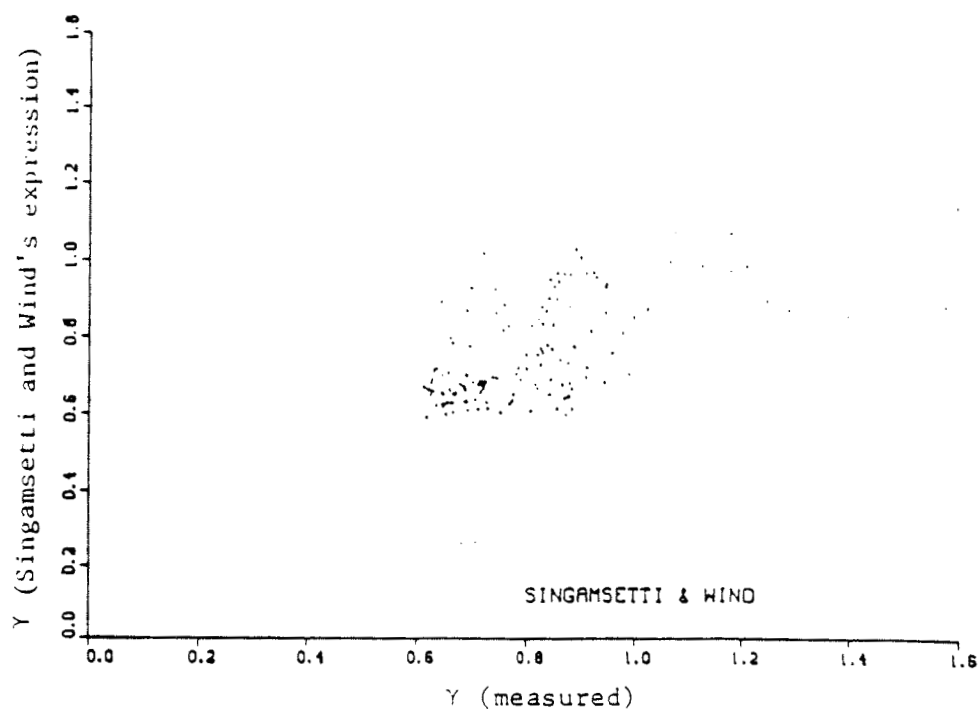


Figure 2-7. Comparison of Y calculated by the expression of Singamsetti and Wind (1980) and experimental results

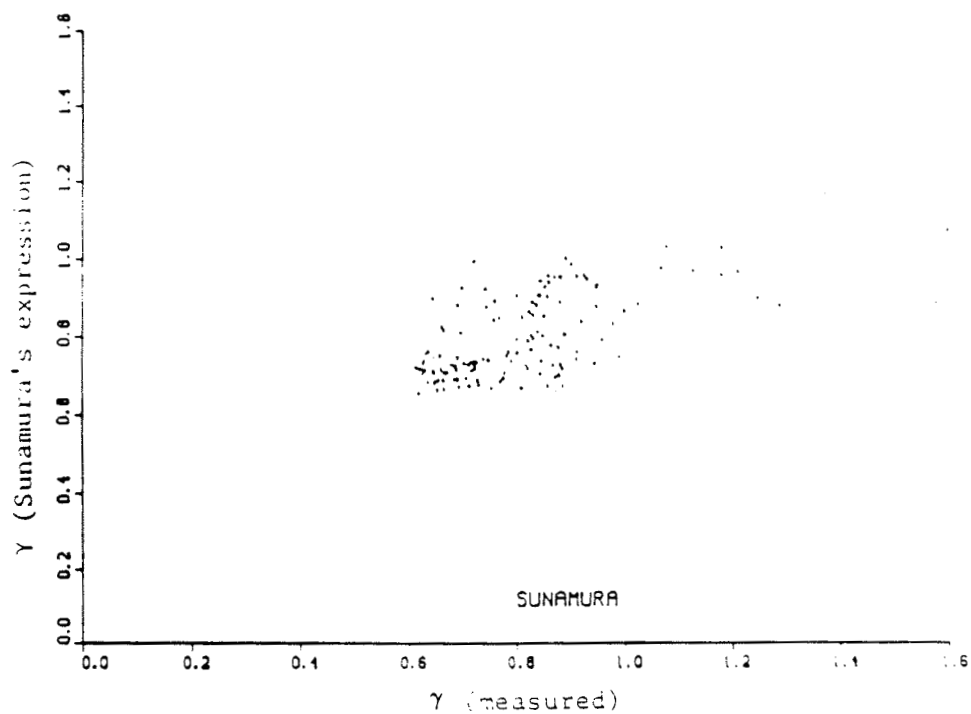


Figure 2-8. Comparison of Y calculated by the expression of Sunamura (1981) and experimental results

is plotted in Figure 2-8 against the data. Equations 2-6 and 2-7 are quite similar. The equations give a rough estimate of the measured value of γ , but they do not explain all of the measured variation in γ .

Plots of the measured γ versus H_o/L_o (Figure 2-9) and beach slope (Figure 2-10) show that γ decreases with increasing wave steepness and increases with increasing slope. Figure 2-11 is a plot of γ versus a combination of these two parameters, $m/(H_o/L_o)^{1/2}$, known as the surf similarity parameter (Battjes 1975). The plot shows some increase in γ with an increasing surf similarity parameter, but the relationship is weak and the data are very scattered. Obviously much effort has been expended in the past to determine H_b/h_b . Although none of the expressions presented gives an excellent fit to the data, the expressions of Singamsetti and Wind, and of Sunamura provide the best predictions. It is evident that both the measurement and the process of wave breaking are very complex and that the phenomenon has a large variability.

The second parameter needed to quantify the wave height decay in this study is the exponent n . The n -value in Equation 2-4, obtained as a best fit to each of the decay profiles in the data, was calculated by regression analysis. Equation 2-4 is nonlinear, but it was transformed to a linear form using natural logarithms, and the curves were fit to the data by the method of least squares (Miller and Freund 1977). The method of least squares minimizes the sum of the squares of the vertical distances from the data points to the regression curve. Equation 2-4 transforms to

$$\ln H = \ln (\gamma h_b) + n \ln (h/h_b)$$

in which \ln is the logarithm to the base e . The previous equation is of the form

$$Y = a + b X$$

where n is unknown. The (γh_b) -term can be treated either as a known or unknown in the analysis. The value of γh_b for a particular run is

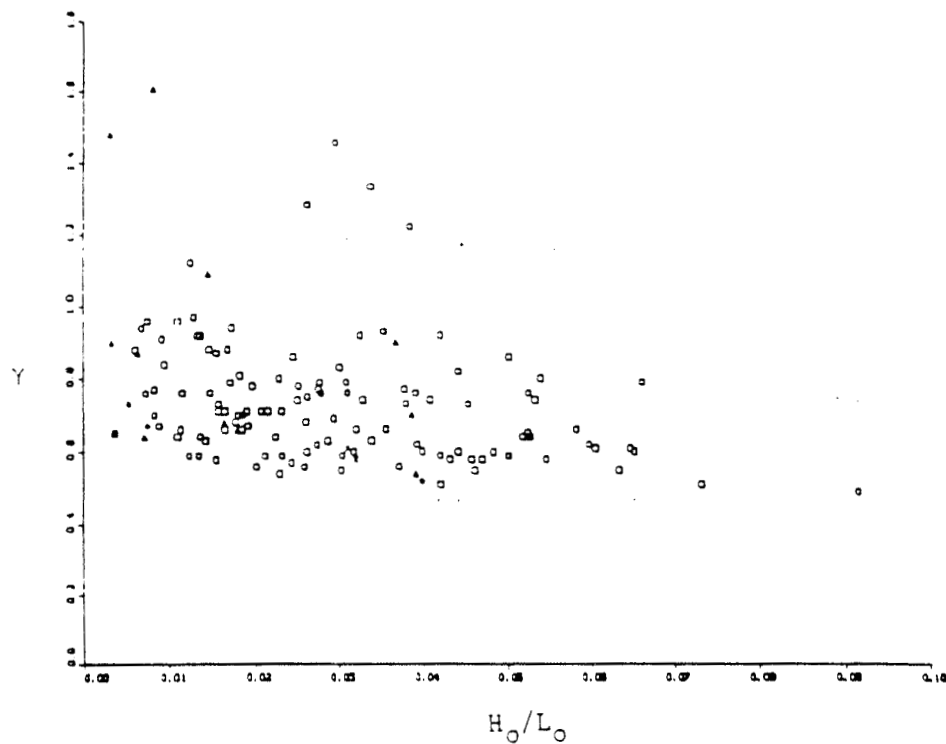


Figure 2-9. Gamma versus wave steepness for experimental results

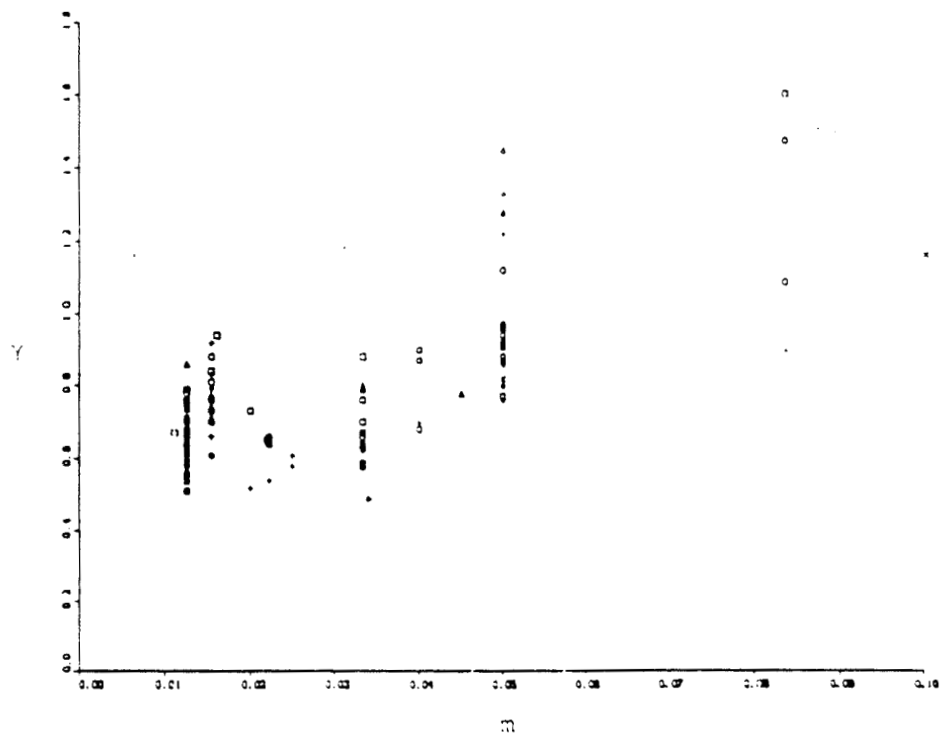


Figure 2-10. Gamma versus beach slope for experimental results

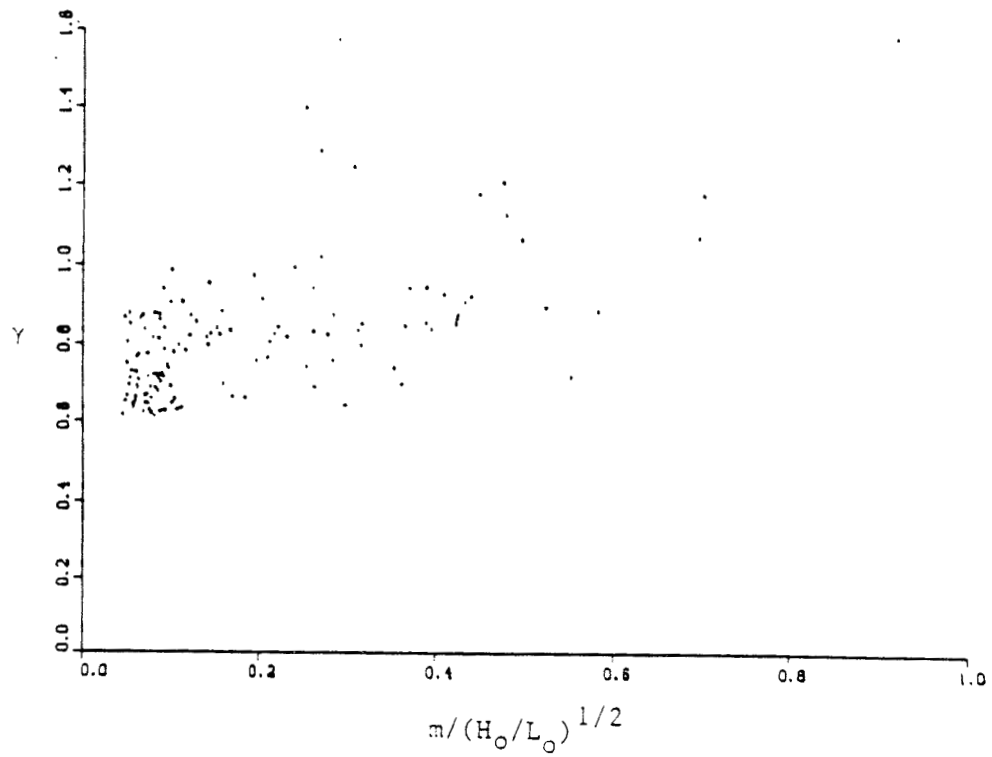


Figure 2-11. Gamma versus surf similarity parameters for experimental results

equal to H_b , which is available in the data set. If the value of γh_b is calculated by the regression, this gives a better fit of the curve to the data. But, by letting γ "float" as a free parameter, it is no longer equal to H_b/h_b . Therefore, the value of γh_b is set to H_b for each run, and only the value of n is allowed to vary to fit the data.

The first attempt to quantify n was to calculate it for each data run with the regression analysis, and to plot these n -values against significant parameters for respective runs. The parameters chosen to relate with the n -values were beach slope, wave steepness, surf similarity parameter, and surf similarity parameter at wave breaking, $m/(H_b/L_b)^{1/2}$. Figure 2-12 shows n versus beach slope for each run. The plot shows an inverse or hyperbolic relationship between n and slope, but there is much scatter. An n -value greater than 1.0 indicates a concave upward decay profile, so larger n -values associated with smaller slopes fits the trend in Figure 2-1. Figure 2-13 is a plot of n versus H_o/L_o . No correlation between n and H_o/L_o is obvious. Figures 2-14 and 2-15 are plots of n versus the deepwater surf similarity parameter and the surf similarity parameter at breaking. The correlation takes a hyperbolic shape in both cases. These four plots show that n and H_o/L_o do not have a strong relationship, but n and slope are related, as was known from the onset. The plots show that for steep bottom slopes, the n -value is lower and less variable, whereas on gentle bottom slopes, the n -value is extremely variable.

This first attempt was encouraging, but not conclusive. The n -values for the individual runs on small slopes were extremely variable. Closer examination of these runs (Horikawa and Kuo 1/80 and 1/65 slopes) showed that some runs had as few as four data points, and in some cases the data spanned only one-third of the surf zone (from the breaker line inshore). In runs with few data points, the n -values were higher. The lack of inshore data points in the decay profiles evidently biased the results.

To eliminate the problem of sparse data in some runs, all data for each slope were nondimensionalized and combined. The wave height was

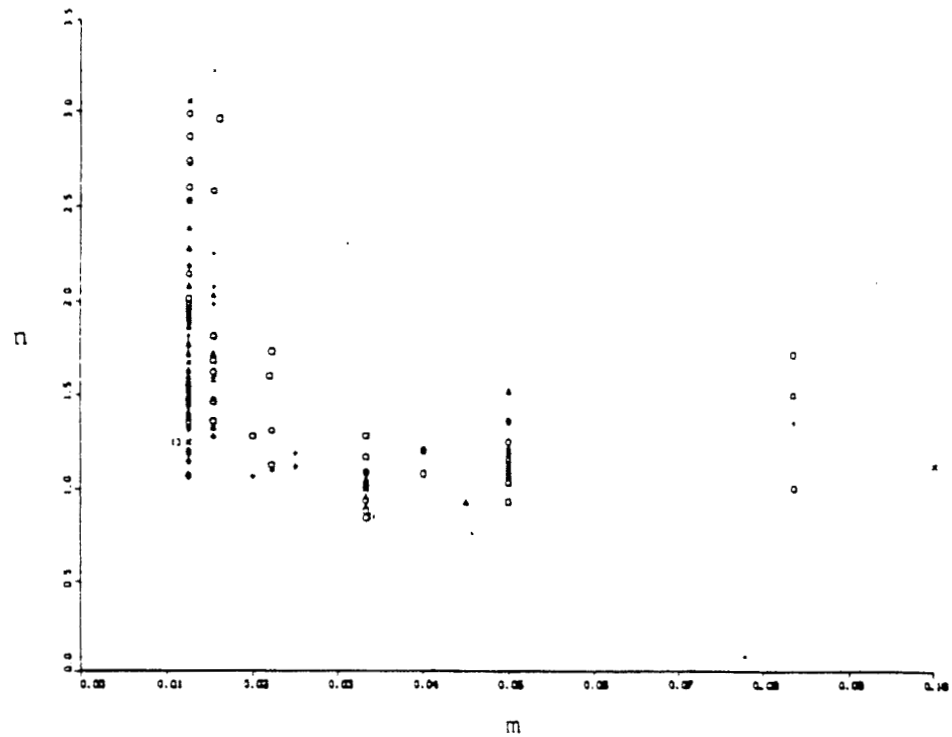


Figure 2-12. Power law exponent versus beach slope for experimental results (exponent determined from each experimental run)

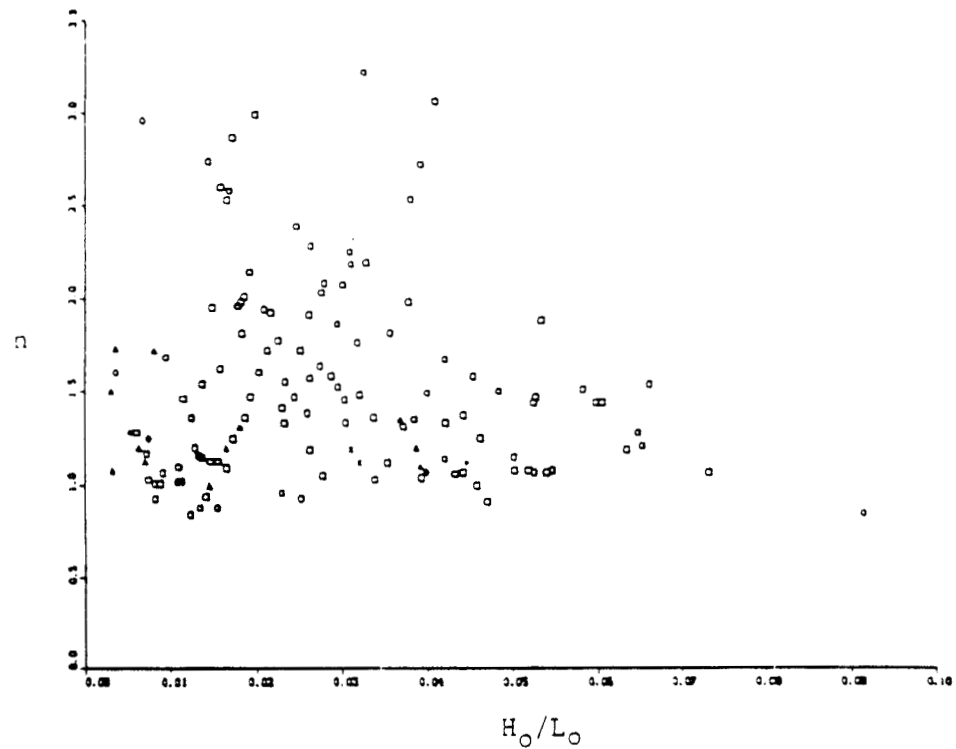


Figure 2-13. Power law exponent versus wave steepness for experimental results (exponent determined from each experimental run)

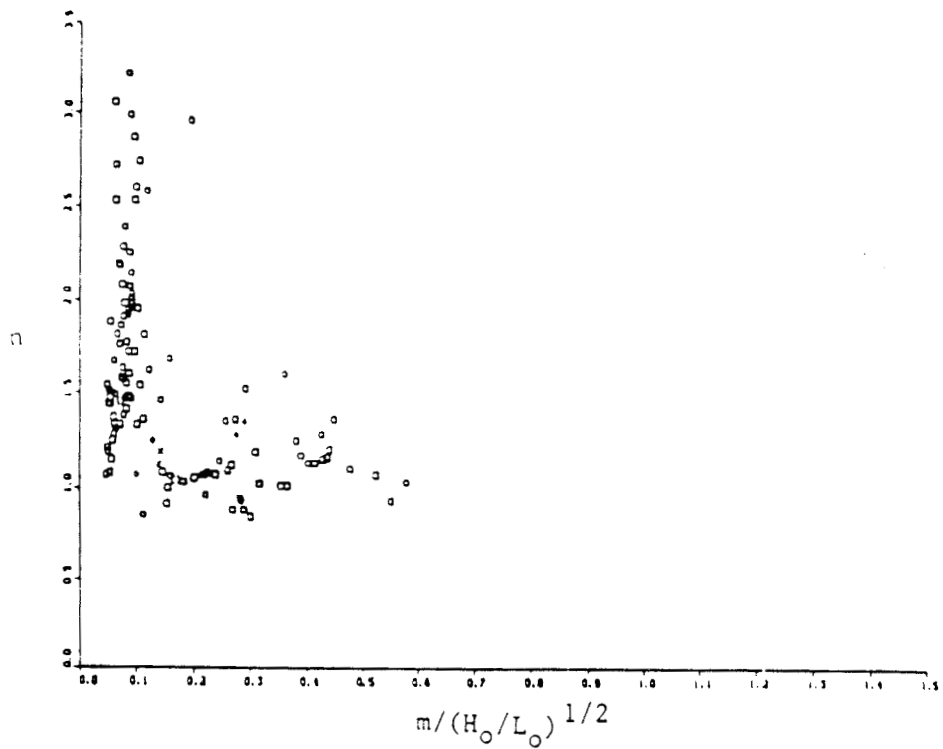


Figure 2-14. Power law exponent versus deepwater surf similarity parameter for experimental results (exponent determined from each experimental run)

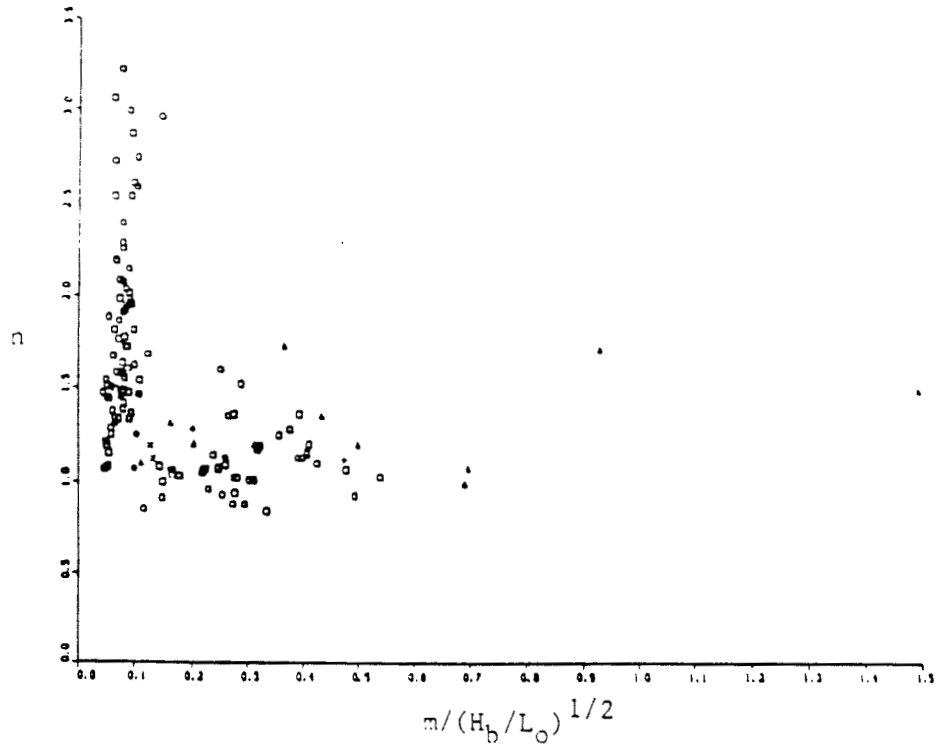


Figure 2-15. Power law exponent versus surf similarity parameter at wave breaking for experimental results (exponent determined from each experimental run)

nondimensionalized by the breaking wave height and the water depth was nondimensionalized by the water depth at breaking. Equation 2-4 becomes

$$H/H_b = (h/h_b)^n$$

The equation was transformed to the linear form

$$\ln (H/H_b) = n \ln (h/h_b)$$

and a regression analysis was performed. The results of the regression are given in Table 2-2. The n -value is the result of the regression for the lumped nondimensional data. The values of γ and H_o/L_o are the averages of the combined runs. Figure 2-16 is a plot of the "lumped" n versus the inverse of bottom slope. A linear regression of n as a function of slope gave the equation

$$n = 1.35 + 0.009/m$$

with a correlation coefficient, r , equal to 0.71. A regression was also done on a subset of the data, the Horikawa and Kuo data, and gave the equation

$$n = 0.89 + 0.017/m$$

with a correlation coefficient equal to 0.86. The Horikawa and Kuo data set was selected as a subset because it includes more runs and data points per slope than the other data sets and thus would be more statistically stable. Figure 2-17 is a plot of the "lumped" n versus the averaged H_o/L_o . The plot shows no obvious correlation.

Although the relationship between n and beach slope is fairly clear for the combined data, the scatter in the data implies there may be another important factor, assuming that random experimental variability is not the major cause. To resolve the variation in n for a given slope, n versus H_o/L_o and n versus γ were plotted for selected slopes. Figures 2-18 and 2-19 are plots of n versus H_o/L_o and n versus γ for a slope of 1/20. The values of n , H_o/L_o , and γ are from each of the individual runs, not

TABLE 2-2

Regression Results for $n = f(\text{slope})$

Slope	n	\bar{Y}_{ave}	H_C/L_O	No. of Data Points	No. of Runs	Source
1/90	1.75	0.86	.0075	23	1	Sasaki and Saeki
1/80	1.97	0.71	.0341	515	57	Horikawa and Kuo
1/65	2.38	0.87	.0275	142	16	Horikawa and Kuo
1/63	3.99	0.97	.0068	7	1	Maruyama et al.
1/50	1.52	0.83	.0226	73	2	Saeki and Saski
1/46	1.96	0.70	.0037	6	1	Maruyama et al.
1/45	1.84	0.88	.0170	35	4	Van Dorn
1/40	1.70	0.81	.0315	22	2	Stive
1/30	1.32	0.78	.0230	248	19	Horikawa and Kuo
1/29	1.12	0.64	.0913	7	1	Maruyama et al.
1/25	1.51	0.94	.0162	39	4	Van Dorn
1/22	1.11	0.88	.0252	5	1	Maruyama et al.
1/20	1.20	0.99	.0258	169	21	Horikawa and Kuo
1/12	1.49	1.25	.0156	24	4	Van Dorn
1/10	1.30	1.21	.0446	7	1	Mizuguchi

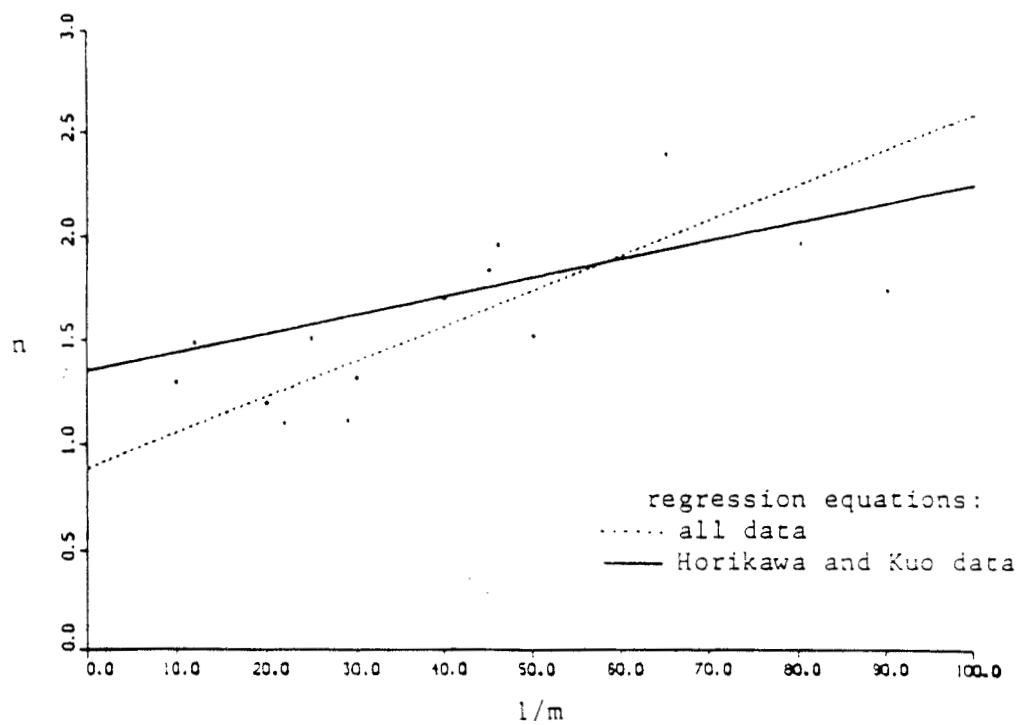


Figure 2-16. Power law exponent versus 1/slope for experimental results and regression equations (exponent determined from combined data for each slope)

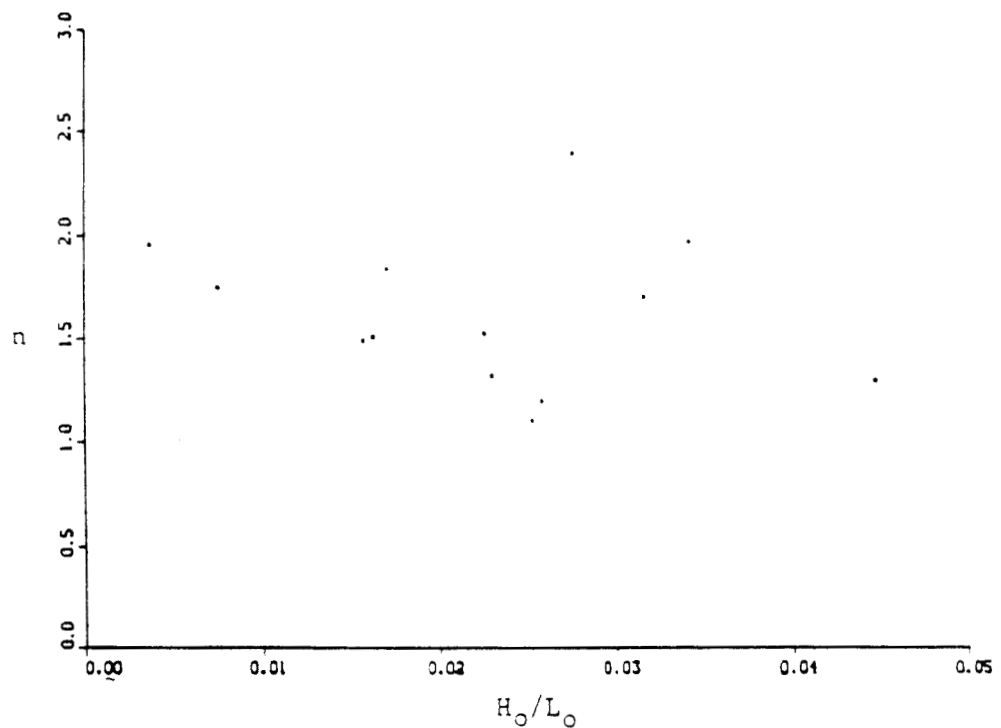


Figure 2-17. Power law exponent versus wave steepness for experimental results (exponent determined from combined data for each slope)

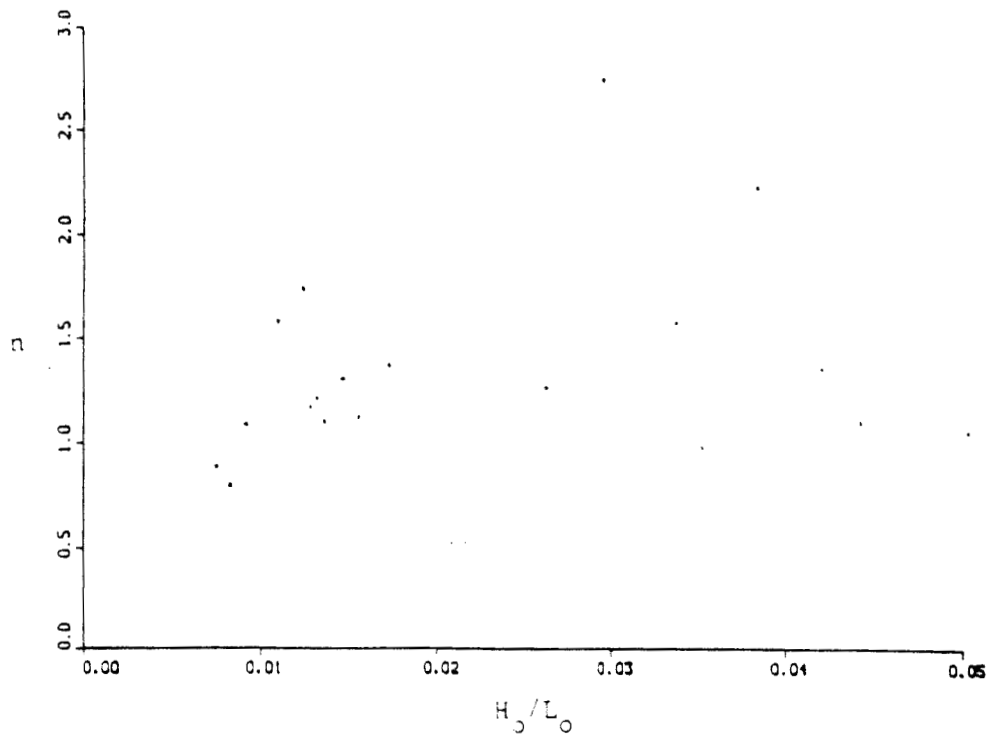


Figure 2-18. Power law exponent versus wave steepness for experimental results with slope = 1/20 (exponent determined from each experimental run)

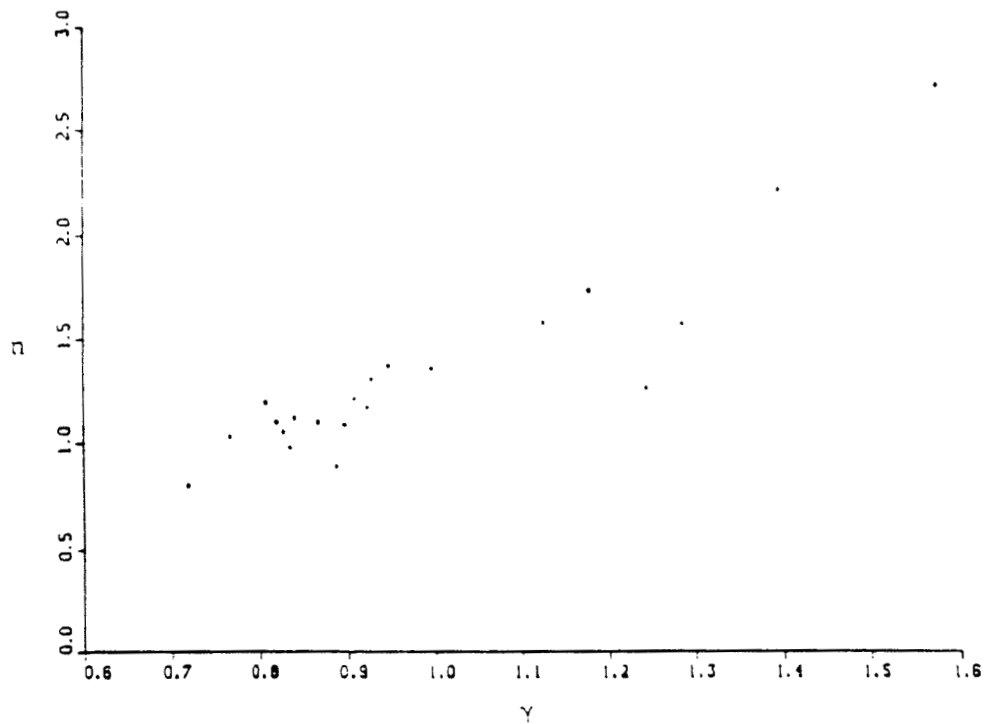


Figure 2-19. Power law exponent versus γ for experimental results with slope = 1/20 (exponent determined from each experimental run)

averages. The n -value still shows no relation to H_o/L_o , but n does increase as Y increases. To summarize, n is a function of slope and Y , but n does not appear to be related to H_o/L_o or to the surf similarity parameter (a function of H_o/L_o).

As a next step, to avoid the problem of sparse data in some runs without combining all the data of the same slope, runs with similar Y were combined (so the effect of Y is seen). Slopes with multiple runs were divided into groups with Y centered on whole tenths of Y (0.6, 0.7, 0.8, etc...). Regressions were run on each of the groups to calculate a best fit n . These n -values, the average Y , and the slope for each group were used as input to a multiple regression of n in terms of Y and slope. The assumed form of the equation is

$$n = b_0 + b_1/m + b_2Y + b_3Y/m$$

The method of least squares was used again to fit a family of curves to the data. The multiple regression was run on a subset of the data, the Horikawa and Kuo data, because it included more data points per slope. The result of the multiple regression is

$$n = 0.657Y + 0.043Y/m - 0.0096/m + 0.032 \quad (2-8)$$

Equation 2-8 is plotted in Figure 2-20. The plot shows that n increases with increasing Y and decreasing slope. The interaction term of Y and slope accounts for the increased steepness of the curves as the slope decreases. Figure 2-21 shows all the data plotted against Equation 2-8. The second term in Equation 2-8 is the leading term for moderate-to-mild beach slopes. The value of n is mainly controlled by Y , but is also sensitive to m because the beach slope varies over an order of magnitude whereas the value of Y deviates little from unity.

Figures 2-22 through 2-27 give examples of the fit of the power law wave height decay model to the Horikawa and Kuo laboratory data. The solid line represents the power law model. The n -values used were calculated from Equation 2-8 with the measured values of n and beach slope. The dashed line is the fit of the Dally et al. model described earlier. The recommended value

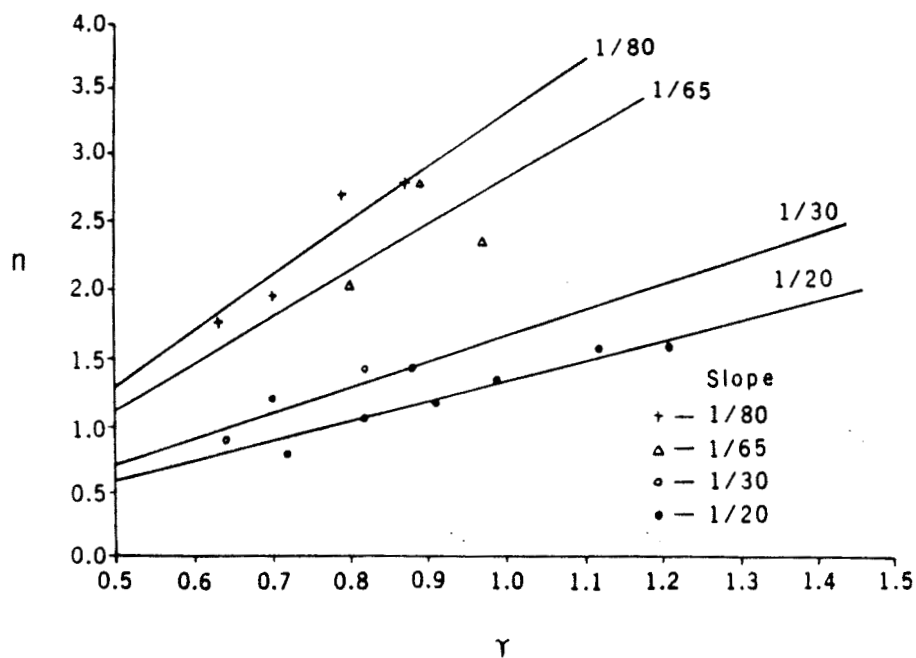


Figure 2-20. Power law exponent versus γ from Equation 2-8 and experimental results from Horikawa and Kuo (1967) (exponent determined from combined data with similar γ and slope)

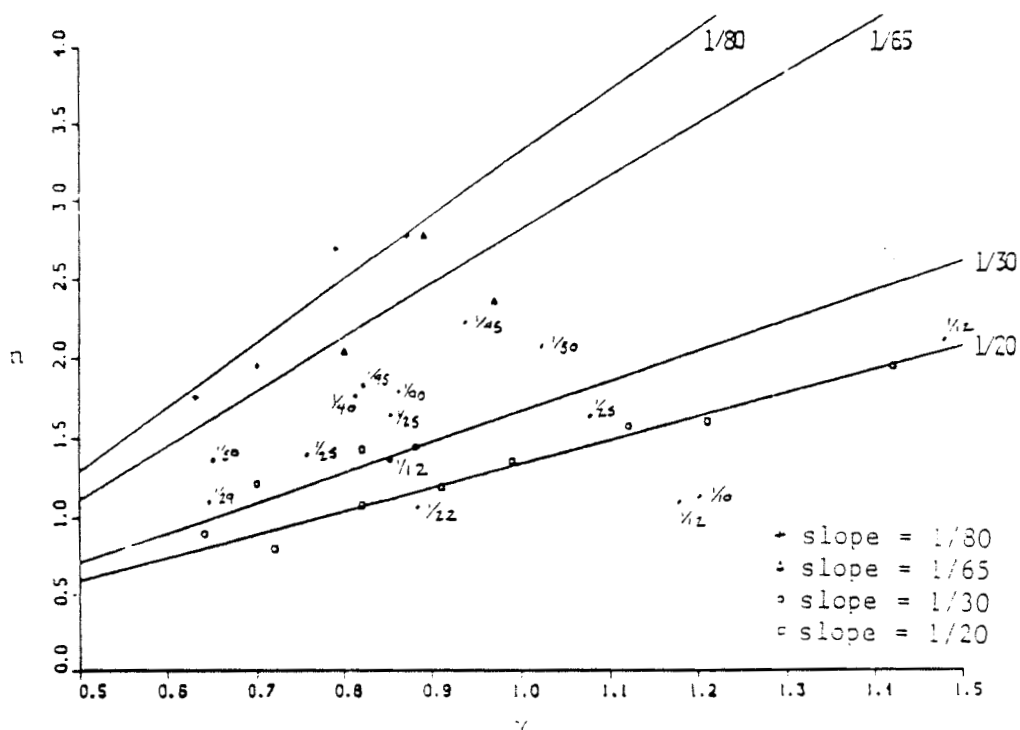


Figure 2-21. Power law exponent versus γ from Equation 2-8 and experimental results (exponent determined from combined data with similar γ and slope)

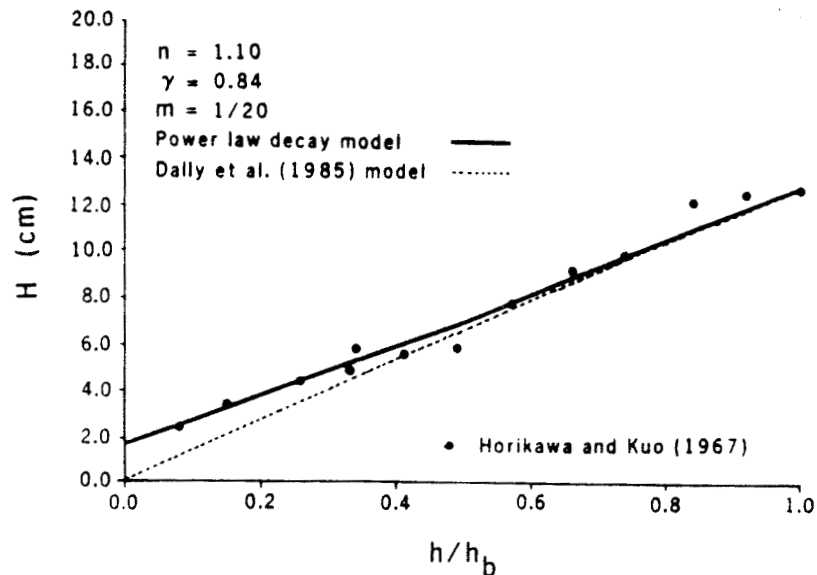


Figure 2-22. Comparison of wave height from experimental results, power law model ($n=1.10$, $\gamma=1.18$, and slope= $1/20$), and Dally et al. (1985a, 1985b) model

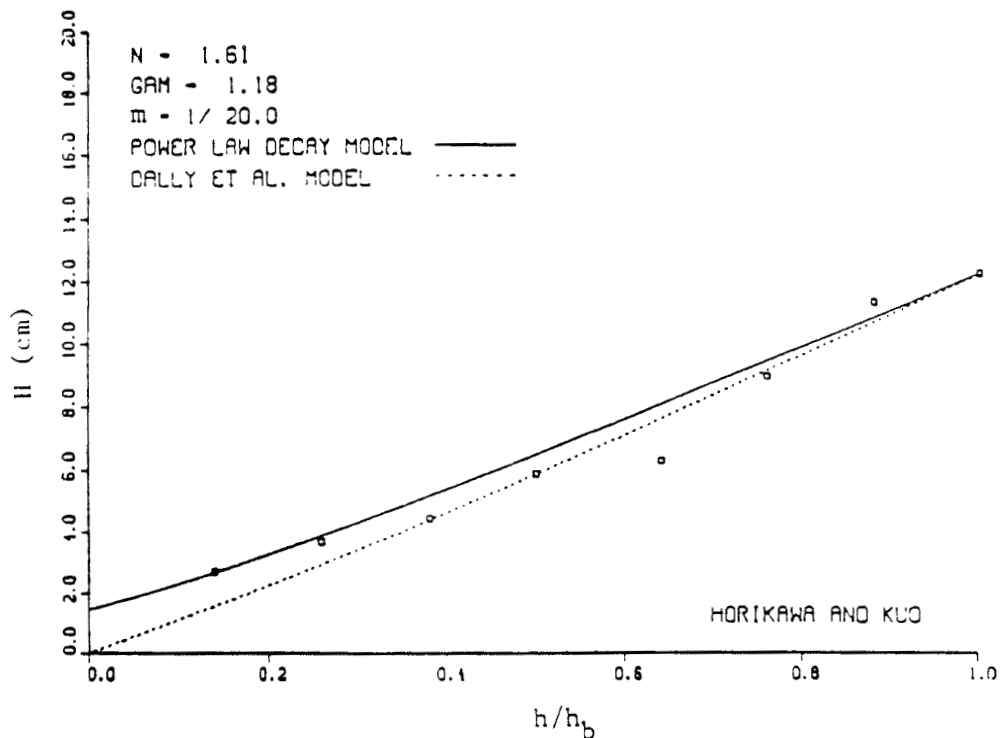


Figure 2-23. Comparison of wave height decay from experimental results, power law model ($n=1.61$, $\gamma=1.18$, and slope= $1/20$), and Dally et al. (1985a, 1985b) model

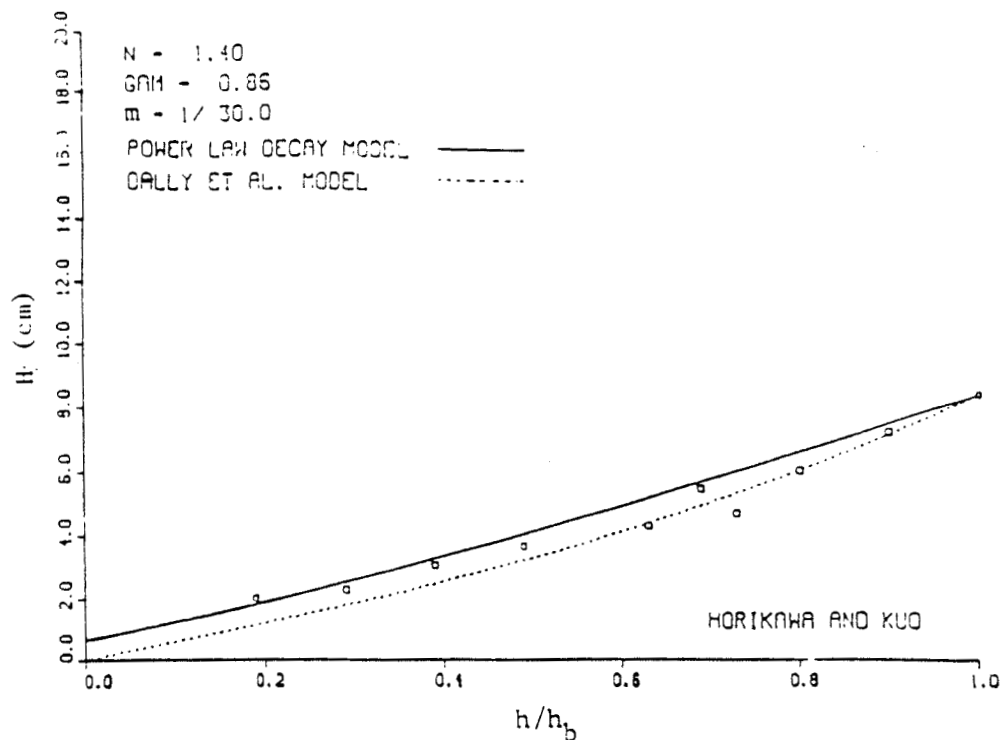


Figure 2-24. Comparison of wave height decay from experimental results, power law model ($n=1.40$, $Y=0.86$, and slope= $1/30$), and Dally et al. (1985a, 1985b) model

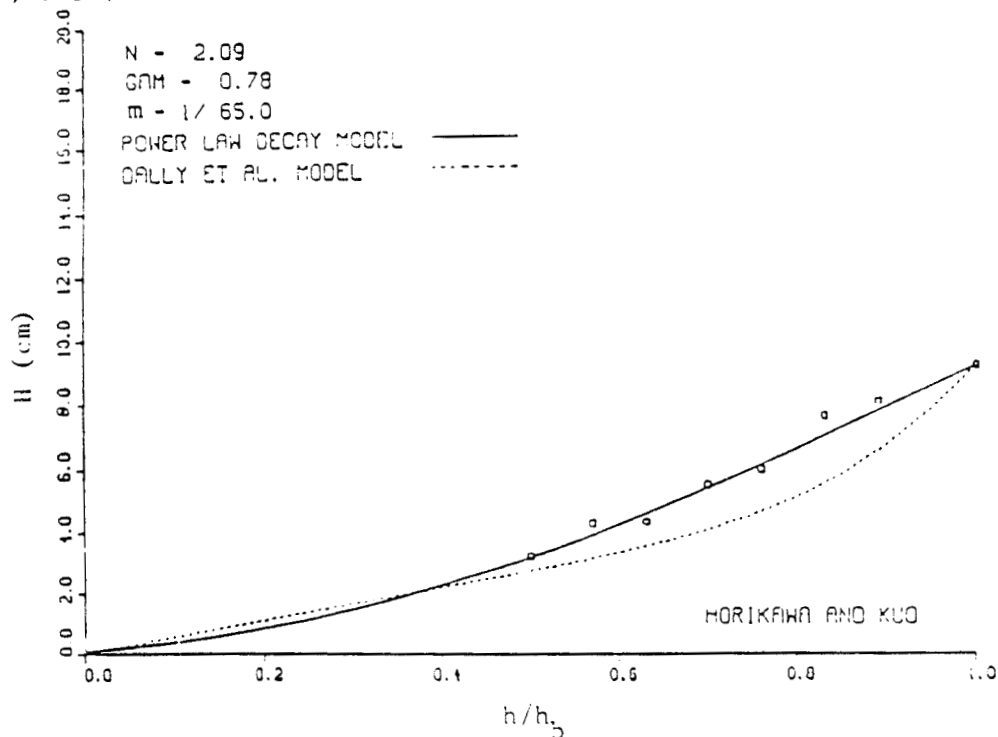


Figure 2-25. Comparison of wave height decay from experimental results, power law model ($n=2.09$, $Y=0.78$, and slope= $1/65$), and Dally et al. (1985a, 1985b) model

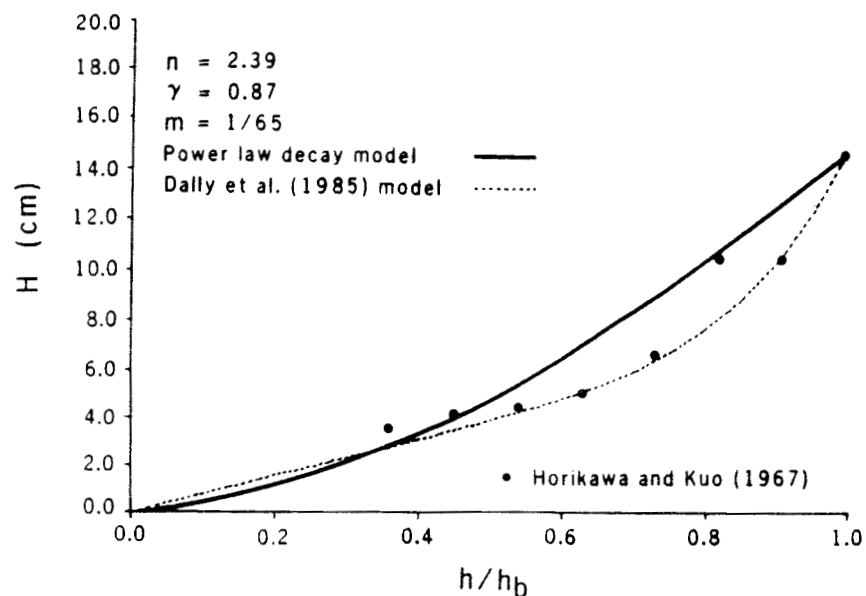


Figure 2-26. Comparison of wave height decay from experimental results, power law model ($n=2.39$, $\gamma=0.87$, and slope= $1/65$), and Dally et al. (1985a,1985b) model

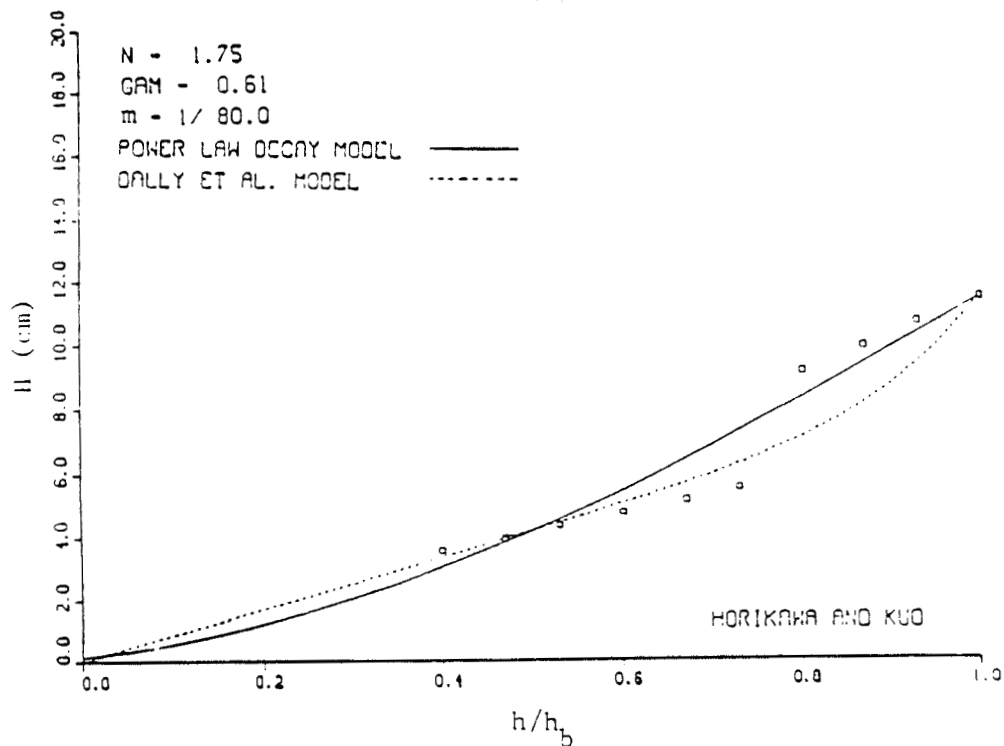


Figure 2-27. Comparison of wave height decay from experimetnal results, power law model ($n=1.75$, $\gamma=0.61$, and slope= $1/80$), and Dally et al. (1985a,1985b) model

of $k = 0.15$ and the stable wave height of $H_s = 0.40 h$ were used to calculate the Dally et al. wave height decay. The decay profiles on the steep beach slopes show almost linear decay with a pronounced setup (not included in the Dally et al. curve). The decay profiles on the mild slopes show a concave upward shape as predicted by both models. The Dally et al. model appears to fit the profile shape better on the mild slopes, characterizing the reformation of the wave. Overall, the power law model gives a good prediction of the wave height decay.

The power law model predicts the wave height decay better than the linear decay model assumed in previous longshore current models. The power law model also compares favorably to the more complex model of Dally et al. (1985a, 1985b). The specification of two parameters, Y and n , is required in the power law model. The parameter Y is the ratio of wave height to water depth at wave breaking. This parameter is best estimated by the expression of Singamsetti and Wind (Equation 2-6) or the expression of Sunamura (Equation 2-7). The exponent, n , of the power law is a function of Y and the beach slope as specified in Equation 2-8. A closed-form solution for the longshore current distribution is derived in the next chapter using the power law model of wave height decay.

CHAPTER III: DERIVATION OF THE LONGSHORE CURRENT DISTRIBUTION MODEL

This chapter describes the derivation of the closed-form mathematical model of the longshore current distribution based on the power law of wave height decay in the surf zone developed in Chapter II. The model is intended to be an engineering tool for predicting longshore currents and for studying relationships between physical factors generating the currents. The momentum balance in the longshore direction is the basis for the model, but many simplifying assumptions are made in order to provide a solution in a form for practical use. The model may be viewed as an extension of the model of Longuet-Higgins (1970a, 1970b). The effect of incident wave angles is included in the form presented by Kraus and Sasaki (1978a, 1978b), but truncated at second order to allow easier application. The longshore current model is compared to laboratory data and to the Longuet-Higgins model.

Assumptions

The assumptions used in the derivation of the longshore current model are listed in Table 1-2. These assumptions simplify the mathematical development, so an analytical solution becomes possible. Similar assumptions have been made in most previous longshore current models, including numerical models. The assumptions picture a highly oversimplified environment, somewhat removed from the real world. The longshore current is never completely steady (see, e.g., Meadows 1977), in contrast to the steady state assumption. The longshore current varies significantly over time periods as short as 5 minutes. The longshore current is also assumed to be homogeneous in the longshore direction. Harris (1969) describes this as an "alongshore system" as opposed to a cellular system with the longshore current feeding rip currents. Harris notes that alongshore systems occurred in only 10 percent of his field observations performed on the Natal coast of South Africa. In laboratory wave basins, more conditions can be controlled (e.g., the wave field and the beach slope), but the lateral boundary condition of a homogenous

current in the longshore direction is difficult to achieve. If proper care is not taken, a large circulation cell will tend to form in a wave basin. Although the assumptions made are restrictive, the trends observed in the model are expected to be applicable to more complex situations. If a cellular system is present, a circulation model (e.g., Keeley and Bowen 1977) should be used. The model presented in this report predicts the depth-averaged longshore current distribution. This level of sophistication is consistent with most available measurements of the longshore current.

Equations of Motion

The equations of motion are statements of Newton's Second Law, conservation of momentum. The equations of motion for the depth-averaged, steady flow that must be satisfied are

$$u \partial u / \partial x + v \partial u / \partial y - f_c v = -g (h + \bar{\eta}) \partial \bar{\eta} / \partial x + (1/\rho) \Sigma \text{ stresses}_x \quad (3-1)$$

for the x-direction (shore normal) and

$$u \partial v / \partial x + v \partial v / \partial y + f_c u = -g (h + \bar{\eta}) \partial \bar{\eta} / \partial y + (1/\rho) \Sigma \text{ stresses}_y \quad (3-2)$$

for the y-direction (shore parallel), where u is the mean current speed in the x-direction, v is the mean current speed in the y-direction, f_c is the Coriolis parameter, g is the gravitational acceleration, and $\bar{\eta}$ is the mean setup (Figure 3-1). A derivation of the equations of motion is found in Dean and Dalrymple (1984). The continuity equation,

$$\partial / \partial x [u(\bar{\eta} + h)] + \partial / \partial y [v(\bar{\eta} + h)] = 0 \quad (3-3)$$

expressing conservation of mass, must also be satisfied. All y-derivatives are zero because of the assumption of homogeneity in the y-direction and, applying the continuity equation (Equation 3-3), $u=0$. The Coriolis force is

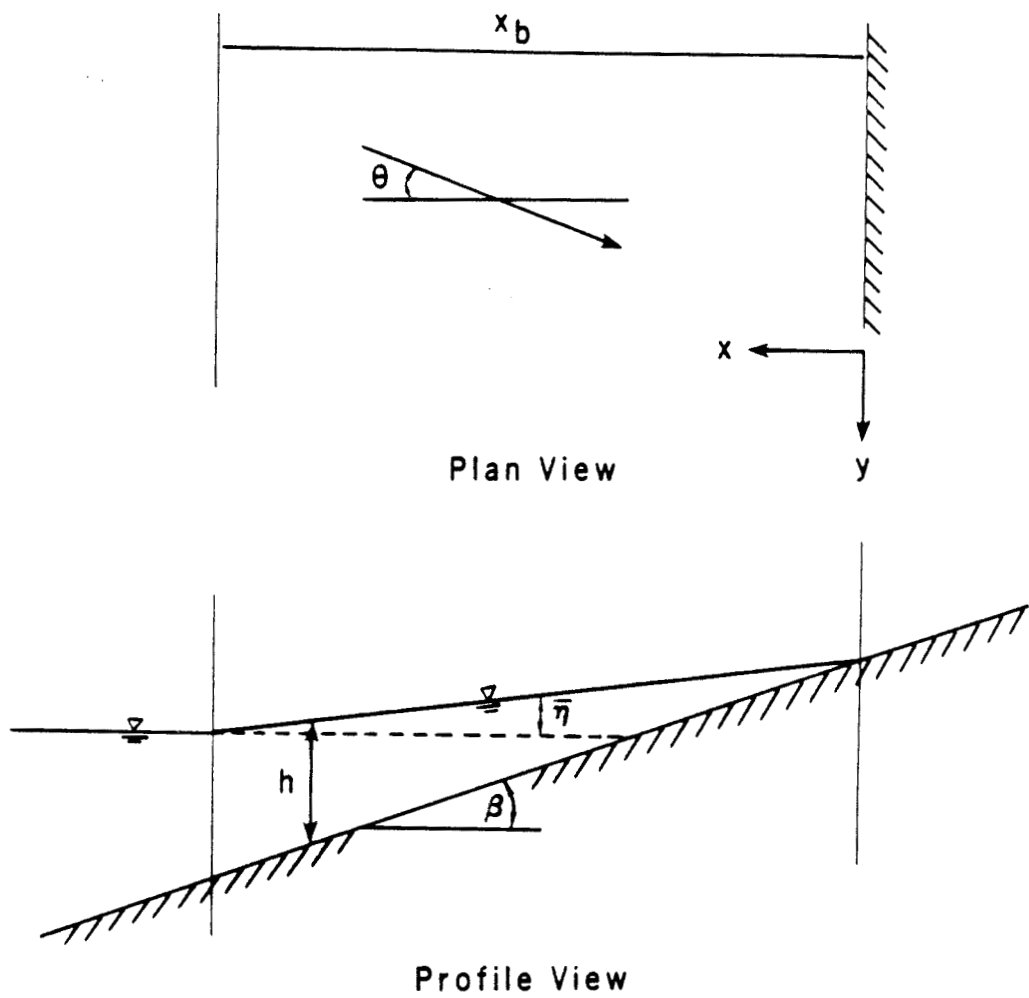


Figure 3-1. Definition sketch for momentum balance

neglected. Equations 3-1 and 3-2 simplify to

$$0 = -g (h + \bar{\eta}) \partial \bar{\eta} / \partial x + (1/\rho) \Sigma \text{ stresses}_x \quad (3-4)$$

and

$$0 = \Sigma \text{ stresses}_y \quad (3-5)$$

Equation 3-4 (x-momentum) is used in Chapter IV to derive the wave setup.

Equation 3-5 is expanded to derive the longshore current distribution.

The stresses referred to in Equation 3-5 are the local wave stress, τ_y , the wind stress, τ_{wy} , the stress due to lateral mixing, B_L , and the frictional stress on the bottom, $\langle B_y \rangle$. Equation 3-5 becomes

$$-\tau_y - \tau_{wy} = B_L - \langle B_y \rangle \quad (3-6)$$

The wind stress is not included in the general derivation, but it is discussed later in this chapter.

Local Wave Stress

The local wave stress is the longshore force exerted on the nearshore water mass by the incoming waves, and it is typically assumed to be the only driving force of the longshore current. The local wave stress is calculated using the concept of radiation stress developed by Longuet-Higgins and Stewart (1962, 1963, 1964). Longuet-Higgins and Stewart define radiation stress as the excess flow of momentum due to the presence of waves. The flux of y-momentum parallel to the shore across a plane $x=\text{constant}$ is

$$S_{xy} = F_x (\sin \theta / C) \quad (3-7)$$

where S_{xy} represents the radiation stress component which is the excess flux

of x-directed momentum in the y-direction. F_x is the energy flux in the x-direction per unit distance alongshore, C is the wave celerity, and θ is the local wave angle. By Snell's law, $(\sin\theta/C)$ is a constant and is therefore equal to the same ratio at breaking. Equation 3-7 can then be written as

$$S_{xy} = F_x (\sin\theta_b/C_b) \quad (3-8)$$

Applying linear wave theory, the x-directed energy flux is

$$F_x = E C_g \cos\theta \quad (3-9)$$

where C_g is the local group celerity of the waves, and E is the local energy density per unit surface area. The energy density is

$$E = 1/8 \rho g H^2 \quad (3-10)$$

If waves do not lose energy (by wave breaking or bottom friction), the energy flux is constant, but in the surf zone, wave energy is certainly lost. The wave energy decays through the surf zone, and it is zero at approximately the shoreline. The rate of energy dissipation, D , is

$$\partial F_x / \partial x = -D \quad (3-11)$$

The net stress per unit area exerted by the waves on the water in the surf zone is

$$\tau_y = - \partial S_{xy} / \partial x \quad (3-12)$$

and from Equations 3-7, 3-11, and 3-12,

$$\begin{aligned} \tau_y &= - \partial / \partial x (F_x) (\sin\theta_b/C_b) \\ &= D (\sin\theta_b/C_b) \end{aligned} \quad (3-13)$$

The local wave stress is proportional to the rate of energy dissipation. Therefore, outside the surf zone, where energy loss is small (minimal wave breaking; weak bottom orbital velocities, producing little bottom friction) the wave stress is considered zero. Inside the surf zone, energy loss by wave breaking is dominant, and bottom friction is also believed to be significant.

To this point, the derivation is not original, but has followed that of Longuet-Higgins (1970a, 1970b). Next, the wave height decay power law is incorporated by applying Equation 2-4 to describe the broken wave height in the surf zone. The local wave energy (Equation 3-10) becomes

$$E = 1/8 \rho g [\gamma h_b (h/h_b)^n]^2 \quad (3-14)$$

and the energy flux (Equation 3-9) becomes

$$F_x = 1/8 \rho g [\gamma h_b (h/h_b)^n]^2 C_g \cos \theta \quad (3-15)$$

In shallow water, the wave group celerity and the wave celerity are equal and expressed as

$$C_g = C = (g h)^{1/2} \quad (3-16)$$

by linear shallow-water wave theory. Using Equation 3-16, Equation 3-15 reduces to

$$F_x = 1/8 \rho g^{3/2} \gamma^2 h^{(2n+1/2)} / (h_b)^{(2n-2)} \cos \theta \quad (3-17)$$

Wave setup is accounted for inside the surf zone by altering the beach slope, $\tan \beta$, as suggested by Longuet-Higgins (1970a)

$$- dh/dx = \tan \beta^* = \tan \beta / (1 + 3/8 \gamma^2) \quad (3-18)$$

The wave setup is assumed to be a linear function of water depth by applying Equation 3-18.

The derivative of the energy flux in the x-direction is computed as an intermediate step to calculating the local wave stress. From Equation 3-17 and Equation 3-18

$$\partial F_x / \partial x = -\tan\beta^* \partial F_x / \partial h \quad (3-19)$$

$$= -\tan\beta^* \frac{1}{8} \rho g^{3/2} \gamma^2 / (h_b)^{(2n-2)} \partial / \partial h (h^{(2n+1/2)} \cos\theta)$$

The local driving wave stress inside the surf zone follows directly from Equation 3-19 substituted in to Equation 3-13, and the wave stress outside the surf zone, where D is negligible, is zero

$$\tau_y = \begin{cases} \tan\beta^* \frac{1}{8} \rho g^{3/2} \gamma^2 / (h_b)^{(2n-2)} \partial / \partial h (h^{(2n+1/2)} \cos\theta) & x < x_b \\ 0 & x > x_b \end{cases} \quad (3-20)$$

$(\sin\theta_b / C_b)$

Lateral Mixing Stress

The lateral mixing stress is the exchange of momentum caused by horizontal turbulent eddies. A review of the influence of lateral mixing in longshore current modeling was recently made by McDougal and Hudspeth (1986). Neglect of lateral mixing predicts an unrealistic discontinuity in the longshore current profile at the breaker line. The lateral mixing stress employed is of the form used by Longuet-Higgins (1970b)

$$B_L = \partial / \partial x (\rho \epsilon_L h \partial v / \partial x) \quad (3-21)$$

where ϵ_L is the lateral viscosity coefficient defined as the product of a representative mixing length and velocity. The lateral viscosity coefficient used is from Madsen et al. (1978). The representative mixing length used is the distance to the mean shoreline, and the representative velocity is the maximum orbital velocity, $U_{o\max}$,

$$\epsilon_L = \Gamma \times U_{o\max} \quad (3-22)$$

where Γ is a constant. The maximum orbital velocity is

$$\begin{aligned} U_{o_{\max}} &= H C / (2h) \\ &= H g^{1/2} / (2 h^{1/2}) \end{aligned} \quad (3-23)$$

by linear shallow-water wave theory. Applying Equation 3-23 and the power law expression for the broken wave height in the surf zone, Equation 3-22 becomes

$$\epsilon_L = \Gamma x g^{1/2} / 2 \begin{cases} \gamma h^{(n-1/2)} / (h_b)^{n-1} & x < x_b \\ H/h^{1/2} & x > x_b \end{cases} \quad (3-24)$$

The expression for the lateral mixing stress in the surf zone from Equation 3-21 and 3-24 becomes

$$B_L = \begin{cases} \partial/\partial x (\rho \Gamma x g^{1/2} / 2 \gamma h^{(n+1/2)} / (h_b)^{(n-1)} \partial v / \partial x) & x < x_b \\ \partial/\partial x (\rho \Gamma x g^{1/2} / 2 H h^{1/2} \partial v / \partial x) & x > x_b \end{cases} \quad (3-25)$$

Bottom Friction Stress

The bottom friction stress resists the flow along the bottom. The bottom friction stress is described by

$$\vec{B} = c_f \rho |\vec{U}| \vec{U} \quad (3-26)$$

where, c_f is the friction coefficient and \vec{U} is the total velocity, composed of the wave orbital velocity, \vec{U}_o , and the longshore current velocity. The total velocity for a longshore current system is

$$\vec{U} = \vec{U}_0 + (0, v) \quad (3-27)$$

where the notation $(0, v)$ is used to denote the x and y -components of the steady current. The arrows indicate vector quantities. The absolute value of the bottom velocity is

$$|\vec{U}| = (\vec{U}_0^2 + 2 \vec{U}_0 (0, v) + v^2)^{1/2} \quad (3-28)$$

Applying the assumption that v is much smaller than $|\vec{U}|$ and expanding Equation 2-28 with a truncated binomial series (retaining only first order terms), yields

$$|\vec{U}| = |\vec{U}_0| + \vec{U}_0 v / |\vec{U}_0| \quad (3-29)$$

The y -component of $|\vec{U}| \vec{U}$ is

$$\begin{aligned} (|\vec{U}| \vec{U})_y &= [|\vec{U}_0| + (\vec{U}_0 \sin \theta v) / |\vec{U}_0|] (\vec{U}_0 \sin \theta + v) \\ &= |\vec{U}_0| \vec{U}_0 \sin \theta + v |\vec{U}_0| + \vec{U}_0^2 \sin^2 \theta v / |\vec{U}_0| \\ &\quad + v^2 \vec{U}_0 \sin \theta / |\vec{U}_0| \end{aligned} \quad (3-30)$$

Since the time average of the bottom friction is required to compute the mean longshore current, linear terms of U_0 do not contribute and can be dropped,

$$(|\vec{U}| \vec{U})_y = |\vec{U}_0| v (1 + \sin^2 \theta) \quad (3-31)$$

The resulting y -component of the bottom stress is

$$B_y = c_f \rho |\vec{U}_0| v (1 + \sin^2 \theta)^2 \quad (3-32)$$

The time average of the orbital velocity is

$$\langle U_o \rangle = (2/\pi) U_{o_{\max}} \quad (3-33)$$

where $U_{o_{\max}}$ is given in Equation 3-23. Equation 3-32 simplifies to

$$\langle B_y \rangle = c_f / \pi \rho v \begin{cases} \gamma g^{1/2} h^{(n-1/2)} / (h_b)^{(n-1)} (1 + \sin^2 \theta) & x < x_b \\ g^{1/2} H / h^{1/2} (1 + \sin^2 \theta) & x > x_b \end{cases} \quad (3-34)$$

Longshore Current Velocity

Special case: small incident wave angle. Further simplifications can be made by assuming the angle of wave incidence is small. The small-angle assumption also facilitates comparison between the present model and the model of Longuet-Higgins, since Longuet-Higgins assumes the wave angle is small.

For this special case, $\cos \theta$ is approximately equal to unity and $\sin \theta$ is approximately equal to zero. Substituting the longshore stresses applicable to the surf zone (Equations 3-20, 3-25, and 3-34) into the stress balance (Equation 3-6) gives

$$\begin{aligned} - \tan \beta^* (4n+1)/16 \rho g^{3/2} \gamma^2 h^{(2n-1/2)} / (h_b)^{(2n-2)} \sin \theta_b / C_b = \\ + \partial/\partial x (\rho \gamma \gamma x g^{1/2} / 2 h^{(n+1/2)} / (h_b)^{(n-1)} \partial v / \partial x) \\ - c_f / \pi \rho v \gamma g^{1/2} h^{(n-1/2)} / (h_b)^{n-1} \end{aligned} \quad (3-35)$$

Applying the plane beach assumption ($h = \tan \beta^* x$), and simplifying, Equation 3-35 becomes

$$- \tan \beta^* (4n+1)/16 g^{1/2} \gamma x^{(2n-1/2)} h_b^{1/2} / (x_b)^n \sin \theta_b = \quad (3-36)$$

$\Gamma/2 \tan\beta^* \partial/\partial x (x^{(n+3/2)} \partial v/\partial x) - 1/\pi c_f v x^{(n-1/2)}$
Nondimensionalizing x , letting $X = x/x_b$, results in

$$- \tan\beta^* (4n+1)/16 g^{1/2} \gamma (h_b)^{1/2} X^{(2n-1/2)} \sin\theta_b = \quad (3-37)$$

$$\Gamma/2 \tan\beta^* \partial/\partial X (X^{(n+3/2)} \partial v/\partial X) - 1/\pi c_f v X^{(n-1/2)}$$

If the lateral mixing term is neglected, the first term to the right of the equal sign in Equation 3-37 is zero, and the longshore current speed is solved for directly

$$v = \pi/c_f \tan\beta^* (4n+1)/16 g^{1/2} (h_b)^{1/2} \gamma X^n \sin\theta_b \quad (3-38)$$

The velocity at the breaker line ($X = 1$) for $n = 1$, neglecting lateral mixing, is defined as v_0

$$v_0 = \frac{5\pi}{16} \frac{\tan\beta^*}{c_f} \gamma (gh_b)^{1/2} \sin\theta_b \quad (3-39)$$

following Longuet-Higgins (1970a). The value of v_0 is the maximum possible current speed for $n = 1$. As n varies, the maximum current speed is given by

$$v_{\max} = (4n + 1)/5 v_0 \quad (3-40)$$

Nondimensionalizing the current speed v by v_0 , $V = v/v_0$, simplifies Equation 3-37 to

$$-(4n+1)/5 X^{(2n-1/2)} = P \partial/\partial X (X^{(n+3/2)} \partial V/\partial X) - V X^{(n-1/2)} \quad (3-41)$$

where

$$P = (\Gamma\pi)/(2 c_f) \tan\beta^* \quad (3-42)$$

The parameter P is nondimensional, and it expresses the relative importance of lateral mixing (Γ) and bottom friction (c_f).

Calculating the derivative in Equation 3-41 and rearranging the terms gives

$$P X^2 V'' + P (n+3/2) X V' - V = -(4n+1)/5 X^n \quad (3-43)$$

where the primes denote derivatives with respect to X. Equation 3-43 is a nonhomogeneous second-order differential equation solved by the method of variation of parameters. The solution to the differential equation is

$$V = B X^p + A X^n \quad (3-44)$$

where

$$A = (4n+1)/5 [1/(1 - n P (2n+1/2))]$$

$$p = -(2n+1)/4 + [((2n+1)^2/16) + 1/P]^{1/2}$$

Substituting the longshore stresses applicable outside the surf zone (Equations 3-20, 3-25, and 3-34) into the stress balance equation (Equation 3-6) yields

$$\begin{aligned} 0 = \partial/\partial x (\rho \Gamma x g^{1/2}/2 H h^{1/2} \partial v/\partial x) \\ - c_f/\pi \rho v g^{1/2} H/h^{1/2} (1+\sin^2 \theta) \end{aligned} \quad (3-45)$$

Outside the surf zone the wave height is approximated by linear shallow-water wave theory (Green's Law) as

$$H = (\cos \theta / \cos \theta_b)^{1/2} (h_b/h)^{1/4} H_b \quad (3-46)$$

Applying the small angle assumption and noting $H_b = \gamma h_b$, Equation 3-45 simplifies to

$$H = \gamma h_b^{5/4} / h^{1/4} \quad (3-47)$$

Applying the small angle assumption, the plane beach assumption, and Equation 3-47, Equation 3-45 simplifies to

$$0 = Q \partial/\partial x (x^{5/4} \partial v/\partial x) - v/x^{3/4} \quad (3-48)$$

or in nondimensional form

$$0 = Q \partial/\partial X (X^{5/4} \partial V/\partial X) - V/X^{3/4} \quad (3-49)$$

where

$$Q = \Gamma\pi/(2 c_f) \tan\theta$$

The parameter Q is used instead of P seaward of the breaker line because the effect of wave setup is negligible in this region. Calculating the derivative in Equation 3-49 and rearranging the terms gives

$$x^2 v'' + 5/4 x v' - v/Q = 0 \quad (3-50)$$

Equation 3-50 is a homogeneous second-order differential equation with the solution

$$v = C x^q \quad (3-51)$$

where $q = -1/8 - (1/64 + 1/Q)^{1/2}$

The quantities B from Equation 3-44 and C from Equation 3-51 were obtained by equating the current and the derivative of the current inside and outside the surf zone at the breaker line. The general solution for the longshore current distribution assuming a small incident wave angle is

$$V = \begin{cases} B X^p + A X^n & X < 1 \\ C X^q & X > 1 \end{cases} \quad (3-52)$$

where $A = (4n+1)/5 [1/(1 - n P (2n+1/2))]$

$$p = -(2n+1)/4 + [(2n+1)^2/16 + 1/Q]^{1/2}$$

$$q = -1/8 - (1/64 + 1/P)^{1/2}$$

$$B = (q-n)/(p-q) A$$

$$C = (p-n)/(p-q) A$$

Combinations of n and P that satisfy the relation

$$n = -1/8 \pm (1/64 + 1/(2P))^{1/2} \quad (3-53)$$

cause the solution for A in Equation 3-49 to become indefinite. For these special cases, particular solutions to Equation 3-42 must be calculated. For example, with $n = 1.5$ and $P = 4/21$, the solution is

$$V = -(147/100) [X^{3/2} \ln X - X^{3/2}/5] \quad (3-54)$$

Next, the more general case without the small angle assumption is considered.

General case: wave angle not necessarily small. On gently sloping beaches, the wave angle at breaking is usually small due to wave refraction, but this is not always the case. Liu and Dalrymple (1978) and Kraus and Sasaki (1979a) show that the breaking wave angle has a significant effect on the magnitude of the longshore current and the shape of the current distribution. The method of Kraus and Sasaki is followed to include the effect of wave angles on the longshore current distribution.

By Snell's law and Equation 3-16

$$\begin{aligned}\sin\theta &= C/C_b \sin\theta_b \\ &= (h/h_b)^{1/2} \sin\theta_b\end{aligned}\quad (3-55)$$

Using a trigonometric identity, the cosine of the wave angle may be written as

$$\cos\theta = (1 - (h/h_b) \sin^2\theta_b)^{1/2} \quad (3-56)$$

Equations 3-55 and 3-56 express the sine and cosine of the local wave angle in terms of water depth and constants.

Using Equation 3-56, the local wave stress in the surf zone, Equation 3-20, becomes

$$\begin{aligned}\tau_y &= \tan\beta^* 1/8 \rho g^{3/2} \gamma^2 / (h_b)^{(2n-2)} \sin\theta_b / C_b \\ &\quad \partial/\partial h (h^{(2n+1/2)} (1 - (h/h_b) \sin^2\theta_b)^{1/2})\end{aligned}\quad (3-57)$$

Taking the derivative and simplifying, Equation 3-57 becomes

$$\begin{aligned}\tau_y &= \rho g \gamma^2 \tan\beta^* / 16 \sin\theta_b h^{(2n-1/2)} / (h_b)^{(2n-3/2)} \\ &\quad [(4n+1) (1 - (h/h_b) \sin^2\theta_b)^{1/2} - (h/h_b) \sin^2\theta_b / (1 - (h/h_b) \sin^2\theta_b)^{1/2}]\end{aligned}\quad (3-58)$$

The expression for the local wave stress outside the surf zone remains the same. The lateral mixing stress was unaffected by the small angle assumption, therefore Equation 3-25 is still valid. The bottom friction stress (Equation 3-34) becomes

$$\langle B_y \rangle = c_f / \pi \rho v \begin{cases} \gamma g^{1/2} h^{(n-1/2)} / (h_b)^{(n-1)} (1 + (h/h_b) \sin^2\theta_b) & x < x_b \\ g^{1/2} H/h^{1/2} (1 + (h/h_b) \sin^2\theta_b) & x > x_b \end{cases} \quad (3-59)$$

The stress balance inside the breaker line from Equations 3-57, 3-25, and 3-34 is

$$\begin{aligned}
 & -\rho g \gamma^2 \tan \beta^* / 16 \sin \theta_b h^{(2n-1/2)} / (h_b)^{(2n-3/2)} \\
 & [(4n+1)(1-(h/h_b) \sin^2 \theta_b)^{1/2} - \\
 & (h/h_b) \sin^2 \theta_b / (1-(h/h_b) \sin^2 \theta_b)^{1/2}] = \\
 & \rho \Gamma / 2 \gamma g^{1/2} / (h_b)^{(n-1)} \partial / \partial x (x h^{(n+1/2)} \partial v / \partial x) - \\
 & c_f / \pi \rho g^{1/2} v \gamma h^{(n-1/2)} / (h_b)^{(n-1)} (1 + X \sin^2 \theta_b)
 \end{aligned} \tag{3-60}$$

Equation 3-60 is nondimensionalized and simplified, resulting in

$$\begin{aligned}
 & P \partial / \partial X (X^{(n+3/2)} \partial v / \partial X) - v X^{(n-1/2)} (1 + X \sin^2 \theta_b) = \\
 & -(4n+1)/5 X^{(2n-1/2)} [(1 - X \sin^2 \theta_b)^{1/2} - X / (4n+1) \sin^2 \theta_b / (1 - X \sin^2 \theta_b)^{1/2}]
 \end{aligned} \tag{3-61}$$

Taking the derivative in Equation 3-61 yields

$$\begin{aligned}
 & P (n+3/2) X v' + P X^2 v'' - v (1 + X \sin^2 \theta_b) = \\
 & -(4n+1)/5 X^n [(1 - X \sin^2 \theta_b)^{1/2} - X / (4n+1) \sin^2 \theta_b / (1 - X \sin^2 \theta_b)^{1/2}]
 \end{aligned} \tag{3-62}$$

The quantity in square brackets in Equation 3-62 is approximated by a binomial expansion truncated to second order

$$\begin{aligned}
 & [1 - (4n+3)/(2(4n+1)) X \sin^2 \theta_b - \\
 & (4n+5)/(8(4n+1)) X^2 \sin^4 \theta_b]
 \end{aligned} \tag{3-63}$$

Kraus and Sasaki (1979a, 1979b) obtained a solution to Equation 3-62 in the form of an infinite series by retaining all orders of the binomial expansion of the breaking wave angle. Truncation past second order is here considered to be sufficiently accurate and allows a more convenient solution for engineering application. Equation 3-62 then becomes

$$P(n+3/2) X V' + P X^2 V'' - V(1 + X \sin^2 \theta_b) = \quad (3-64)$$

$$-b_1 X^n + b_2 X^{n+1} + b_3 X^{n+2}$$

where

$$b_1 = (4n+1)/5$$

$$b_2 = (4n+3) \sin^2 \theta_b / (10)$$

$$b_3 = (4n+5) \sin^2 \theta_b / (40)$$

Equation 3-64 is a second-order nonhomogeneous differential equation. The solution to Equation 3-64 for the region shoreward of the breaker line is approximated by a power series truncated to second order

$$V = A_0 X^n + A_1 X^{n+1} + A_2 X^{n+2} + B_0 X^p + B_1 X^{p+1} + B_2 X^{p+2} \quad (3-65)$$

where

$$A_0 = [(4n+1)/5] / [1-(n)(2n+0.5)P]$$

$$A_1 = [-(4n+3)\sin^2 \theta_b / 10 - A_0 \sin^2 \theta_b] / [1-(n+1)(2n+1.5)P]$$

$$A_2 = [-(4n+5)\sin^4 \theta_b / 40 - A_1 \sin^2 \theta_b] / [1-(n+2)(2n+2.5)P]$$

$$B_1 = (B_0 \sin^2 \theta_b) / [(p+1)(p+n+1.5)P-1]$$

$$B_2 = (B_1 \sin^2 \theta_b) / [(p+2)(p+n+2.5)P-1]$$

$$p = -(2n+1)/4 + [(2n+1)^2 / 16 + 1/P]^{1/2}$$

The stress balance seaward of the breaker line (Equation 3-44) with the wave height approximated by Green's Law (Equation 3-45) in nondimensional form is

$$Q \partial/\partial X (X^{5/4} \partial V/\partial X) - X^{-3/4} V (1 + X \sin^2 \theta_b) = 0 \quad (3-66)$$

Calculating the derivative in Equation 3-66 and rearranging the terms yields

$$Q X^2 V'' + 5/4 Q X V' - V (1 + X \sin^2 \theta_b) = 0 \quad (3-67)$$

Equation 3-67 is a homogeneous second-order differential equation. The solution of Equation 3-67 is approximated by a power series truncated to second order

$$V = C_0 X^q + C_1 X^{q-1} + C_2 X^{q-2} \quad (3-68)$$

where

$$q = -(1/8) - (1/64 + 1/Q)^{1/2}$$

$$C_1 = C_0 \sin^2 \theta_b / [(q-1)(q-3/4)Q-1]$$

$$C_2 = C_1 \sin^2 \theta_b / [(q-2)(q-7/4)Q-1]$$

Expressions for the coefficients B from Equation 3-65 and C from Equation 3-68 are obtained by equating the current and the derivative of the current inside and outside the surf zone at the breaker line. The general solution for the longshore current distribution truncated to second order in the breaking wave angle is

$$V = \begin{cases} A_0 X^n + A_1 X^{n+1} + A_2 X^{n+2} + B_0 X^p + B_1 X^{p+1} + B_2 X^{p+2} & X < 1 \\ C_0 X^q + C_1 X^{q-1} + C_2 X^{q-2} & X > 1 \end{cases} \quad (3-69)$$

where

$$p = -(2n+1)/4 + [(2n+1)^2/16 + 1/P]^{1/2}$$

$$q = -1/8 - (1/64 + 1/Q)^{1/2}$$

$$A_0 = [(4n+1)/5]/[1-(n)(2n+0.5)P]$$

$$A_1 = [-(4n+3)\sin^2\theta_b/10 - \sin^2\theta_b A_0]/[1-(n+1)(2n+1.5)P]$$

$$A_2 = [-(4n+5)\sin^4\theta_b/40 - \sin^2\theta_b A_1]/[1-(n+2)(2n+2.5)P]$$

$$B_1 = (B_0 \sin^2\theta_b)/[(p+1)(p+n+1.5)P-1]$$

$$B_2 = (B_1 \sin^2\theta_b)/[(p+2)(p+n+2.5)P-1]$$

$$C_1 = C_0 \sin^2\theta_b/[(q-1)(q-3/4)Q-1]$$

$$C_2 = C_1 \sin^2\theta_b/[(q-2)(q-7/4)Q-1]$$

$$P = \Gamma\pi/(2c_f) \tan\delta^*$$

$$Q = \Gamma\pi/(2 c_f) \tan\delta$$

$$B_0 = (S'_A S_C - S_A S'_C)/(S_B S'_C - S'_B S_C)$$

$$C_0 = (S'_A S_B - S_A S'_B)/(S_B S'_C - S'_B S_C)$$

with

$$S_A = A_0 + A_1 + A_2$$

$$S'_A = n A_0 + (n+1) A_1 + (n+2) A_2$$

$$S_B = 1 + b_1 + b_2$$

$$S'_B = p + (p+1) b_1 + (p+2) b_2$$

$$S_C = 1 + c_1 + c_2$$

$$S'_C = q + (q-1) c_1 + (q-2) c_2$$

and

$$b_1 = B_1/B_0$$

$$b_2 = B_2/B_0$$

$$c_1 = C_1/C_0$$

$$c_2 = C_2/C_0$$

Wind Stress

The possibility of adding an additional term to the stress balance to include the effect of wind stress on the water surface was explored. The wind stress in open water is generally taken to be

$$\tau_{wy} = \rho c_D w^2 \sin \phi \quad (3-70)$$

where τ_{wy} is the wind stress in the y-direction, c_D the drag coefficient (Garrett 1977), w is the wind speed, and ϕ is the incident wind direction (Wilson 1960). Birkemeier and Dalrymple (1975) present a nearshore circulation model that includes the effect of wind stress. The analytical solution of the stress balance with the addition of the wind stress as given in Equation 3-70 with lateral mixing neglected is

$$V = (1/(1+X \sin^2 \theta_b)) [(4n+1)/5 X^n ((1-X \sin^2 \theta_b)^{1/2} - 1/(4n+1) X \sin^2 \theta_b / (1-X \sin^2 \theta_b)^{1/2}) + \pi c_D w^2 \sin \phi / (v_o \gamma (gh)_b c_f) (1/X^{(n-1/2)})] \quad (3-71)$$

The solution becomes indefinite near the shoreline. This problem could be overcome by representing the fluid flow and wind stress in the swash zone more accurately. Such a task is beyond the scope of this report.

Discussion of Results

The main points discussed in this section are: a) the effect of the wave height decay power law on the longshore current distribution, b) a comparison of the longshore current model with data, and c) the model limitations.

The longshore current model does not reduce exactly to the model of Longuet-Higgins (1970a, 1970b) for $n = 1$ and small incident wave angle because the form of the lateral viscosity coefficient follows Madsen et al. (1978) instead of Longuet-Higgins. This is not a fundamental difference, and it will not be considered in the discussion.

The effect of the exponent, n , on the longshore current profile is shown in Figure 3-2. Increasing n -values steepen the current profile and increase the distance from the shoreline to the maximum velocity. Therefore, for mild beach slopes and large values of γ the n -value will be large, the current distribution will be more peaked, and the location of the maximum current will be closer to the breaker line. Typical values of n range from 1.0 to 2.0. Figures 3-3 and 3-4 show the effect of varying the P -value. A

small value of P indicates the bottom friction stress dominates the lateral mixing stress, and a large value of P indicates the lateral mixing stress dominates the bottom friction stress. Larger values of P flatten and broaden the current profile. The value of $n = 1$ in Figure 3-3 corresponds to the Longuet-Higgins model. For $n = 1$ and $P = 0$, the current profile is triangular (note the discontinuity at the breaker line as explained earlier for the no-lateral mixing case). In Figure 3-4, for $n = 1.5$ and $P = 0$, the profile is concave upward with the same discontinuity at the breaker line. Figures 3-2, 3-3, and 3-4 are for an approximately zero incident wave angle, implying the higher order wave angle effect was omitted.

The effects associated with increased wave angle are shown in Figure 3-5. The nondimensional current decreases with increasing breaking wave angle. The value of V in Figure 3-5 for an incident breaking wave angle of 30 degrees ($n = 1.0$ and $P = 0.05$) is 30 percent lower than for an incident breaking wave angle of 0 degrees. Also, the location of the maximum current is closer to the shoreline with increasing breaking wave angle.

The longshore current model developed herein was compared to laboratory data from Mizuguchi et al. (1978) and to the model of Longuet-Higgins. A summary of the laboratory data is found in Kraus and Sasaki (1979a). As noted by Kraus and Sasaki, the position of the maximum current velocity varies considerably, and is therefore a good parameter for correlating the current model prediction with the laboratory observations. The position of the maximum velocity is used to determine P , c_f , and Γ , given Y , and θ_0 . The method employed by Kraus and Sasaki to estimate the parameters from the data is used with the additional step to determining n from Y and $\tan\theta$.

Figures 3-6, 3-7, 3-8, and 3-9 illustrate the fit of the longshore current model and the Longuet-Higgins model to the Mizuguchi et al. data. The current velocity is normalized by the maximum velocity. Inside the surf zone, the model fits the data well. Near the shoreline, the effect of the power law decay can be seen in the slightly concave upward shape of the profile. Table 3-1 gives the values of P and c_f calculated by fitting the data. The P and c_f values for the model are slightly higher than for the model of Longuet-Higgins. The results of the present model represent the data

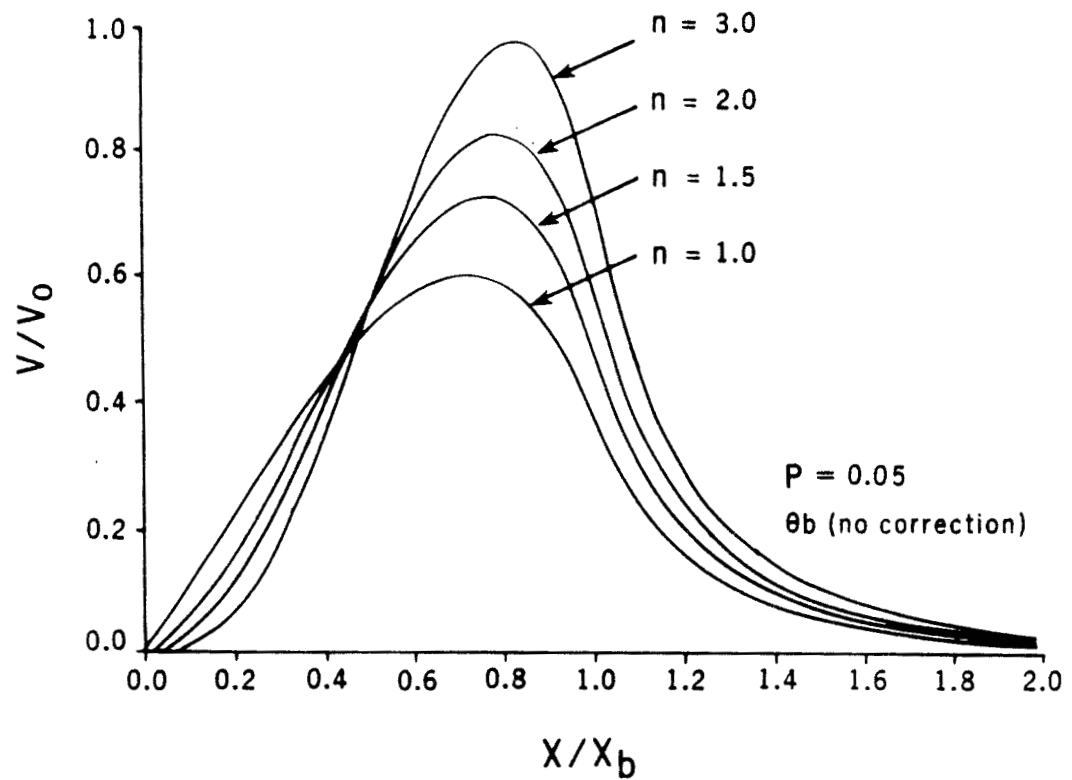


Figure 3-2. Longshore current distribution showing the dependence on the power law exponent ($n=1.0, 1.5, 2.0, 3.0$; $P=0.05$; $\theta_b=0.0^\circ$ implies higher-order wave angle effect was omitted)

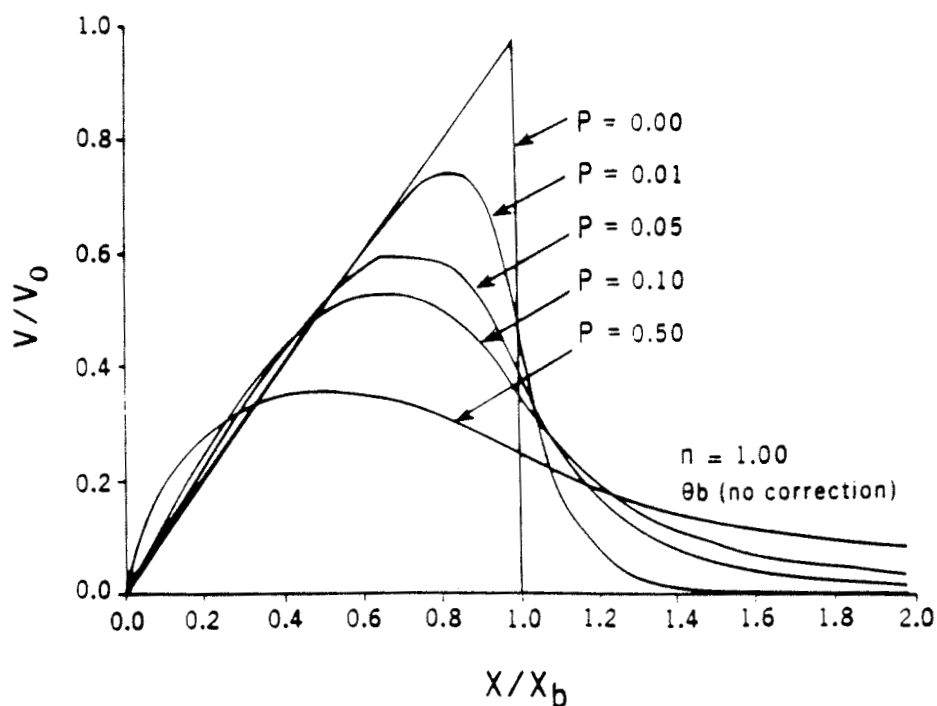


Figure 3-3. Longshore current distribution showing the dependence on the parameter P ($P=0.00, 0.01, 0.05, 0.10, 0.50$; $n=1.0$; $\theta_b=0.0$ implies higher order wave angle effect was omitted)

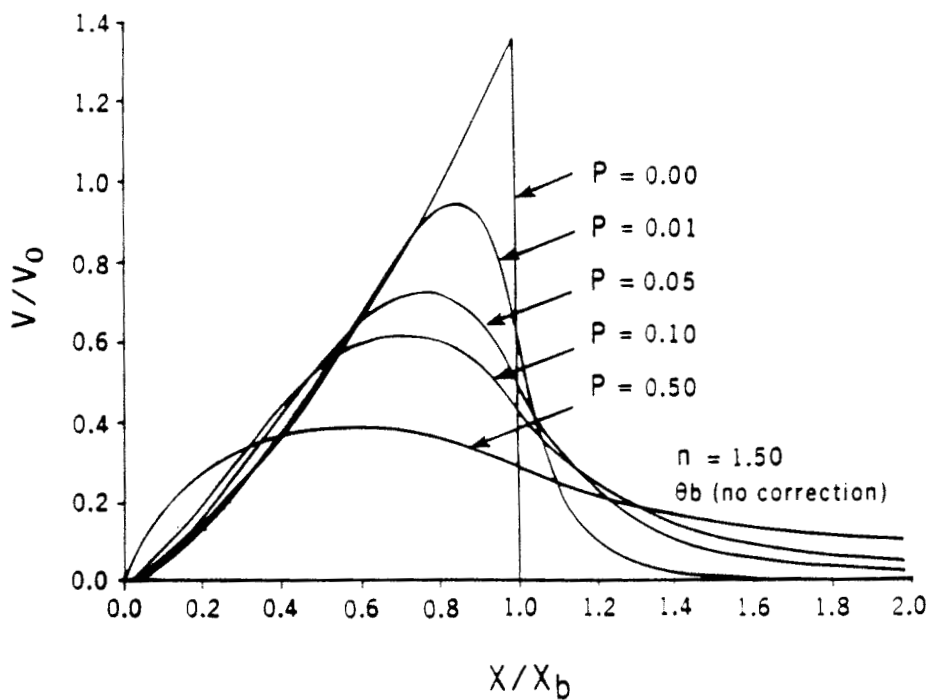


Figure 3-4. Longshore current distribution showing the dependence on the parameter P ($P=0.00, 0.01, 0.05, 0.10, 0.50$; $n=1.5$; $\theta_b=0.0$ implies higher order wave angle effect was omitted)

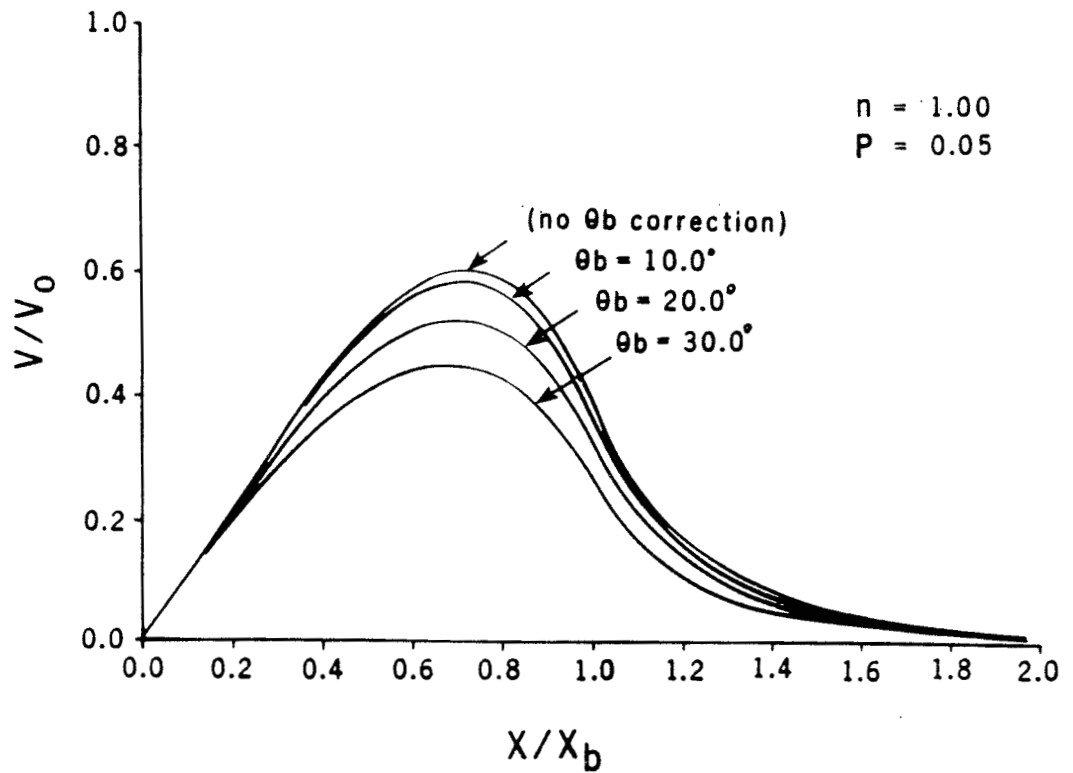


Figure 3-5. Longshore current distribution showing the dependence on the breaking wave angle ($\theta_b = 0.0^\circ$ (no high-order angle effects), 10.0° , 20.0° , 30.0° ; $n = 1.00$, $P = 0.05$)

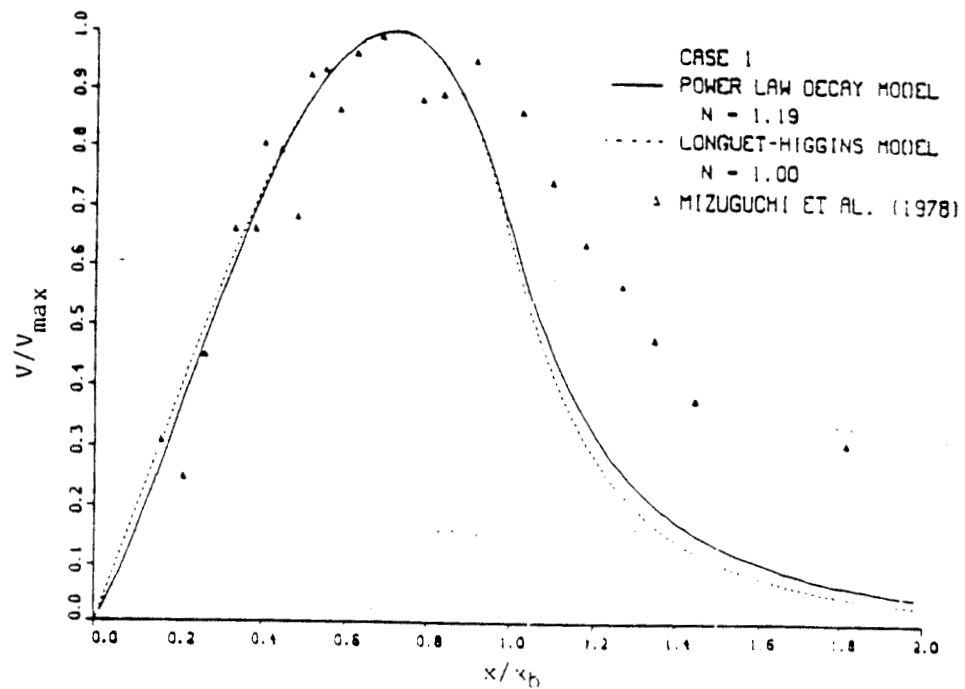


Figure 3-6. Comparison of the longshore current distribution from Case 1 experimental results of Mizuguchi et al. (1978), the present model, and the model of Longuet-Higgins (1970b)

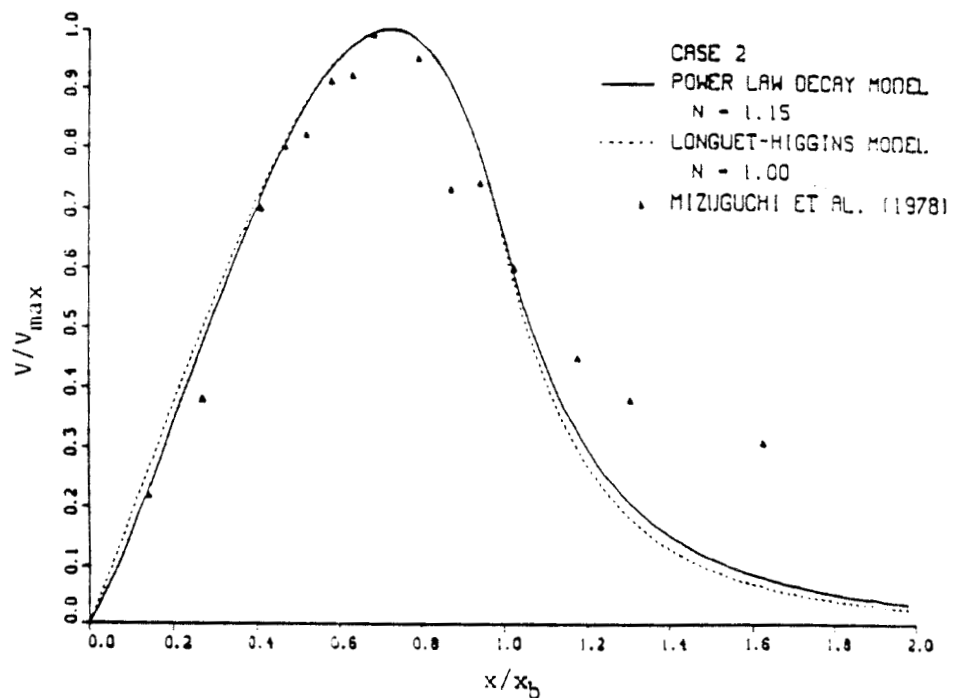


Figure 3-7. Comparison of the longshore current distribution from Case 2 experimental results of Mizuguchi et al. (1978), the present model, and the model of Longuet-Higgins (1970b)

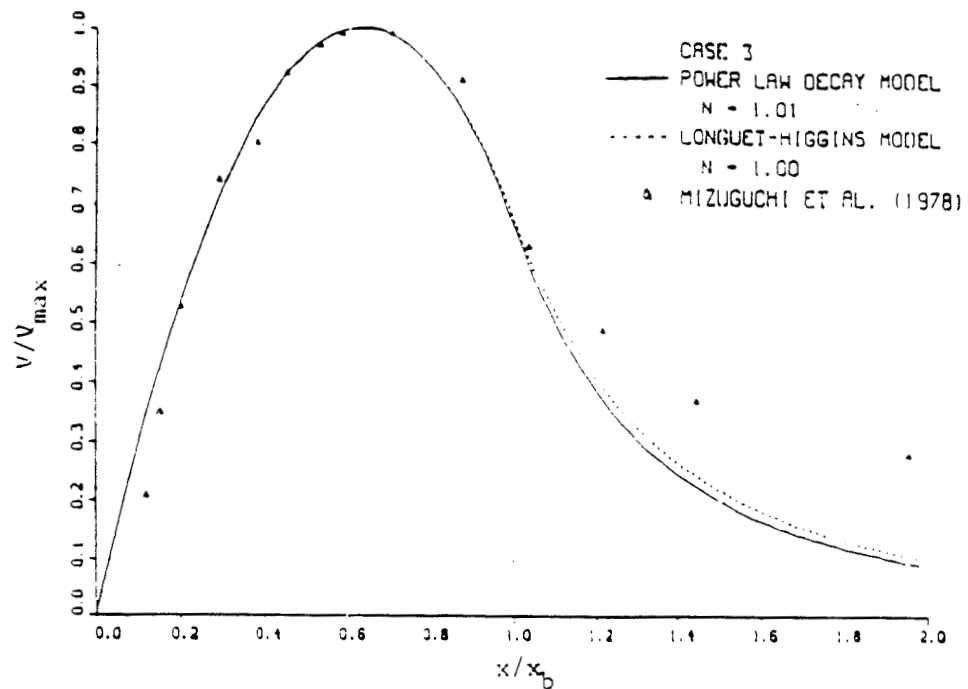


Figure 3-8. Comparison of the longshore current distribution from Case 3 experimental results of Mizuguchi et al. (1978), the present model, and the model of Longuet-Higgins (1970b)

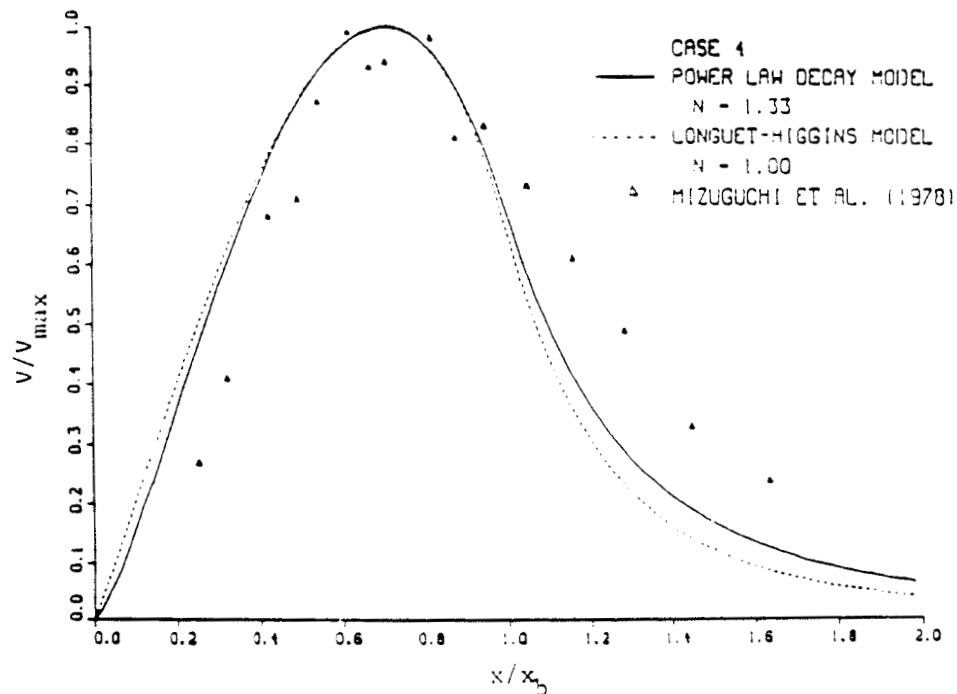


Figure 3-9. Comparison of the longshore current distribution from Case 4 experimental results of Mizuguchi et al. (1978), the present model, and the model of Longuet-Higgins (1970b)

outside the surf zone slightly better than the Longuet-Higgins model, but the departure from the data is still large. The reasons for this difference are not known, but may be due, in part, to the accuracy of measuring the breaker position, the accuracy of measuring low current velocities, and the effect of circulation in the enclosed wave basin.

The data set of Mizuguchi et al. does not rigorously test the current model. The data were collected on a slope of 1/10.4, so the expected values of n are close to 1.0 as shown in Chapter II. An n -value of 1.0 reduces the broken wave height to a linear function of the water depth, and the current model reduces to a truncated version of the model of Kraus and Sasaki, or to

Table 3-1
Mizuguchi et al. (1978) Longshore Current Data

	Case 1	Case 2	Case 3	Case 4
θ_b (deg)	4.5	4.8	15.4	11.4
h_b (cm)	3.8	2.4	4.2	2.5
v_{max} (cm/s)	16.4	15.2	22.0	20.0
X_{max}	0.71	0.72	0.63	0.70
$\tan\beta$	0.064	0.066	0.070	0.060
Y	1.15	1.12	0.99	1.28
$P(LH)$	0.055	0.040	0.15	0.063
P	0.071	0.058	0.14	0.094
$c_f(LH)$	0.013	0.012	0.026	0.021
c_f	0.013	0.012	0.025	0.017
n	1.19	1.15	1.01	1.33

(LH) indicates the value for the Longuet-Higgins model

the model of Longuet-Higgins if the incident wave angle is small. Beaches in the United States consisting of 0.2-mm sand typically have slopes in the range

of 1/40 to 1/70. The n -values for these milder slopes would be greater than 1.0, and the effect of the power law wave height decay on the current profile would be more pronounced.

Table 3-1 illustrates a more subtle point. Earlier work, corresponding to a value of $n = 1$, may require somewhat different values of c_f and P to fit the data. Again, the data of Mizuguchi et al. does not test this point rigorously because the values of n are close to unity.

The application of the longshore current model is limited not only by the assumptions listed in Table 1-2, but also by the truncation of the power series solution to second order. The effect of the truncation increases as the values of θ_b , P , and n increase. The effect of varying these parameters over typical ranges is examined. The value of θ_b is limited to less than approximately 30 degrees because of the truncation of the bottom friction stress. Typical values of P range from 0.01 to 0.10, and typical values of n range from 1.0 to 2.0. For a value of P equal to 0.5 and $\theta_b = 30^\circ$, the maximum difference between the infinite power series solution and the truncated solution is only 6 percent and at $\theta_b = 20^\circ$ the difference reduces to less than 1 percent. Figure 3-5 shows the truncated solution for $n = 1.0$ and $P = 0.05$, and Figure 3-10 shows the infinite series solution. For a P -value of 0.10, the difference between the infinite series and truncated series solutions is 11 percent for $\theta_b = 30^\circ$ and 1 percent for $\theta_b = 20^\circ$. For an n -value of 2.0 ($P = 0.05$) the difference between the infinite series and truncated series solutions are 37 percent for $\theta_b = 30^\circ$ and 4 percent for $\theta_b = 20^\circ$. Figure 3-11 shows the truncated series solution and Figure 3-12 shows the infinite series solution for $n = 2.0$ and $P = 0.05$. In summary, the present model, which is a truncated power series, estimates the infinite power series well for incident breaking wave angles up to approximately 20° . For incident breaking wave angles between 20° and 30° , the model still estimates the infinite series well for relatively small values of P and n , but caution should be used applying the model for large values of P and n .

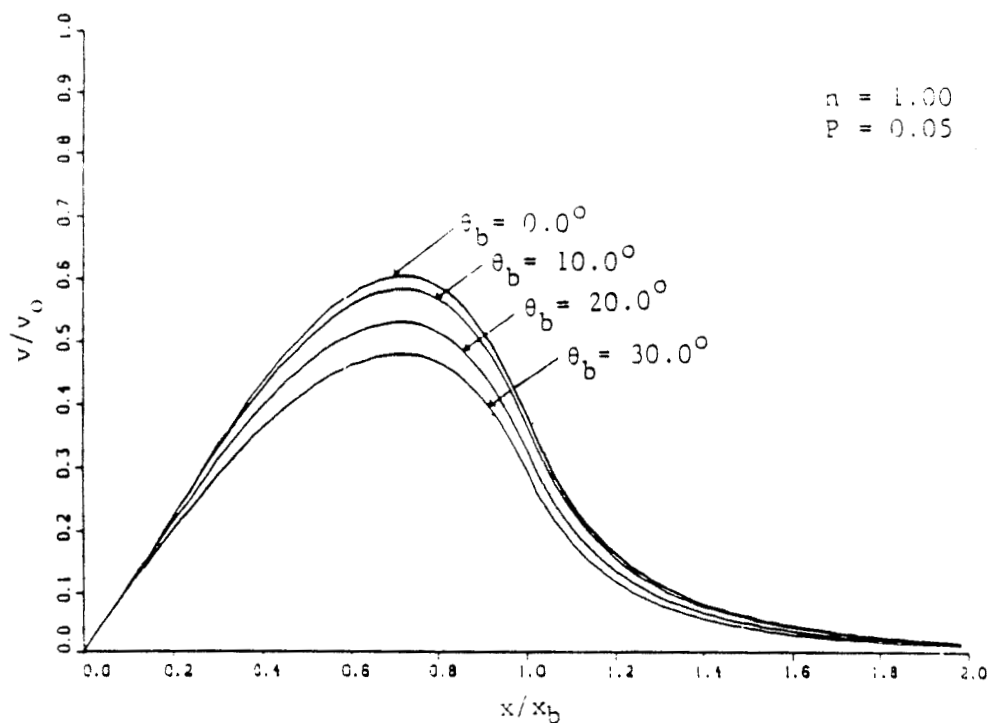


Figure 3-10. Infinite series solution for the longshore current distribution showing the dependence on the breaking wave angle ($\theta_b = 0.0^\circ$ (no high-order angle effect), 10.0° , 20.0° , 30.0° ; $n = 1.00$; $P = 0.05$)

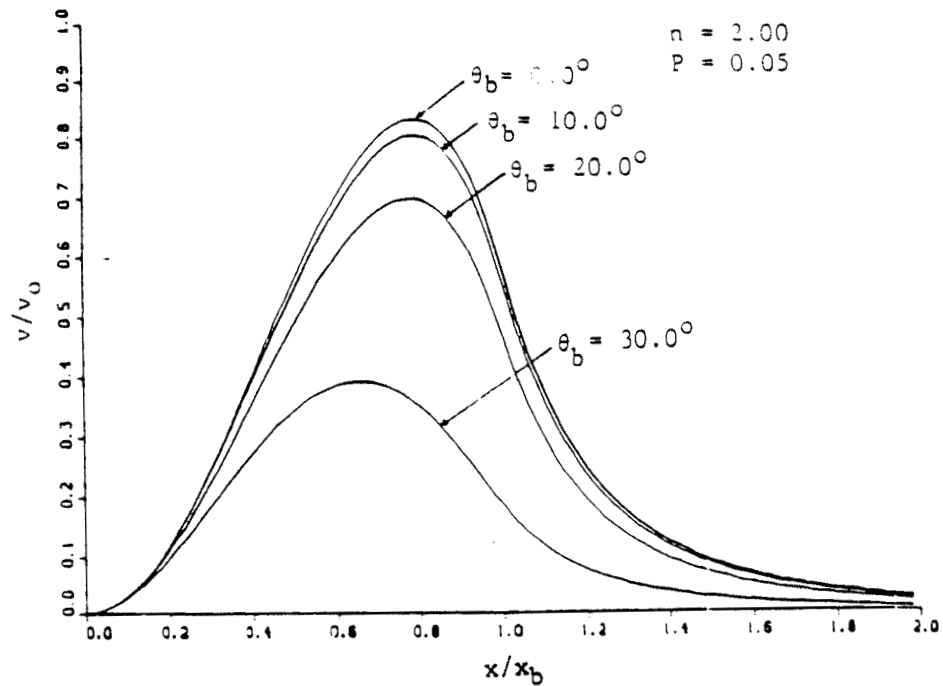


Figure 3-11. Longshore current distribution showing the dependence on the breaking wave angle ($\theta_b = 0.0^\circ$ (no high-order angle effects), 10.0° , 20.0° , 30.0° ; $n=2$; $p=0.05$)

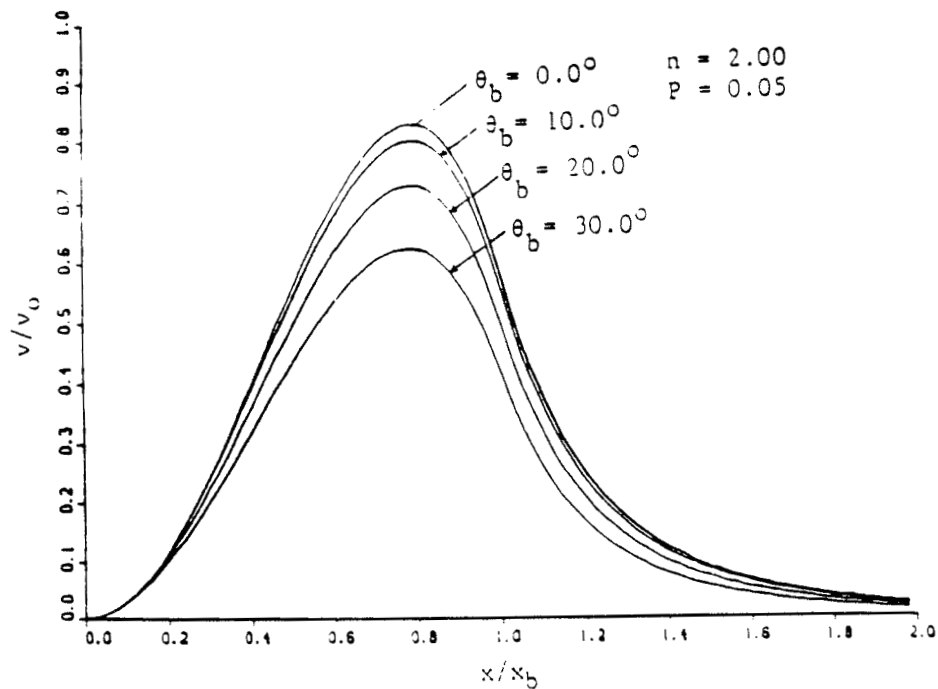


Figure 3-12. Infinite series solution for the longshore current distribution showing the dependence on the breaking wave angle ($\theta_b = 0.0^\circ$ (no high-order angle effects), 10.0° , 20.0° , 30.0° ; $n=2.0$; $P=0.05$)

CHAPTER IV: WAVE SETUP

Wave setup and setdown are the change in the mean water level due to excess momentum in the x-direction. In the surf zone there is normally a setup of the water level, whereas seaward of the breaker line there is a setdown. The wave setup in the longshore current model is approximated by altering the beach slope as given by Equation 3-18. This chapter describes the derivation of the wave setup from the equation of motion in the x-direction (Equation 3-4) based on the power law description of the broken wave height. Although this form of the wave setup is not included in the longshore current model, it is an application of the power law wave height decay.

The equation of motion in the x-direction becomes

$$0 = \rho g (h + \bar{\eta}) \partial \bar{\eta} / \partial x + \partial S_{xx} / \partial x \quad (4-1)$$

with the only x-directed stress being the principle component of the radiation stress, S_{xx} . The quantity $\bar{\eta}$ is the time-mean water surface elevation due to wave-induced momentum. The mean flux of momentum across a plane $x =$ constant is

$$S_{xx} = 3/2 E \quad (4-2)$$

in shallow water (Longuet-Higgins and Stewart 1964). Substituting in the energy density given by Equation 3-10, Equation 4-2 becomes

$$S_{xx} = 3/16 \rho g H^2 \quad (4-3)$$

and the momentum balance (Equation 4-1) expands to

$$0 = \rho g (h + \bar{\eta}) \partial \bar{\eta} / \partial x + \partial / \partial x (3/16 \rho g H^2) \quad (4-4)$$

Shoreward of the breaker line, the power law wave height decay is applied to describe the broken wave height, and Equation 4-4 becomes

$$0 = \rho g (h + \bar{\eta}) \frac{\partial \bar{\eta}}{\partial x} + \frac{3}{16} \rho g \frac{\partial}{\partial x} (\gamma^2 (h_b + \bar{\eta}_b)^2 [(h + \bar{\eta}) / (h_b + \bar{\eta}_b)]^{2n}) \quad (4-5)$$

Calculating the derivative in Equation 4-5 and simplifying, yields

$$0 = (h + \bar{\eta}) \frac{\partial \bar{\eta}}{\partial x} + \frac{3}{16} \gamma^2 / (h_b + \bar{\eta}_b)^{(2n-2)} (2n) (h + \bar{\eta})^{(2n-1)} (\frac{\partial \bar{\eta}}{\partial x} + \frac{\partial h}{\partial x}) \quad (4-6)$$

Rearranging the terms gives

$$\frac{\partial \bar{\eta}}{\partial x} = -1/[1 + K/(h + \bar{\eta})^{(2n-1)}] \frac{\partial h}{\partial x} \quad (4-7)$$

where

$$K = 8(h_b + \bar{\eta}_b)^{(2n-2)} / (3n\gamma^2)$$

Solving for $\bar{\eta}$ by treating $(h + \bar{\eta})$ as a single variable and integrating gives

$$\bar{\eta} = -(h + \bar{\eta})^{(2n-1)} / (K(2n-1)) + C' \quad (4-8)$$

where C' is a constant of integration.

Seaward of the breaker line the energy flux is constant and the setdown is given by

$$\bar{\eta} = -H^2 / (16h) \quad (4-9)$$

in shallow water (Longuet-Higgins and Stewart 1964). This is referred to as "setdown" because it is a depression of the mean water surface. Equating the solutions for $\bar{\eta}$ seaward and shoreward of the breaker line at the breaker line and noting $H_b = \gamma h_b$ yields the solution for the integration constant

$$C' = (\gamma^2 h_b / 16) [(-3n\gamma^2 / 8) + 4n + 1] / (2n - 1) \quad (4-10)$$

The solution of Equation 4-8 becomes

$$\bar{\eta} = - (h + \bar{\eta})^{(2n-1)} / (K(2n - 1)) + (\gamma^2 h_b / 16) [(-3n\gamma^2 / 8) + 4n + 1] / (2n - 1) \quad (4-11)$$

The solution for $\bar{\eta}$ must be found iteratively because Equation 4-11 is implicit. For the special case of $n = 1$ (linear wave height decay), $\bar{\eta}$ can be expressed explicitly

$$\bar{\eta} = (3\gamma^2 / (8 + 3\gamma^2)) (-h + h_b / 16 (-\gamma^2 + 40/3)) \quad (4-12)$$

For this special case the setup is a linear function of the water depth. For values of n greater than one, the profile of the wave setup is concave downward.

Figures 4-1 and 4-2 illustrate the effect of the exponent from the power law wave height decay, n , on the wave setup profile. Figure 4-1 shows the profile of the wave setup calculated from Equation 4-11 ($n = 1.79$) and Equation 4-12 ($n = 1.00$) for the small-scale experimental run of Stive (1985). The setup measured by Stive is also plotted. Figure 4-2 shows the profile of the wave setup calculated from Equation 4-11 ($n = 1.52$) and Equation 4-12 ($n = 1.00$) for the large-scale experimental run of Stive. Again, the setup measured by Stive is also plotted. The n -values used in Equation 4-12 were calculated with Equation 2-8 from the beach slope (1/40) and the measured γ -values.

The setup profiles calculated using both Equation 4-11 and Equation 4-12 overestimate the wave setup, but the calculated setup based on the power law wave height decay represents the data better than the calculated setup based on linear wave height decay. The difference between the two calculated profiles is greatest at the point of maximum setup, which is the critical point in most engineering studies.

In summary, the wave setup is calculated based on the power law expression of the broken wave height developed in Chapter II. For the limited amount of setup data examined, the calculated setup based on the power law wave height decay describes the trend of the measurements better than the calculated setup based on linear wave height decay. Both expressions overestimate the data.

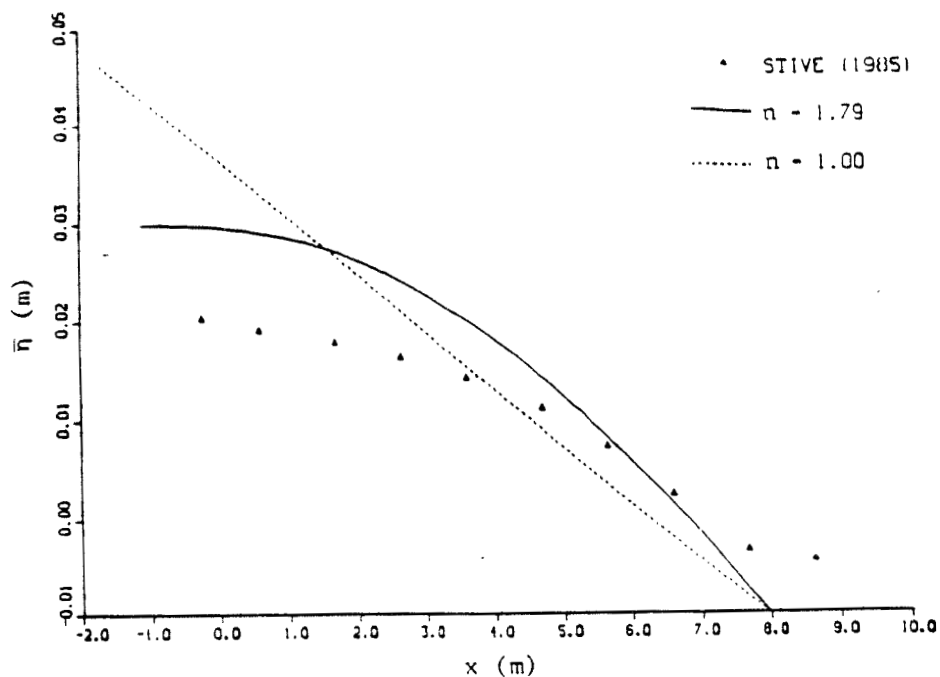


Figure 4-1. Comparison of wave setup from the small scale experimental results of Stive (1985), setup based on the power law wave height decay $n=1.79$), and setup based on linear wave height decay

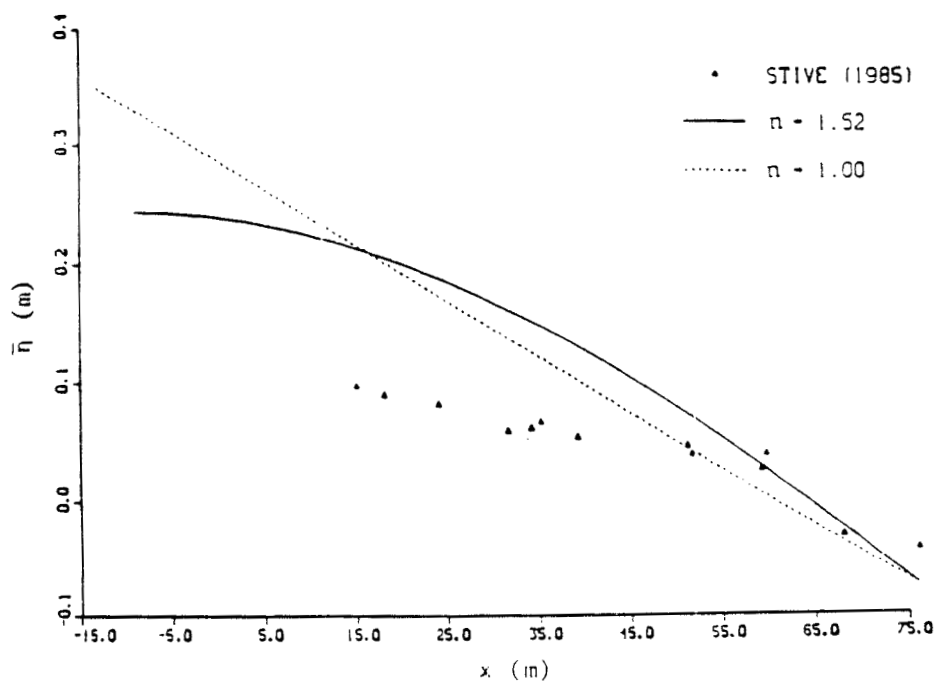


Figure 4-1. Comparison of wave setup from the small scale experimental results of Stive (1985), setup based on the power law wave height decay $n=1.52$), and setup based on linear wave height decay

CHAPTER V: CONCLUSIONS

The purpose of this report was to develop an analytical model of the longshore current based on a power law expression for the broken wave height in the surf zone. The model was intended to be an improvement over present models based on linear wave height decay. For use as an engineering tool, the model was to be as general as possible, including the effect of wave setup, finite wave angle, and lateral mixing.

An empirical power law expression for the broken wave height was developed based on seven independent data sets consisting of 135 experimental runs. The exponent of the power law expression is a function of the beach slope and the ratio of wave height to water depth at wave breaking. From the data, typical values of the exponent range from 1.0 to 2.0. High values of the exponent correspond to mild beach slopes, small ratios of the wave height to water depth at wave breaking, and concave upward wave height profiles. For an exponent equal to 1.0, the broken wave height reduces to a linear function of the water depth. In previous longshore current models, a linear wave height decay was assumed for all beach slopes and breaker height to breaker depth ratios. The power law decay is shown to represent the wave height decay profiles significantly better than linear decay. The power law decay expression also compared favorably to the more complex decay model of Dally et al. (1985a, 1985b). To use the power law expression in a predictive mode, the ratio of wave height to water depth at wave breaking must be estimated. This ratio is best estimated by the expression of Singamsetti and Wind (1980) or the expression of Sunamura (1981).

The longshore current model is based on the momentum balance in the longshore direction. Many simplifying assumptions are made in the model in order to provide a solution in a form for practical use. The driving force of the longshore current is the local wave stress which is calculated using the concept of radiation stress. The lateral mixing stress, caused by horizontal turbulent eddies, redistributes momentum. Flow of water along the bottom is resisted by the bottom friction stress. The derivation of the longshore

current follows the method used by Longuet-Higgins (1970a, 1970b). The effect of incident wave angles is included in the form presented by Kraus and Sasaki (1979a, 1979b). Wave setup is accounted for by altering the beach slope. The longshore current is expressed as a power series in the wave angle truncated to second order. Wind stress is not included in the general solution, although some examination was made of its effect.

The longshore current model was compared to laboratory data from Mizuguchi et al. (1978) and the model of Longuet-Higgins (1970b). The longshore current model represents the data well, although it appears to underestimate the current speed seaward of the breaker line. There is some doubt about the validity of the data, however, for the seaward region. The longshore current model follows the trends of the data slightly better than the Longuet-Higgins model, but the data set is not a rigorous test of the model. The experiment was performed on a steep beach slope, so the expected exponent in the power law decay expression is close to 1.0, reducing the wave height decay to approximately a linear function of water depth. The range of incident wave angles for which the model can be applied is limited by the truncation of the power series solution, but covers the useful range of realistic breaking wave angles.

The mean wave setup and setdown are derived from the momentum balance in the shore normal direction based on the power law wave height decay. The profile of the wave setup is concave downward for an exponent in the power law wave height decay greater than unity, whereas the setup calculated from linear wave height decay is linear. The estimated setup based on the power law wave height decay represents the setup data collected by Stive (1985) better than the estimated setup based on linear wave height decay. Both calculated estimates of setup overestimate the measurements.

The understanding of wave height decay and longshore currents gained from this investigation suggests areas of future study: a) collection of additional longshore current data to verify the longshore current model over the range of typical beach slopes, wave height to water depth ratios at wave breaking, and incident wave angles; b) collection of additional longshore current data to quantify the friction coefficient and the eddy viscosity, so

the model could be better applied in a predictive mode; c) application of the longshore current model to predict the distribution of sediment transport across the surf zone; d) application of the power law wave height decay directly to other wave energy problems in the surf zone (e.g., sediment transport and wave setup); and e) extension to random wave breaking.

REFERENCES

- Basco, D. R. 1982. "Surf Zone Currents," Miscellaneous Report No. 82-7 (I), U. S. Army, Corps of Engineers Coastal Engineering Research Center, Fort Belvoir, VA.
- Basco, D. R., and Coleman, R. A. 1982. "Surf Zone Currents," Miscellaneous Report No. 82-7 (II), U. S. Army, Corps of Engineers Coastal Engineering Research Center, Fort Belvoir, VA.
- Battjes, J. A. 1975. "Surf Similarity," Proceedings of the 14th Coastal Engineering Conference, American Society of Civil Engineers, pp 466-480.
- Battjes, J. A., and Janssen, J. P. F. M. 1979. "Energy Loss and Setup due to Breaking of Random Waves," Proceedings of the 16th Coastal Engineering Conference, American Society of Civil Engineers, pp 569-587.
- Birkemeier, W. A., and Dalrymple, R. A. 1975. "Nearshore Water Circulations Induced by Wind and Waves," Symposium on Modeling Techniques, American Society of Civil Engineers, pp 1062-1081.
- Bowen, A. J. 1969. "The Generation of Longshore Currents on a Plane Beach," Journal of Marine Research, Vol 27, No. 1, pp 206-215.
- Bowen, A. J., Inman, D. L., and Simmons, V. P. 1968. "Wave 'Set-Down' and Setup," Journal of Geophysical Research, Vol 73, No. 8, pp 2569-2577.
- Collins, J. I., and Wier, W. 1969. "Probabilities of Wave Characteristics in the Surf Zone," Tetra Tech Report #TC-149.
- Dally, W. R., Dean, R. G., and Dalrymple, R. A. 1985a. "A Model for Breaker Decay on Beaches," Proceedings of the 19th Coastal Engineering Conference, American Society of Civil Engineers, pp 82-98.
- _____. 1985b. "Wave Height Variation Across Beaches of Arbitrary Profile," Journal of Geophysical Research, Vol 90, No. C6, pp 11917-11927.
- Dean, R. G. 1977. "Equilibrium Beach Profiles: U.S. Atlantic and Gulf Coasts," Ocean Engineering Report 12, Department of Civil Engineering, University of Delaware, Newark, DE.
- Dean, R. G., and Dalrymple, R. A. 1984. Water Wave Mechanics for Engineers and Scientist, 1st ed., Prentice-Hall, Inc., Englewood Cliffs, NJ.
- Divoky, D., Le Mehaute, B., and Lin, A. 1970. "Breaking Waves on Gentle Slopes," Journal of Geophysical Research, Vol 75, No. 9, pp 1681-1692.

- Galvin, C. J. 1967. "Longshore Current Velocity: A Review of Theory and Data," Review of Geophysics, Vol 5, No. 3, pp 287-304.
- _____. 1969. "Breaker Travel and Choice of Design Wave Height," Journal of the Waterways and Harbors Division, American Society of Civil Engineers, Vol 95, No. WW2, pp 175-200.
- Garrett, J. R. 1977. "Review of Drag Coefficients over Oceans and Continents," Monthly Weather Review, Vol 105, pp 915-929.
- Goda, Y. 1970. "A Synthesis of Breaker Indices," Transactions of the Japan Society of Civil Engineers, Vol 2, Part 2, pp 227-230.
- Harris, T. F. W. 1969. "Nearshore Circulations; Field Observations and Experimental Investigations of an Underlying Cause in Wave Tanks," Symposium on Coastal Engineering, Stellenbosch, South Africa.
- Horikawa, K., and Kuo, C. 1967. "A Study on Wave Transformation Inside the Surf Zone," Proceedings of the 10th Coastal Engineering Conference, American Society of Civil Engineers, pp 217-233.
- Hwang, L., and Divoky, D. 1971. "Breaking Wave Setup and Decay on Gentle Slope," Proceedings of the 12th Coastal Engineering Conference, American Society of Civil Engineers, pp 377-389.
- James, I. D. 1974. "A Non-linear Theory of Longshore Currents," Estuarine and Coastal Marine Science, Vol 2, No. 3, pp 235-249.
- Jonsson, I. G. 1967. "Wave Boundary Layers and Friction Factors," Proceedings of the 10th Coastal Engineering Conference, American Society of Civil Engineers, pp 127-148.
- Jonsson, I. G., Skovgaard, O., and Jacobsen, T. S. 1975. "Computation of Longshore Currents," Proceedings of the 14th Coastal Engineering Conference, American Society of Civil Engineers, pp 699-714.
- Keely, J. R., and Bowen, A. J. 1977. "Longshore Variation in Longshore Currents," Canadian Journal of Earth Science, Vol 14, No. 8, pp 1897-1905.
- Kraus, N. C., and Sasaki, T. O. 1979a. "Influence of Wave Angle and Lateral Mixing on the Longshore Current," Marine Science Communications, Vol 5, No. 2, pp 91-126.
- _____. 1979b. "Effects of Wave Angle and Lateral Mixing on the Longshore Current," Coastal Engineering in Japan, Japan Society of Civil Engineers, Vol 22, pp 59-74.
- Kuo, C. T. 1965. "A Study on Wave Transformation After Breaking," unpublished M. S. Thesis, Department of Civil Engineering, University of Tokyo, Tokyo, Japan. (in Japanese)

- Le Mehaute, B. 1963. "On the Nonsaturated Breaker Theory and the Wave Run Up," Proceedings of the 8th Coastal Engineering Conference, American Society of Civil Engineers, pp 77-92.
- Liu, P. L.-F., and Dalrymple, R. 1978. "Bottom Frictional Stresses and Longshore Currents Due to Waves with Large Angles of Incidence," Journal of Marine Research, Vol 36, No. 2, pp 357-375.
- Longuet-Higgins, M. S. 1970a. "Longshore Currents Generated by Obliquely Incident Sea Waves, 1," Journal of Geophysical Research, Vol 75, No. 33, pp 6778-6789.
- _____. 1970b. "Longshore Currents Generated by Obliquely Incident Sea Waves, 2," Journal of Geophysical Research, Vol 75, No. 33, pp 6790-6801.
- Longuet-Higgins, M. S., and Stewart, R. W. 1962. "Radiation Stress and Mass Transport in Gravity Waves, with Application to 'Surf Beats'," Journal of Fluid Mechanics, Vol 13, No. 4, pp 481-504.
- _____. 1963. "A Note on Wave Setup," Journal of Marine Research, Vol 21, No. 1, pp 4-10.
- _____. 1964. "Radiation Stress in Water Waves; A Physical Discussion with Applications," Deep Sea Research, Vol 11, No. 4, pp 529-562.
- Madsen, O. S., Ostendorf, D. W., and Reyman, A. S. 1978. "A Longshore Current Model," Symposium on Technical, Environmental, Socioeconomic, and Regulatory Aspect of Coastal Zone Management Coastal Zone '78, American Society of Civil Engineers, pp 2332-2341.
- Maruyama, K., Sakakiyama, T., Kajima, R., Saito, S., and Shimizu, T. 1983. "Experimental Study on Wave Height and Water Particle Velocity Near the Surf Zone Using a Large Wave Flume," Civil Engineering Laboratory Report No. 382034, The Central Research Institute of Electric Power Industry, Chiba, Japan. (in Japanese)
- McCowan, J. 1891. "On the Solitary Wave," Philosophical Magazine, Journal of Science, London, Edinburgh, Dublin, Vol 32, No. 5.
- McDougal, W. G., and Hudspeth, R. T. 1986. "Influence of Lateral Mixing on Longshore Currents," Ocean Engineering, Vol 13, No. 5, pp 419-433.
- Meadows, G. A. 1977. "Time Dependent Fluctuations in Longshore Currents," Proceedings of the 15th Coastal Engineering Conference, American Society of Civil Engineers, pp 660-680.
- Melville, W. K. 1977. "Wind Stress and Roughness Length Over Breaking Waves," Journal of Physical Oceanography, Vol 7, pp 702-710.

Miller, I., and Freund, J. E. 1977. Probability and Statistics for Engineers, 3d ed., Prentice-Hall, Inc., Englewood Cliffs, NJ.

Mizuguchi, M., Oshima, Y., and Horikawa, K. 1978. "Longshore Currents," Proceedings of the 25th Japanese Conference on Coastal Engineering, Japan Society of Civil Engineers. (in Japanese)

Mizuguchi, M. 1981. "An Heuristic Model of Wave Height Distribution in Surf Zone," Proceedings of the 17th Coastal Engineering Conference, American Society of Civil Engineers, pp 278-289.

Nakamura, M., Shirashi, H., and Sasaki, Y. 1967. "Wave Decaying Due to Breaking," Proceedings of the 10th Coastal Engineering Conference, American Society of Civil Engineers, pp 234-253.

Saeki, H., and Sasaki, M. 1973. "A Study of the Deformation of Waves After Breaking (1)," Proceedings of the 20th Japanese Conference on Coastal Engineering, Japan Society of Civil Engineers, pp 559-564. (in Japanese)

Sasaki, M., and Saeki, H. 1974. "A Study of the Deformation of Waves After Breaking (2)," Proceedings of the 21st Japanese Conference on Coastal Engineering, Japan Society of Civil Engineers, pp 39-44. (in Japanese)

Sawaragi, T., and Iwata, K. 1975. "On Wave Deformation After Breaking," Proceedings of the 14th Coastal Engineering Conference, American Society of Civil Engineering, pp 481-499.

Singamsetti, S. R., and Wind, H. G. 1980. "Characteristics of Breaking and Shoaling Periodic Waves Normally Incident on to Plane Beaches of Constant Slope," Report M1371, Delft Hydraulics Laboratory.

Stive, M. J. F. 1985. "A Scale Comparison of Wave Breaking on a Beach," Coastal Engineering, Vol 9, pp 151-158.

Street, R. L., and Camfield, F. E. 1967. "Observation and Experiments on Solitary Wave Deformation," Proceedings of the 10th Coastal Engineering Conference, American Society of Civil Engineers, pp 284-293.

Suhayda, J., and Pettigrew, N. R. 1977. "Observations of Wave Height and Wave Celerity in the Surf Zone," Journal of Geophysical Research, Vol 82, No. 9, pp 1419-1424.

Sunamura, T. 1981. "A Laboratory Study of Offshore Transport of Sediment and a Model for Eroding Beaches," Proceedings of the 17th Coastal Engineering Conference, American Society of Civil Engineers, pp 1051-1070.

Svendsen, I. A. 1984. "Wave Heights and Setup in a Surf Zone," Coastal Engineering, Vol 8, pp 303-329.

Thornton, E. B. 1971. "Variation of Longshore Current Across the Surf Zone," Proceedings of the 12th Coastal Engineering Conference, American Society of Civil Engineers, pp 291-308.

Thornton, E. B., and Guza, R. T. 1983. "Transformation of Wave Height Distribution," Journal of Geophysical Research, Vol 88, pp 5925-5938.

Van Dorn, W. G. 1977. "Setup and Run-up in Shoaling Breakers," Proceedings of the 15th Coastal Engineering Conference, American Society of Civil Engineers, pp 738-751.

Weggel, J. R. 1972. "Maximum Breaker Height," Journal of the Waterways, Harbors, and Coastal Engineering Division, American Society of Civil Engineers, Vol 98, No. WW4, pp 529-548.

Wilson, B. W. 1960. "Note on Surface Wind Stress over Water at Low and High Wind Speeds," Journal of Geophysical Research, Vol 65, No. 10, pp 3377-3382.

APPENDIX A: WAVE HEIGHT DECAY DATA

KEY: S = slope
 T = wave period (s)
 HO = deepwater wave height
 DB = water depth at wave breaking
 H = wave height
 D = water depth
 (cm) = heights and depths in centimeters
 (m) = heights and depths in meters

S = 1/80.0 T = 1.2 HO = 8.75 DB = 12.5 (cm)

H	D/DB
8.58	1.00
8.08	.90
6.47	.80
3.23	.70
2.91	.60

S = 1/80.0 T = 1.2 HO = 9.13 DB = 12.5 (cm)

H	D/DB
9.08	1.00
8.15	.90
4.38	.80
3.13	.70
2.51	.60

S = 1/80.0 T = 1.2 HO = 11.95 DB = 13.8 (cm)

H	D/DB
12.16	1.00
9.60	.91
5.54	.82
5.17	.73
4.80	.64
4.44	.55

S = 1/80.0 T = 1.2 HO = 14.78 DB = 16.3 (cm)

H	D/DB
14.18	1.00
12.92	.92
9.60	.85
8.36	.77
6.68	.69
6.26	.62
5.85	.54
5.42	.46

S = 1/80.0 T = 1.2 HO = 11.74 DB = 16.3 (cm)

H	D/DB
11.60	1.00
11.26	.92
8.61	.85
5.96	.77
5.64	.69
5.30	.62
4.97	.54
4.64	.46

S = 1/80.0 T = 1.2 HO = 13.01 DB = 16.3 (cm)

H	D/DB
13.14	1.00
11.80	.92
6.74	.85
6.07	.77
5.73	.69
5.39	.62
5.06	.54
4.38	.46

S = 1/80.0 T = 1.2 HO = 13.34 DB = 17.5 (cm)

H	D/DB
13.15	1.00
12.80	.93
7.75	.86
6.07	.79
5.72	.71
5.39	.64
5.06	.57
4.72	.50
4.37	.43

S = 1/80.0 T = 1.2 HO = 13.53 DB = 20.0 (cm)

H	D/DB
13.31	1.00
12.98	.94
11.35	.88
9.74	.81
6.82	.75
6.17	.69
5.52	.63
5.20	.56
4.87	.50
4.55	.44
4.20	.38

S = 1/80.0 T = 1.2 HO = 14.59 DB = 22.5 (cm)

H	D/DB
14.70	1.00
14.00	.94
12.65	.89
11.95	.83
8.20	.78
7.87	.72
7.18	.67
6.16	.61
8.82	.56
8.47	.50
8.12	.44
4.78	.39
3.42	.33

S = 1/80.0 T = 1.2 HO = 14.17 DB = 21.3 (cm)

H	D/DB
13.90	1.00
13.60	.94
11.08	.88
7.27	.82
6.96	.76
6.65	.71
6.34	.65
6.02	.59
8.38	.53
5.06	.47
4.42	.41
4.11	.35

S = 1/80.0 T = 1.2 HO = 11.80 DB = 21.3 (cm)

H	D/DB
18.18	1.00
13.88	.94
11.95	.88
8.07	.82
7.75	.76
7.42	.71
7.11	.65
6.78	.59
6.46	.53
5.82	.47
4.52	.41
3.55	.35

S = 1/80.0 T = 1.2 HO = 16.36 DB = 26.3 (cm)

H	D/DB
16.25	1.00
15.92	.95

10.40	.90
9.75	.86
9.75	.81
9.42	.76
8.77	.71
8.45	.67
8.12	.62
7.90	.57
7.48	.52
7.14	.48
6.50	.43
4.87	.38
4.54	.33
4.22	.29

S = 1/80.0 T = 1.4 HO = 7.98 DB = 12.5 (cm)

H	D/DB
7.77	1.00
7.77	.90
6.20	.80
4.03	.70
3.63	.60

S = 1/80.0 T = 1.4 HO = 9.00 DB = 13.8 (cm)

H	D/DB
9.25	1.00
9.08	.91
7.14	.82
4.38	.73
4.22	.64
3.89	.55

S = 1/80.0 T = 1.4 HO = 9.73 DB = 15.0 (cm)

H	D/DB
9.37	1.00
7.85	.92
7.25	.83
5.13	.75
4.23	.67
3.62	.58
3.32	.50

S = 1/80.0 T = 1.4 HO = 11.60 DB = 15.0 (cm)

H	D/DB
11.60	1.00
8.39	.92
7.41	.83
5.71	.75
4.03	.67
3.32	.58
2.35	.50

S = 1/80.0 T = 1.4 HO = 11.36 DB = 16.3 (cm)

H	D/DB
11.52	1.00
9.98	.92
5.61	.85
5.30	.77
5.30	.69
5.30	.62
4.68	.54
4.05	.46

S = 1/80.0 T = 1.4 HO = 12.85 DB = 18.8 (cm)

H	D/DB
12.30	1.00
11.03	.93
9.45	.87
7.89	.80
5.33	.73
5.03	.67
4.73	.60
4.09	.53
3.79	.47
3.15	.40

S = 1/80.0 T = 1.4 HO = 13.52 DB = 20.0 (cm)

H	D/DB
12.95	1.00
11.60	.94
10.94	.88
10.01	.81
8.02	.75
5.97	.69
5.68	.63
5.30	.56
4.97	.50
4.64	.44
4.31	.38

S = 1/80.0 T = 1.4 HO = 14.14 DB = 21.3 (cm)

H	D/DB
13.53	1.00
12.86	.94
9.57	.88
8.91	.82
8.25	.76
7.59	.71
5.94	.65
5.61	.59
5.28	.53
4.95	.47
4.62	.41
4.28	.35

S = 1/80.0 T = 1.4 HO = 14.82 DB = 21.3 (cm)

H	D/DB
13.80	1.00
13.47	.94
11.50	.88
11.17	.82
8.54	.76
6.90	.71
5.58	.65
5.26	.59
4.93	.53
4.60	.47
4.27	.41
3.94	.35

S = 1/80.0 T = 1.4 HO = 15.32 DB = 22.5 (cm)

H	D/DB
16.40	1.00
13.84	.94
11.65	.89
10.20	.83
9.46	.78
8.74	.72
8.01	.67
7.28	.61
6.92	.56
6.55	.50
5.82	.44
5.46	.39
5.10	.33

S = 1/80.0 T = 1.4 HO = 16.70 DB = 25.0 (cm)

H	D/DB
17.32	1.00
14.00	.95
13.64	.90
13.28	.85
11.07	.80
9.22	.75
8.85	.70
8.48	.65
8.48	.60
8.11	.55
7.74	.50
7.37	.45
5.90	.40
5.53	.35
5.16	.30

S = 1/80.0 T = 1.6 HO = 7.88 DB = 11.3 (cm)

H	D/DB
7.93	1.00
7.58	.89
4.32	.78
2.89	.67

S = 1/80.0 T = 1.6 HO = 9.82 DB = 12.5 (cm)

H	D/DB
10.22	1.00
8.26	.90
8.25	.80
4.50	.70
3.75	.60

S = 1/80.0 T = 1.6 HO = 10.48 DB = 15.0 (cm)

H	D/DB
10.32	1.00
9.60	.92
9.60	.83
5.90	.75
4.43	.67
3.69	.58
2.95	.50

S = 1/80.0 T = 1.6 HO = 11.14 DB = 16.3 (cm)

H	D/DB
11.65	1.00
11.30	.92
10.20	.85
6.56	.77
5.83	.69
5.10	.62
4.37	.54
2.92	.46

S = 1/80.0 T = 1.6 HO = 12.35 DB = 16.3 (cm)

H	D/DB
13.69	1.00
11.40	.92
7.60	.85
6.84	.77
6.08	.69
4.56	.62
3.80	.54
3.04	.46

S = 1/80.0 T = 1.6 HO = 13.08 DB = 16.3 (cm)

H	D/DB
14.25	1.00
11.25	.92

7.50	.85
6.00	.77
5.25	.69
4.50	.62
3.75	.54
3.00	.46

S = 1/80.0 T = 1.6 HO = 14.18 DB = 17.5 (cm)

H	D/DB
15.16	1.00
10.11	.93
7.95	.86
7.23	.79
5.78	.71
5.05	.64
4.33	.57
3.61	.50
3.61	.43

S = 1/80.0 T = 1.6 HO = 15.92 DB = 21.3 (cm)

H	D/DB
14.70	1.00
14.00	.94
11.90	.88
10.50	.82
8.40	.76
6.30	.71
5.60	.65
4.90	.59
4.55	.53
4.55	.47
4.55	.41
4.20	.35

S = 1/80.0 T = 1.6 HO = 16.80 DB = 22.5 (cm)

H	D/DB
14.95	1.00
13.90	.94
11.12	.89
9.73	.83
6.25	.78
6.25	.72
5.56	.67
5.56	.61
4.87	.56
4.87	.50
4.52	.44
4.17	.39
3.82	.33

S = 1/80.0 T = 1.8 HO = 7.44 DB = 11.3 (cm)

H	D/DB
8.80	1.00
6.80	.89
5.20	.78
4.40	.67

S = 1/80.0 T = 1.8 HO = 8.33 DB = 12.5 (cm)

H	D/DB
9.20	1.00
8.40	.90
4.00	.80
3.60	.70
3.20	.60

S = 1/80.0 T = 1.8 HO = 8.95 DB = 15.0 (cm)

H	D/DB
9.41	1.00
9.00	.92
8.18	.83
6.55	.75
4.09	.67
3.68	.58
3.28	.50

S = 1/80.0 T = 1.8 HO = 9.64 DB = 13.8 (cm)

H	D/DB
10.00	1.00
8.00	.91
6.80	.82
4.80	.73
4.00	.64
3.20	.55

S = 1/80.0 T = 1.8 HO = 10.51 DB = 15.0 (cm)

H	D/DB
10.80	1.00
9.20	.92
8.80	.83
5.60	.75
4.80	.67
4.00	.58
3.60	.50

S = 1/80.0 T = 1.8 HO = 10.93 DB = 16.3 (cm)

H	D/DB
11.60	1.00
11.20	.92
9.20	.85
6.80	.77
5.20	.69
4.40	.62
4.00	.54
3.60	.46

S = 1/80.0 T = 1.8 HO = 11.34 DB = 16.3 (cm)

H	D/DB
11.76	1.00
11.16	.92
6.78	.85
5.98	.77
5.18	.69
4.38	.62
3.98	.54
3.59	.46

S = 1/80.0 T = 1.8 HO = 11.76 DB = 18.8 (cm)

H	D/DB
11.52	1.00
10.72	.93
9.95	.87
9.16	.80
5.57	.73
5.17	.67
4.78	.60
4.37	.53
3.98	.47
3.58	.40

S = 1/80.0 T = 1.8 HO = 13.10 DB = 18.8 (cm)

H	D/DB
12.40	1.00
10.46	.93
9.68	.87
6.59	.80
5.82	.73
5.49	.67
5.04	.60
4.65	.53
4.26	.47
3.88	.40

S = 1/80.0 T = 1.8 HO = 13.86 DB = 20.0 (cm)

H	D/DB
12.60	1.00
11.81	.94
11.45	.88
9.55	.81
7.25	.75
6.11	.69
5.73	.63
4.96	.56
4.20	.50
3.82	.44
3.44	.38

S = 1/80.0 T = 1.8 HO = 14.50 DB = 21.3 (cm)

H	D/DB
13.75	1.00
14.13	.94
13.35	.88
10.70	.82
8.40	.76
6.87	.71
5.73	.65
5.31	.59
4.96	.53
4.58	.47
4.20	.41
3.82	.35

S = 1/80.0 T = 1.8 HO = 15.28 DB = 21.3 (cm)

H	D/DB
13.78	1.00
13.00	.94
9.55	.88
7.65	.82
7.26	.76
6.88	.71
6.12	.65
5.35	.59
4.58	.53
4.20	.47
3.82	.41
3.44	.35

S = 1/80.0 T = 1.8 HO = 15.35 DB = 22.5 (cm)

H	D/DB
15.00	1.00
14.80	.94
12.80	.89
10.00	.83
8.80	.78
8.40	.72
7.60	.67
6.40	.61
5.60	.56
5.40	.50
5.20	.44
4.80	.39
4.40	.33

S = 1/80.0 T = 2.0 HO = 8.48 DB = 13.1 (cm)

H	D/DB
8.26	1.00
7.80	.90

6.42	.81
5.05	.71
4.13	.62
3.67	.52

S = 1/80.0 T = 2.0 HO = 8.92 DB = 13.8 (cm)

H	D/DB
9.07	1.00
6.90	.91
4.75	.82
3.45	.73
3.02	.64

S = 1/80.0 T = 2.0 HO = 9.78 DB = 15.0 (cm)

H	D/DB
10.35	1.00
9.90	.92
6.30	.83
4.95	.75
4.05	.67
3.15	.58

S = 1/80.0 T = 2.0 HO = 10.65 DB = 15.0 (cm)

H	D/DB
11.20	1.00
10.27	.92
7.00	.83
5.60	.75
4.67	.67
2.80	.58

S = 1/80.0 T = 2.0 HO = 11.32 DB = 15.0 (cm)

H	D/DB
11.82	1.00
9.45	.92
6.62	.83
5.67	.75
4.73	.67
4.25	.58
3.31	.50

S = 1/80.0 T = 2.0 HO = 11.52 DB = 16.8 (cm)

H	D/DB
12.00	1.00
11.07	.93
7.37	.85
5.69	.78
5.53	.70
4.61	.63
3.69	.55
3.23	.48

S = 1/80.0 T = 2.0 HO = 11.95 DB = 16.5 (cm)

H	D/DB
11.88	1.00
10.56	.92
8.80	.85
7.48	.77
6.16	.70
5.28	.62
4.84	.55
4.40	.47
3.52	.39
2.64	.32

S = 1/80.0 T = 2.0 HO = 12.62 DB = 20.0 (cm)

H	D/DB
12.51	1.00
11.60	.94
9.36	.88
7.13	.81
6.25	.75
5.80	.69
5.35	.63
4.90	.56
4.46	.50
3.57	.44
2.68	.38

S = 1/80.0 T = 2.0 HO = 13.25 DB = 20.0 (cm)

H	D/DB
13.56	1.00
11.30	.94
9.03	.88
8.13	.81
7.23	.75
6.33	.69
4.97	.63
4.52	.56
4.07	.50
3.62	.44
2.71	.38

S = 1/80.0 T = 2.0 HO = 14.35 DB = 21.3 (cm)

H	D/DB
14.60	1.00
13.67	.94
10.83	.88
8.48	.82
6.12	.76
5.89	.71
5.66	.65

5.18	.59
4.72	.53
4.47	.47
4.23	.41
3.77	.35

S = 1/80.0 T = 2.0 HO = 15.22 DB = 21.3 (cm)

H	D/DB
15.35	1.00
13.55	.94
9.95	.88
8.58	.82
7.23	.76
6.32	.71
5.87	.65
5.42	.59
4.97	.53
4.52	.47
4.07	.41
3.61	.35

S = 1/80.0 T = 2.0 HO = 16.33 DB = 25.0 (cm)

H	D/DB
15.50	1.00
15.00	.95
14.06	.90
13.60	.85
11.25	.80
9.37	.75
7.50	.70
7.03	.65
6.66	.60
6.10	.55
5.16	.50
4.69	.45
4.22	.40
3.75	.35
3.28	.30

S = 1/65.0 T = 2.0 HO = 19.26 DB = 27.4 (cm)

H	D/DB
24.00	1.00
22.60	.91
18.10	.89
14.70	.84
13.50	.78
8.71	.73
7.21	.67
7.21	.61
6.82	.56
6.31	.50
5.56	.44

S = 1/65.0 T = 2.0 HO = 17.20 DB = 25.0 (cm)

H	D/DB
21.05	1.00
18.05	.98
16.55	.92
13.55	.86
12.04	.79
11.29	.73
9.41	.67
8.28	.61
6.62	.55

S = 1/65.0 T = 2.0 HO = 14.50 DB = 18.3 (cm)

H	D/DB
18.05	1.00
12.02	.92
9.00	.83
9.00	.75
6.81	.67
5.72	.58
5.86	.50
5.11	.41
4.51	.33
3.00	.25

S = 1/65.0 T = 2.0 HO = 11.60 DB = 18.2 (cm)

H	D/DB
16.53	1.00
12.00	.92
10.50	.84
8.42	.75
6.00	.67
5.70	.58
5.40	.50
5.21	.42
4.21	.33

S = 1/65.0 T = 2.0 HO = 9.82 DB = 16.8 (cm)

H	D/DB
14.67	1.00
10.52	.91
10.52	.82
6.61	.73
5.11	.63
4.51	.54
4.21	.45
3.61	.36

S = 1/65.0 T = 2.0 HO = 5.90 DB = 10.9 (cm)

H	D/DB
9.64	1.00
7.82	.90
6.77	.83
5.11	.69
3.91	.55
2.86	.42

S = 1/65.0 T = 2.0 HO = 7.20 DB = 13.4 (cm)

H	D/DB
12.79	1.00
8.42	.91
6.61	.79
5.41	.68
4.81	.56
3.91	.45
3.00	.34

S = 1/65.0 T = 1.6 HO = 24.50 DB = 35.2 (cm)

H	D/DB
27.00	1.00
22.60	.96
20.30	.91
19.50	.87
16.50	.83
15.00	.78
13.50	.74
12.40	.70
11.60	.65
11.30	.61
9.60	.53
7.25	.35
5.10	.24
4.20	.21

S = 1/65.0 T = 2.0 HO = 20.00 DB = 28.0 (cm)

H	D/DB
22.80	1.00
17.40	.93
16.20	.88
11.80	.82
11.50	.76
10.40	.71
9.20	.65
10.20	.60
10.20	.54

S = 1/65.0 T = 1.6 HO = 17.20 DB = 24.5 (cm)

H	D/DB
19.00	1.00
19.00	.93
16.00	.87
12.00	.81
9.78	.75
9.25	.69
8.10	.62
8.45	.56
8.40	.50

S = 1/65.0 T = 1.6 HO = 14.30 DB = 19.3 (cm)

H	D/DB
17.00	1.00
15.50	.95
9.65	.87
9.10	.79
6.75	.71
6.78	.63
6.17	.55

S = 1/65.0 T = 1.6 HO = 12.30 DB = 18.3 (cm)

H	D/DB
15.80	1.00
13.50	.92
11.00	.87
9.80	.83
7.84	.75
7.15	.67
3.00	.58

S = 1/65.0 T = 1.6 HO = 11.40 DB = 15.2 (cm)

H	D/DB
14.30	1.00
13.30	.95
10.50	.90
9.45	.85
7.50	.80
5.70	.75
6.01	.70
4.95	.65
5.71	.60
5.40	.55
3.60	.50

S = 1/65.0 T = 1.6 HO = 9.50 DB = 12.8 (cm)

H	D/DB
11.60	1.00
10.20	.95

7.52	.89
5.60	.83
5.90	.77
4.80	.71
4.50	.68
4.80	.65
4.80	.59
4.35	.53

S = 1/65.0 T = 1.6 HO = 6.90 DB = 11.9 (cm)

H	D/DB
9.32	1.00
8.14	.89
7.67	.83
6.02	.76
5.56	.70
4.37	.63
4.33	.57
3.26	.50

S = 1/65.0 T = 1.6 HO = 6.37 DB = 10.2 (cm)

H	D/DB
8.40	1.00
9.00	.97
6.10	.89
6.00	.81
5.25	.74
3.30	.66
2.70	.59

S = 1/30.0 T = 2.2 HO = 12.95 DB = 17.3 (cm)

H	D/DB
12.84	1.00
12.21	.94
11.29	.88
10.85	.83
10.51	.84
8.63	.78
7.87	.72
7.55	.66
6.84	.63
6.14	.58
5.79	.51
5.22	.45
5.33	.47
4.79	.41
4.12	.36
4.05	.30
3.15	.28
3.10	.22
2.68	.16
2.65	.11

S = 1/30.0 T = 2.2 HO = 12.10 DB = 14.5 (cm)

H	D/DB
10.00	1.00
9.05	.93
7.65	.86
6.72	.79
6.16	.76
6.20	.72
5.62	.61
5.28	.54
5.74	.56
4.51	.49
4.28	.43
3.80	.36
3.64	.33
3.03	.26
2.67	.20
2.77	.13

S = 1/30.0 T = 2.2 HO = 10.40 DB = 15.2 (cm)

H	D/DB
11.52	1.00
10.53	.97
10.08	.90
7.81	.84
6.34	.77
5.94	.78
5.86	.71
5.45	.65
5.52	.58
5.72	.54
4.67	.47
4.27	.41
4.06	.34
3.96	.32
3.58	.25
2.94	.19
2.63	.12

S = 1/30.0 T = 2.2 HO = 10.82 DB = 13.5 (cm)

H	D/DB
11.15	1.00
8.46	.93
6.92	.85
6.35	.80
6.02	.73
5.52	.65
5.76	.58
5.71	.61
4.99	.53

4.55	.46
4.08	.38
4.03	.36
3.40	.28
2.64	.21
2.40	.14

S = 1/30.0 T = 2.2 HO = 9.47 DB = 11.8 (cm)

H	D/DB
7.59	1.00
6.73	.92
5.77	.83
5.79	.75
5.43	.73
4.92	.65
4.58	.56
4.56	.48
3.73	.41
3.26	.32
2.59	.24
2.40	.15

S = 1/30.0 T = 2.2 HO = 8.64 DB = 13.5 (cm)

H	D/DB
11.30	1.00
10.31	.94
7.42	.86
6.91	.79
6.89	.80
5.95	.73
5.25	.65
4.92	.58
5.26	.61
4.71	.53
4.68	.46
4.20	.38
3.84	.36
3.32	.28
2.49	.21
2.21	.14

S = 1/30.0 T = 2.2 HO = 8.45 DB = 13.5 (cm)

H	D/DB
10.77	1.00
9.78	.93
7.68	.85
5.66	.78
5.32	.73
5.19	.65
4.83	.58

4.39	.51
4.30	.36
2.93	.28
2.49	.21
1.96	.14

S = 1/30.0 T = 2.2 HO = 6.76 DB = 11.8 (cm)

H	D/DB
8.73	1.00
7.56	.92
6.84	.83
5.71	.75
4.43	.69
4.87	.61
4.77	.52
4.04	.44
4.34	.41
3.80	.32
2.55	.24
1.77	.15

S = 1/30.0 T = 2.2 HO = 6.32 DB = 10.8 (cm)

H	D/DB
9.15	1.00
7.53	.91
5.43	.82
5.24	.72
4.76	.66
4.97	.57
3.95	.46
3.42	.37
3.90	.45
3.16	.35
2.38	.26
2.33	.17

S = 1/30.0 T = 2.2 HO = 5.57 DB = 9.8 (cm)

H	D/DB
8.38	1.00
7.23	.90
6.07	.80
5.49	.69
4.70	.73
4.32	.63
3.67	.49
3.04	.39
2.25	.29
2.00	.19

S = 1/30.0 T = 2.2 HO = 4.67 DB = 6.8 (cm)

H	D/DB
5.96	1.00
5.32	.90
4.99	.76
3.11	.61
2.93	.46

S = 1/30.0 T = 1.4 HO = 16.10 DB = 20.2 (cm)

H	D/DB
16.71	1.00
16.16	.95
13.93	.87
10.16	.84
9.30	.78
9.26	.74
7.79	.69
7.18	.64
6.96	.59
6.65	.54
5.94	.50
5.36	.45
4.55	.36
4.70	.31
4.34	.25
4.37	.20

S = 1/30.0 T = 1.4 HO = 14.60 DB = 18.4 (cm)

H	D/DB
15.51	1.00
11.43	.95
8.18	.84
8.74	.81
8.96	.80
8.47	.74
6.77	.66
7.04	.61
6.03	.54
5.39	.49
4.66	.41
4.83	.35
4.42	.27
3.39	.22
2.94	.15
3.00	.11

S = 1/30.0 T = 1.4 HO = 14.00 DB = 18.3 (cm)

H	D/DB
15.09	1.00
13.04	.95
9.46	.87

7.96	.82
7.62	.75
6.70	.70
5.68	.61
5.93	.55
5.13	.49
4.83	.44
4.08	.40
4.27	.35
4.19	.26
3.80	.21

S = 1/30.0 T = 1.4 HO = 13.30 DB = 18.2 (cm)

H	D/DB
12.67	1.00
10.62	.93
10.58	.87
8.57	.83
9.01	.77
6.88	.71
5.95	.65
5.75	.62
5.91	.57
5.43	.50
4.60	.44
3.74	.40
4.02	.35
3.82	.27
3.22	.21

S = 1/30.0 T = 1.4 HO = 11.71 DB = 18.2 (cm)

H	D/DB
12.09	1.00
11.26	.93
9.40	.87
7.31	.65
6.44	.61
7.34	.55
5.77	.49
5.06	.43
3.80	.36
3.95	.30
3.69	.24
2.97	.18

S = 1/30.0 T = 1.4 HO = 10.01 DB = 15.8 (cm)

H	D/DB
10.44	1.00
9.63	.95
10.01	.94

9.56	.88
8.71	.81
7.00	.75
6.41	.69
7.49	.63
5.66	.56
5.37	.49
4.02	.41
3.82	.35
3.66	.27
3.19	.21

S = 1/30.0 T = 1.4 HO = 8.19 DB = 7.5 (cm)

H	D/DB
6.86	1.00
5.28	.87
4.61	.73
4.02	.67
2.63	.53
2.71	.38
2.31	.24

S = 1/30.0 T = 1.4 HO = 6.90 DB = 7.5 (cm)

H	D/DB
6.34	1.00
5.52	.87
4.75	.73
3.83	.56
2.73	.42
2.37	.27
1.93	.13

S = 1/20.0 T = 1.4 HO = 8.16 DB = 6.0 (cm)

H	D/DB
7.45	1.00
6.22	.71
3.98	.46
2.81	.21

S = 1/20.0 T = 1.4 HO = 9.17 DB = 6.0 (cm)

H	D/DB
9.42	1.00
9.00	.96
6.93	.83
5.27	.67
4.02	.50
3.82	.46
2.69	.21

S = 1/20.0 T = 1.4 HO = 10.53 DB = 8.0 (cm)

H	D/DB
10.26	1.00
9.47	.73
6.97	.69
5.68	.50
4.41	.44
4.51	.36
3.56	.25
2.95	.16

S = 1/20.0 T = 1.4 HO = 11.98 DB = 8.0 (cm)

H	D/DB
11.14	1.00
9.06	.81
5.88	.69
5.37	.56
3.99	.44
3.49	.38
3.25	.25
2.87	.16

S = 1/20.0 T = 1.4 HO = 11.10 DB = 14.0 (cm)

H	D/DB
11.68	1.00
9.55	.64
8.29	.52
5.54	.36
4.48	.25
3.64	.18
2.61	.07

S = 1/20.0 T = 1.4 HO = 13.22 DB = 14.0 (cm)

H	D/DB
13.92	1.00
12.10	.89
8.22	.68
7.13	.52
5.35	.36
3.62	.18
2.80	.09

S = 1/20.0 T = 1.4 HO = 14.20 DB = 16.0 (cm)

H	D/DB
13.11	1.00
12.33	.88
7.67	.59
6.80	.44
4.26	.25
2.70	.08

S = 1/20.0 T = 1.4 HO = 16.10 DB = 16.0 (cm)

H	D/DB
13.24	1.00
11.98	.80
8.03	.59
7.46	.45
4.82	.25
2.76	.08

S = 1/20.0 T = 1.4 HO = 17.30 DB = 20.5 (cm)

H	D/DB
15.71	1.00
12.51	.78
12.68	.71
10.53	.55
7.92	.46
7.09	.34
5.05	.22
2.86	.06

S = 1/20.0 T = 1.4 HO = 16.92 DB = 20.5 (cm)

H	D/DB
16.55	1.00
12.94	.83
11.07	.71
7.94	.51
6.76	.34
4.50	.22
2.52	.05

S = 1/20.0 T = 2.2 HO = 5.61 DB = 7.3 (cm)

H	D/DB
6.47	.97
5.32	.69
6.10	.69
3.83	.55
3.32	.34
2.21	.16

S = 1/20.0 T = 2.2 HO = 6.25 DB = 10.8 (cm)

H	D/DB
7.76	1.00
7.08	.84
6.56	.67
5.53	.49
4.10	.37
2.89	.23
2.41	.12

S = 1/20.0 T = 2.2 HO = 6.95 DB = 9.3 (cm)

H	D/DB
8.33	1.00
8.01	.81
4.90	.59
5.25	.57
4.24	.43
3.01	.27
2.42	.14

S = 1/20.0 T = 2.2 HO = 8.30 DB = 9.3 (cm)

H	D/DB
10.45	1.00
7.58	.81
5.00	.59
5.06	.57
4.02	.43
3.33	.24
2.80	.16

S = 1/20.0 T = 2.2 HO = 9.46 DB = 10.5 (cm)

H	D/DB
12.34	1.00
11.39	.88
9.00	.76
6.32	.64
5.88	.50
4.46	.38
3.71	.26
2.69	.14

S = 1/20.0 T = 2.2 HO = 9.83 DB = 12.3 (cm)

H	D/DB
11.32	1.00
10.76	.86
10.62	.76
7.89	.65
6.22	.54
5.13	.43
4.52	.33
3.82	.22
2.73	.12

S = 1/20.0 T = 2.2 HO = 10.12 DB = 12.8 (cm)

H	D/DB
11.60	1.00
10.40	.88
8.66	.69
6.72	.59
6.26	.49

5.42	.39
4.28	.29
3.26	.20

S = 1/20.0 T = 2.2 HO = 10.57 DB = 13.5 (cm)

H	D/DB
11.69	.98
12.81	1.00
11.89	.91
11.06	.81
10.30	.74
9.71	.72
7.30	.65
6.54	.56
5.38	.46
5.07	.37
4.50	.28
3.83	.19

S = 1/20.0 T = 2.2 HO = 11.34 DB = 13.3 (cm)

H	D/DB
12.31	1.00
11.25	.91
9.29	.81
8.27	.72
6.72	.62
5.73	.47
5.34	.42
5.58	.40
4.84	.30
3.56	.21
2.59	.13

S = 1/20.0 T = 2.2 HO = 12.14 DB = 15.3 (cm)

H	D/DB
12.84	1.00
12.65	.92
12.20	.84
9.98	.74
9.29	.66
7.87	.57
5.97	.49
5.77	.41
5.98	.34
4.95	.33
4.52	.26
3.46	.15
2.49	.08

S = 1/20.0 T = 2.3 HO = 13.65 DB = 16.5 (cm)

H	D/DB
15.58	1.00
14.94	.92
14.79	.85
11.00	.74
10.85	.67
8.19	.59
7.70	.52
6.72	.44
6.13	.36
5.27	.29
4.52	.24
3.62	.17
2.81	.09

S = 1/50.0 T = 1.3 HO = 10.31 DB = 16.4 (cm)

H	D/DB
10.60	1.00
10.34	.98
10.28	.96
10.12	.94
9.65	.92
9.01	.89
8.85	.87
8.37	.85
8.06	.83
7.37	.80
7.26	.80
6.68	.78
6.47	.76
5.83	.75
6.25	.74
5.51	.71
5.14	.67
4.82	.64
4.13	.63
4.45	.62
4.13	.59
4.13	.58
4.35	.57
4.03	.55
4.03	.53
3.98	.52
3.92	.50
4.03	.49
3.60	.48
3.82	.46
3.82	.44
3.55	.41

3.50	.39
3.23	.36
3.39	.29
2.60	.28
2.76	.25
2.07	.24
2.65	.23
2.33	.20
2.01	.19
1.48	.16
1.38	.14
1.11	.12
1.17	.10
1.06	.10
.95	.05
.90	.03
.74	.01

S = 1/50.0 T = 2.5 HO = 5.34 DB = 9.7 (cm)

H	D/DB
9.90	1.00
8.76	.95
6.68	.91
5.74	.87
5.54	.83
5.00	.80
4.75	.75
4.26	.71
4.11	.66
3.66	.62
3.56	.59
3.51	.54
3.27	.50
2.67	.43
2.38	.38
2.13	.34
1.88	.29
1.53	.21
1.19	.16
.99	.12
.89	.09
.79	.07
.69	.05
.54	.03

S = 1/90.0 T = 2.0 HO = 4.65 DB = 8.5 (cm)

H	D/DB
7.30	1.00
6.79	.97
5.55	.93

3.94	.88
3.72	.84
3.50	.75
3.14	.71
3.07	.69
3.36	.64
2.85	.55
2.99	.51
2.96	.47
3.29	.45
2.34	.41
2.19	.39
1.68	.33
1.53	.28
1.39	.24
1.24	.20
.80	.16
.80	.11
.51	.06
.44	.04

S = 1/45.0 T = 1.6 HO = 16.60 DB = 20.8 (cm)

H	D/DB
1.49	.04
2.32	.14
1.66	.16
3.32	.20
2.66	.26
2.82	.38
3.32	.50
5.81	.65
8.13	.68
7.30	.71
14.11	.88
12.78	.90
16.60	1.00

S = 1/45.0 T = 2.4 HO = 15.80 DB = 18.9 (cm)

H	D/DB
.95	.05
4.11	.34
5.21	.48
4.58	.60
9.16	.75
15.80	1.00

S = 1/45.0 T = 3.4 HO = 13.00 DB = 13.8 (cm)

H	D/DB
1.82	.08
1.95	.21

2.47	.35
2.47	.52
4.55	.69
6.50	.81
10.53	.88
10.27	.92
13.00	1.00

S = 1/45.0 T = 4.8 HO = 13.00 DB = 13.8 (cm)

H	D/DB
1.17	.20
1.69	.34
1.95	.50
4.16	.64
6.37	.78
6.37	.85
13.00	1.00

S = 1/25.0 T = 1.6 HO = 16.40 DB = 21.7 (cm)

H	D/DB
2.30	.07
2.79	.15
3.94	.20
3.94	.25
3.77	.27
4.59	.32
5.08	.39
5.25	.45
7.38	.49
6.56	.55
10.66	.68
13.94	.77
15.58	.84
16.40	1.00

S = 1/25.0 T = 2.4 HO = 14.40 DB = 16.9 (cm)

H	D/DB
1.58	.10
3.02	.19
3.46	.32
5.04	.43
5.47	.51
5.76	.59
5.90	.64
6.77	.72
11.66	.82
14.40	1.00

S = 1/25.0 T = 3.4 HO = 11.80 DB = 11.1 (cm)

H	D/DB
2.48	.15
2.48	.28
4.37	.40
5.43	.51
5.90	.79
9.09	.91
11.80	1.00

S = 1/25.0 T = 4.8 HO = 11.90 DB = 11.1 (cm)

H	D/DB
3.21	.14
3.93	.28
4.05	.40
4.76	.50
5.59	.65
9.04	.78
9.76	.91
11.90	1.00

S = 1/12.0 T = 1.6 HO = 15.60 DB = 18.3 (cm)

H	D/DB
2.03	.10
6.24	.27
5.77	.35
6.40	.51
11.08	.70
14.82	.84
15.60	1.00

S = 1/12.0 T = 2.4 HO = 12.70 DB = 10.8 (cm)

H	D/DB
5.46	.17
5.21	.46
7.24	.60
12.70	.88
12.70	1.00

S = 1/12.0 T = 3.4 HO = 14.80 DB = 9.3 (cm)

H	D/DB
3.70	.20
5.77	.37
5.77	.53
10.95	.69
13.47	.88
14.80	1.00

S = 1/12.0 T = 4.8 HO = 11.20 DB = 8.2 (cm)

H	D/DB
3.02	.20
4.82	.35
8.85	.53
7.28	.69
10.75	.87
11.20	1.00

S = 1/40.0 T = 1.8 HO = .16 DB = .2 (m)

H	D/DB
.18	1.00
.12	.87
.09	.76
.07	.65
.06	.53
.04	.42
.04	.28
.03	.19
.02	.07

S = 1/40.0 T = 5.0 HO = 1.21 DB = 1.9 (m)

H	D/DB
1.50	1.00
1.43	.91
.70	.80
.90	.79
.63	.74
.57	.69
.73	.69
.53	.52
.63	.48
.47	.41
.33	.31
.40	.25
.20	.20

S = 1/10.0 T = 1.2 HO = 10.00 DB = 8.3 (cm)

H	D/DB
10.00	1.00
8.78	.85
6.73	.71
6.12	.55
5.10	.40
3.98	.27
2.96	.12

$$S = 1/29.4 \quad T = 3.1 \quad HO = 1.37 \quad DB = 2.0 \quad (m)$$

H	D/DB
1.29	1.00
1.20	.92
.68	.75
.50	.58
.41	.41
.38	.25
.25	.08

$$S = 1/22.2 \quad T = 5.9 \quad HO = 1.36 \quad DB = 1.9 \quad (m)$$

H	D/DB
1.69	1.00
1.49	.88
.88	.65
.73	.42
.59	.18

$$S = 1/62.5 \quad T = 9.0 \quad HO = .86 \quad DB = 1.6 \quad (m)$$

H	D/DB
1.52	1.00
1.23	.95
.85	.85
.66	.74
.38	.54
.25	.44
.08	.33

$$S = 1/45.5 \quad T = 9.0 \quad HO = .47 \quad DB = 1.4 \quad (m)$$

H	D/DB
.97	1.00
.84	.92
.63	.76
.43	.68
.33	.53
.25	.37

APPENDIX B: LONGSHORE CURRENT COMPUTER PROGRAM AND SAMPLE RUN

LONGSHORE CURRENT BASED ON POWER LAW WAVE HEIGHT DECAY

This program calculates the longshore current based on an empirical power law expression for the wave height decay in the surf zone,

$$H = \Gamma * h_b * (h/h_b)^{-n}$$

where: H is the wave height
h is the water depth
h_b is the water depth at breaking
H_b is the wave height at breaking
Γ is the breaker index (H_b/h_b)
n is the exponent (typical range 1.0 to 2.0)

The exponent n is a function of the beach slope and the breaker index. The exponent may be input directly or calculated in the program from the beach slope and breaker index. Other inputs include the parameter P expressing the relative importance of lateral mixing and bottom friction (typical range 0.01 to 0.10) and the wave angle at breaking (typical range 0.0 to 30.0 degrees).

Do you want the program to calculate the power law exponent? (Y or N)
y

Input the beach slope, breaker index (e.g. 0.02,0.8)
0.02,0.78

Input the parameter P
0.05

Input the breaking wave angle (degrees)
10.0

n = 1.74 P = 0.05 Breaking wave angle = 10.0

Longshore Current Distribution

V is the dimensionless longshore current speed

X is the dimensionless distance from the mean shoreline

V =	0.000	0.003	0.009	0.018	0.029	0.043	0.059	0.076	0.096	0.116
X =	0.000	0.020	0.040	0.060	0.080	0.100	0.120	0.140	0.160	0.180
V =	0.138	0.162	0.186	0.212	0.238	0.265	0.292	0.320	0.348	0.377
X =	0.200	0.220	0.240	0.260	0.280	0.300	0.320	0.340	0.360	0.380
V =	0.405	0.434	0.462	0.489	0.516	0.543	0.568	0.593	0.616	0.638
X =	0.400	0.420	0.440	0.460	0.480	0.500	0.520	0.540	0.560	0.580
V =	0.659	0.678	0.695	0.711	0.724	0.735	0.743	0.749	0.752	0.753
X =	0.600	0.620	0.640	0.660	0.680	0.700	0.720	0.740	0.760	0.780
V =	0.750	0.743	0.734	0.720	0.703	0.681	0.656	0.626	0.591	0.551
X =	0.800	0.820	0.840	0.860	0.880	0.900	0.920	0.940	0.960	0.980
V =	0.507	0.462	0.422	0.386	0.354	0.325	0.299	0.275	0.254	0.235
X =	1.000	1.020	1.040	1.060	1.080	1.100	1.120	1.140	1.160	1.180
V =	0.217	0.201	0.186	0.173	0.161	0.150	0.139	0.130	0.121	0.113
X =	1.200	1.220	1.240	1.260	1.280	1.300	1.320	1.340	1.360	1.380
V =	0.106	0.099	0.093	0.087	0.082	0.077	0.072	0.068	0.064	0.060
X =	1.400	1.420	1.440	1.460	1.480	1.500	1.520	1.540	1.560	1.580
V =	0.057	0.054	0.051	0.048	0.045	0.043	0.041	0.039	0.037	0.035
X =	1.600	1.620	1.640	1.660	1.680	1.700	1.720	1.740	1.760	1.780
V =	0.033	0.031	0.030	0.028	0.027	0.026	0.025	0.023	0.022	0.021
X =	1.800	1.820	1.840	1.860	1.880	1.900	1.920	1.940	1.960	1.980

Do you want to make another run? (Y or N)

n

FORTRAN STOP

```

C*****
C
C   Analytical Model of the Longshore Current Based on
C   Power Law Wave Height Decay Including the Effect of
C   Large Incident Wave Angles
C
C   JANE SMITH 29 OCT 86
C
C*****
C
C   Definitions of variables and arrays
C
C   N - power law exponent, input or calculated internally
C       from the beach slope and breaker index
C   P - parameter expressing the relative importance of
C       lateral mixing and bottom friction (0.01 to 0.10)
C   THETA - breaking wave angle in degrees
C   M - order of the solution (2)
C   THETAR - breaking wave angle in radians
C   SINTB2 - sine of the breaking angle squared
C   From Equation 3-69:
C       PP - p, QQ - q, A(1) - Ao, A(2) - A1, A(3) - A2
C       BETA(1) - Bo, BETA(2) - B1, BETA(3) - B2
C       DELTA(1) - Co, DELTA(2) - C1, DELTA(3) - C2
C       SUMA - SA, SUMB - SB, SUMC - SC
C       SNMA - SA', SNMB - SB', SNMC - SC'
C       B(1) - b1, B(2) - b2, C(1) - c1, C(2) - c2
C       X(j) - nondimensional distance from the shoreline,
C               x/xb
C       V(j) - nondimensional longshore current speed,
C               v/v0
C*****
C
C   DIMENSION A(25),BETA(25),DELTA(25),B(25),C(25)
C   DIMENSION X(100),V(100)
C   DATA INO/'N'/,IYES/'Y'/
C   REAL N
C   M=2
C   MM=M+1
C   TYPE 60
60  FORMAT(/,1X,'LONGSHORE CURRENT BASED ON POWER LAW WAVE',
*1X,'HEIGHT DECAY')
C   TYPE 61
61  FORMAT(/1X,'This program calculates the longshore current
based',
*/, ' on an empirical power law expression for the wave',/
*,' height decay in the surf zone',/,5X,'H = gamma*hb*(h/hb)**n',
*//1X,'where: H is the wave height',/9X,'h is the water depth',
*/9X,'hb is the water depth at breaking',/9X,'Hb is the wave',
*1X,'height at breaking',/9X,'gamma is the breaker index (Hb/hb)',
*//9X,'n is the exponent (typical range 1.0 to 2.0)',/)
C   TYPE 62

```

```

62  FORMAT(' The exponent  n  is a function of the beach slope and'
*/' the breaker index. The exponent may be input directly or',
*/' calculated in the program from the beach slope and breaker',
*/' index. Other inputs include the parameter  P  expressing',
*/' the relative importance of lateral mixing and bottom',
*/' friction (typical range 0.01 to 0.10) and the wave angle',
*/' at breaking (typical range 0.0 to 30.0 degrees).')
99  TYPE 63
63  FORMAT(//,1X,'Do you want the program to calculate the power',
*1x,'law exponent? (Y or N)')
    READ 64, IANS
64  FORMAT(A1)
    IF(IANS.EQ.INO) GO TO 70
    TYPE 66
66  FORMAT(1X,'Input the beach slope, breaker index (e.g. 0.02,0.8)')
    READ *,SLOPE,BINDEX
    N=0.032-0.0096/SLOPE+0.657*BINDEX+0.043*BINDEX/SLOPE
    GO TO 74
70  TYPE 72
72  FORMAT(//1X,'Input power law exponent, n')
    READ *,N
74  TYPE 76
76  FORMAT(/1X,'Input the parameter P')
    READ *,P
    TYPE 77
77  FORMAT(/1X,'Input the breaking wave angle (degrees)')
    READ *,THETA
    TYPE 78,N,P,THETA
78  FORMAT(//,1X,'n = ',F4.2,2X,'P = ',F4.2,2X,'Breaking wave',
*1x,'angle = ',F4.1,///)
C
    FACN=1.0
    FACN2=1.0
    THETAR=3.14159*THETA/180.0
    SINTB2=(SIN(THETAR))**2
    PP=(-(2.0*N+1.0)/4.0)+SQRT(((2.0*N+1.0)/4.0)**2+1.0/P)
    QQ=(-1./8.0)-SQRT(1.0/64.0+1.0/P)
    A(1)=(4.0*N+1.0)/5.0/(1.0-P*N*(2.0*N+0.5))
    BETA(1)=1.0
    DELTA(1)=1.0
    SUMA=A(1)
    SUMB=BETA(1)
    SUMC=DELTA(1)
    SNMA=N*A(1)
    SNMB=PP*BETA(1)
    SNMC=QQ*DELTA(1)
C
C
    DO 10 I=1,M
    II=I+1
    Z=FLOAT(I)
    FACN=FACN*Z
    FACN2=(2.0*Z-3.0)*FACN2

```

```

IF(FACN2.LT.1.0)FACN2=1.0
A(II) = (-(2.0*Z+4.0*N+1)*FACN2)/(5.0*2.0**Z*FACN)
A(II) = A(II)*SINTB2**Z-SINTB2*A(II-1)
A(II) = A(II)/(1.0-P*(N+Z)*(2.0*N+Z+0.5))
C
BETA(II) = SINTB2*BETA(II-1)
BETA(II) = BETA(II)/(P*(PP+Z)*(PP+Z+N+0.5)-1.0)
C
DELTA(II) = SINTB2*DELTA(II-1)
DELTA(II) = DELTA(II)/(P*(QQ-Z)*(QQ-Z+0.25)-1.0)
C
SUMA = SUMA + A(II)
SUMB = SUMB + BETA(II)
SUMC = SUMC + DELTA(II)
SNMA = SNMA + (N+Z)*A(II)
SNMB = SNMB + (PP+Z)*BETA(II)
SNMC = SNMC + (QQ-Z)*DELTA(II)
10 CONTINUE
C
C
C
B(1) = (SNMA*SUMC-SUMA*SNMC)/(SUMB*SNMC-SNMB*SUMC)
C(1) = (SNMA*SUMB-SUMA*SNMB)/(SUMB*SNMC-SNMB*SUMC)
C
DO 20 I=2,MM
B(I) = B(1)*BETA(I)
C(I) = C(1)*DELTA(I)
20 CONTINUE
C
DO 100 J=1,50
X(J) = FLOAT(J-1)/50.
X(J+50) = X(J)+1.0
V(J) = 0.0
V(J+50) = 0.0
DO 101 K=1,MM
Z = FLOAT(K)-1.0
V(J) = V(J)+A(K)*X(J)**(N+Z)+B(K)*X(J)**(PP+Z)
V(J+50) = V(J+50)+C(K)*(X(J+50))**(QQ-Z)
101 CONTINUE
100 CONTINUE
TYPE 43
43 FORMAT(1X,'Longshore Current Distribution')
TYPE 44
44 FORMAT(5X,'V is the dimensionless longshore current speed',
*/5X,'X is the dimensionless distance from the mean shoreline',/)
DO 45 I=1,10
K1 = (I-1)*10+1
K2 = K1+9
TYPE 50,(V(K),K=K1,K2)
TYPE 51,(X(K),K=K1,K2)
TYPE 52
45 CONTINUE
50 FORMAT(1X,'V = ',10F7.3)
51 FORMAT(1X,'X = ',10F7.3)

```

```

52  FORMAT(1X,'- - - - -',
      *1X,'- - - - -')
      TYPE 95
95  FORMAT(//1X,'Do you want to make another run? (Y or N)')
      READ 64, IANS
      IF(IANS.EQ.IYES)GO TO 99
      STOP
      END

```

APPENDIX C: NOTATION

B_L	lateral mixing stress
$\langle B_y \rangle$	average bottom friction stress
C	wave celerity
c_D	drag coefficient
c_f	friction coefficient
C_g	group wave celerity
E	wave energy density per unit surface area
f_c	Coriolis parameter
F_x	energy flux in the onshore-direction per unit distance parallel to shore
g	gravitational acceleration
H	wave height
h	water depth
H_b	wave height at wave breaking
h_b	water depth at wave breaking
H_o	deepwater wave height
k	decay coefficient in Dally et al. (1985a, 1985b) wave height decay model
L_o	deepwater wavelength
m	beach slope
n	exponent in power law wave height decay expression
P	parameter expressing the relative importance of lateral mixing and bottom friction (including the effect of wave setup) in the longshore current model
Q	parameter expressing the relative importance of lateral mixing and bottom friction (excluding the effect of wave setup) in the longshore current model
S_{xx}	mean flux of momentum across a plane $x = \text{constant}$, principle component of radiation stress
S_{xy}	mean flux of y -momentum parallel to the shore across a plane $x = \text{constant}$, component of radiation stress
T	wave period
t	time

u	onshore current component
U_0	wave orbital velocity
V	nondimensional longshore current speed, v/v_0
v	longshore current component
v_0	maximum longshore current speed for special case of $n = 1$ and lateral mixing stress neglected
X	dimensionless onshore coordinate, x/x_b
x	onshore coordinate
x_b	location of wave breaking
y	alongshore coordinate
w	wind speed
β	angle of bottom with the horizontal
Γ	constant in the expression for ϵ_L
γ	ratio of wave height to water depth at wave breaking
ϵ	energy dissipation rate
ϵ_L	lateral viscosity coefficient
\bar{n}	wave setup
\bar{n}_b	wave setup at wave breaking
θ	incident wave angle
θ_b	incident wave angle at wave breaking
π	the constant π
ρ	density of water
ϕ	incident wind angle
τ_y	local wave stress
τ_{wy}	wind stress